2014

ACTIVE CURRENT INJECTION METHOD FOR LIMITING GROUND FAULT CURRENT HARMONICS IN UNDERGROUND COAL MINES

Yigong Zhang
University of Kentucky, chamabow@gmail.com

STUDENT AGREEMENT:

I represent that my thesis or dissertation and abstract are my original work. Proper attribution has been given to all outside sources. I understand that I am solely responsible for obtaining any needed copyright permissions. I have obtained needed written permission statement(s) from the owner(s) of each third-party copyrighted matter to be included in my work, allowing electronic distribution (if such use is not permitted by the fair use doctrine) which will be submitted to UKnowledge as Additional File.

I hereby grant to The University of Kentucky and its agents the irrevocable, non-exclusive, and royalty-free license to archive and make accessible my work in whole or in part in all forms of media, now or hereafter known. I agree that the document mentioned above may be made available immediately for worldwide access unless an embargo applies.

I retain all other ownership rights to the copyright of my work. I also retain the right to use in future works (such as articles or books) all or part of my work. I understand that I am free to register the copyright to my work.

REVIEW, APPROVAL AND ACCEPTANCE

The document mentioned above has been reviewed and accepted by the student's advisor, on behalf of the advisory committee, and by the Director of Graduate Studies (DGS), on behalf of the program; we verify that this is the final, approved version of the student's thesis including all changes required by the advisory committee. The undersigned agree to abide by the statements above.

Yigong Zhang, Student

Dr. Joseph Sottile, Major Professor

Dr. Thomas Novak, Director of Graduate Studies

ACTIVE CURRENT INJECTION METHOD FOR LIMITING GROUND FAULT CURRENT HARMONICS IN UNDERGROUND COAL MINES

DISSERTATION

A dissertation submitted in partial fulfillment of the requirements
for the degree of Doctor of Philosophy in the College of
Engineering at the University of Kentucky

By
Yigong Zhang

Lexington, Kentucky

Director: Dr. Joseph Sottile, Professor of Mining Engineering

Lexington, Kentucky

2014

ABSTRACT OF DISSERTATION

ACTIVE CURRENT INJECTION METHOD FOR LIMITING GROUND FAULT CURRENT HARMONICS IN UNDERGROUND COAL MINES

Current practice in U.S. underground coal mine high-voltage distribution systems is to attempt to limit ground fault current to 25 Amperes and de-energize the circuit at 10 Amperes. However, the significant amount of system capacitance due to the use of shielded cables can cause ground fault current to be two or three times the intended ground fault limit. Consequently, this practice can cause several issues such as ground fault currents significantly exceeding the neutral grounding resistor current limit, loss of relay selectivity in the distribution system, and transient overvoltages in certain ground fault situations. These issues are solved to some extent by using a resonance grounded system, currently used in some other countries. However, a shortcoming of traditional resonance grounded systems is the inability to deal with the harmonic components existing in ground fault current. With the increasing use of nonlinear sources such as variable frequency drives, the proportion of harmonic components in ground fault current can be significant. Consequently, although the fundamental component can be almost fully compensated in a traditional resonance grounded system, the harmonic components can still be large enough to maintain arcing and cause personal injury and equipment damage. In this dissertation, a novel method is developed to perform real-time prediction of the harmonics in ground fault currents. Methods for neutralizing the ground fault current harmonics and identifying ground fault location are also developed. Results indicate that the combination of traditional high-resistance grounding and active current injection to neutralize harmonics in the ground fault has the potential to significantly reduce the total ground fault current and reduce arc and flash hazards during ground faults in high voltage distribution systems.

KEYWORDS: High-Resistance Grounding, Petersen Coil, Fault Current Harmonics, Fault Current Prediction, Active Current Compensation.

Yigong Zhang

Author's Signature

December 17th, 2014

Date

ACTIVE CURRENT INJECTION METHOD FOR LIMITING GROUND FAULT CURRENT HARMONICS IN UNDERGROUND COAL MINES

By

Yigong Zhang

Joseph Sottile
Director of Dissertation

Thomas Novak
Director of Graduate Studies

December 17th, 2014
Date

TO MY BELOVED FAMILIES

My mother Xiurong Chen

My wife Yushan Sui

TO THE MEMORY OF MY FATHER

Zhenhu Zhang

ACKNOWLEDGEMENTS

The following dissertation, while an individual work, benefited from the insights and directions of several people. First, I express my deep sense of gratitude and indebtedness to Professor Joseph Sottile for the inspiration, indispensable guidance, constant encouragement, thoughtful suggestions, invaluable helps, and personal attention provided at every stage of carrying out this project. It has been a wonderful opportunity to work with him. Second, I also express my gratitude and indebtedness to Professor Rich Honaker for providing me the opportunity to work in the Department of Mining Engineering at the University of Kentucky. Financial support obtained from Department of Mining Engineering is greatly acknowledged.

I sincerely thank Professor Thomas Novak, Professor Braden Lusk and Professor Yuan Liao for their invaluable helps and suggestions. I also thank Professor Susan Gardner for participating as an outside examiner of my final dissertation defense.

My sincere gratitude is expressed to all others who have helped me either directly or indirectly during the research.

In the end, I thank my families and friends for the support and inspiration I have been receiving from them, in particular my mother Xiurong Chen and my wife Yushan Sui. They have always been the most significant people and the greatest and strongest support in my life. Everything good in my life, I owe to them.

TABLE OF CONTENTS

_Toc406579245

LIST OF TABLES

LIST OF FIGURES

LIST OF SYMBOLS

a	a-operator ($1\angle 120°$)
AWG	American Wire Gauge
C	Capacitance
C_x	Capacitance of line x
CFR	Code of Federal Regulations
CT	Current Transformer
cmil	Circular mile (wire size)
d	Damping coefficient
E_x	Source voltage in phase x
FFT	Fast Fourier transform
f	Frequency
G	Conductance
I	Current
I_0	Zero-sequence current
I_x	Current in line x
j	Imaginary number ($1\angle 90°$)
$\dot{K}_c$	Three-phase asymmetry coefficient
L	Inductance
LF	Load factor
LN	Line-to-neutral

MP-GC 3/C	Mine power feeder cable with a ground check conductor and three power conductors
NGR	Neutral grounding resistor
P	Active power
pf	Power factor
PC	Petersen coil
PT	Potential transformer
Q	Reactive power
R	Resistance
S	Complex power
SIC	Standard Industrial Classification
t	Time
v	Resonance deviation
V	Voltage
V_{L-L}	Line-to-line voltage
V_{L-N}	Line-to-neutral voltage
V_{xy}	Voltage between line x and y
X	Reactance
X_C	Capacitive reactance
X_L	Inductive reactance
Z	Impedance
φ	Phase
φ	Angle

ω	Angular frequency
θ	Angle
δ	Impedance
ε	Dielectric constant of the medium

CHAPTER 1

INTRODUCTION

1.1. Overview

The electrical distribution system is one of the most important parts of the modern mining industry, especially underground coal mines, because nearly all equipment is electrically driven. The system must transmit large amounts of power, sometimes in confined areas, while maintaining safety to personnel during normal and abnormal conditions. Abnormal conditions include insulation failure, open circuits, transients such as those from lightning and switching, and so forth. A properly designed power system should be able to quickly, and automatically, detect and isolate faulted portions of the power system while maintaining electrical service to other portions of the mine.

As with other industrial power distribution systems, mine grounding systems are designed to protect personnel and prevent equipment damage during ground faults and overvoltage conditions. A properly designed grounding system should be capable of maintaining equipment frame potentials to values near ground potential during ground faults, lightning, line surges and unintentional contact with higher voltage lines. This is achieved by providing a low impedance path for ground fault current, limiting ground fault current to protect personnel, detecting the ground fault, and de-energizing the faulted section of the distribution system [Morley, 1990; Sottile and Novak, 2001].

Applications of electricity and electrical equipment to mining operations are regulated by Title 30 – Mineral Resources, of the Code of Federal Regulations (30CFR). Guidelines described in Title 30 have been specifically developed to make the use of electricity in mines as safe as possible. Part 18 and a portion of Part 75 of Title 30 deal with the regulatory requirement for the use of electricity and electrical equipment in underground coal mines [30 CFR, 2003; Sottile and Novak, 2001].

A mine grounding system is a vital part of any mine power distribution system connected to earth or ground through a ground bed. A ground bed is basically a complex of conductors buried in the earth to provide a low impedance path to infinite earth. From the ground bed, grounding conductors extend to the frames of all mining equipment (oftentimes, several miles away) to maintain the equipment frames near ground potential under normal and abnormal system conditions.

A mine distribution system typically has two types of grounding: system grounding and equipment grounding. System grounding is the connection of the power system to the ground bed. This connection is usually made at the neutral point of the substation transformer, either solidly or through intentional impedance between the neutral point and the ground bed. High-resistance system grounding is required for underground coal mines. With equipment grounding, the metal frames of all mining equipment are connected to the ground bed to maintain their frames near ground potential under normal as well as abnormal or faulted system conditions. Equipment grounding is required by Federal regulations for both ungrounded and grounded mine distribution systems [Amoh, 2006; Morley 1990; Sottile and Novak, 2001].

A fault in a power system is defined as any failure interfering with the normal flow of current and normal system operation [Stevenson, 1982]. Power system faults can cause abnormally large current flow in the power conductors and also grounding conductors. Faults may cause damage to both faulted and unfaulted parts of the power system, and the protection system must detect the fault condition and isolate the faulted section as quickly and selectively as possible to minimize damage to equipment and prevent harm to personnel [Amoh, 2006; Nasar and Trutt, 1999].

The power system protection system typically consists of transducers (instrument transformers), relays, and circuit breakers. Currents and voltages are measured by transducers and converted to low level proportional signals for relay operation. Relays receive and process these signals to detect the fault characteristics and energize circuit-breakers trip circuits. Circuit breakers disconnect the faulted section from the power system after receiving trip signals from relays [Faukenberry and Coffer, 1996; Stevenson, 1982; Tripathi, 2007].

Faults involving ground are defined as ground faults, including single-line-to-ground faults, double-line-to-ground faults, and three-line-to-ground faults. The emphasis in this dissertation is on the single-line-to-ground faults because they occur most frequently in distribution systems [Nasar and Trutt, 1999].

1.2. Problem Statement

Federal regulations for US underground coal mine high-voltage distribution systems require that the ground fault protection system limit the voltage in the ground circuit external to the neutral grounding resistor to no more than 100 V [30 CFR, 2003, Tripathi, 2007]. Practically, this requirement is met by limiting the neutral ground resistor (NGR) current to 25 A and establishing a pickup setting of 10 A. US coal mines typically have 15-kV class distribution systems with nominal distribution voltages that include 12.47 kV, 13.2 kV, 13.8 kV, or 14.4 kV

However, because high voltage distribution systems are required to be composed of shielded cables, the distribution system has a relatively high value of capacitance to ground. This high level of system capacitance results in relatively large capacitive charging current during ground faults, that, in many cases, can significantly exceed the NGR current limit of 25 A. Consequently, the 25 A NGR limit is not truly a 25 A ground fault limit. As distribution systems become more extensive, significant distributed capacitance can also lead to overvoltage problems that cause deterioration and untimely failure of power system components. Moreover, high system distributed capacitance combined with low ground-fault pick-up settings can cause loss of relay selectivity that can cause unnecessary tripping of the entire system during a ground fault in one part of it [Novak, 1998, 2001].

As mentioned above, several significant problems can occur in US mines which are required to use a high resistance grounded system. Coal mines in certain other countries, especially in China, are using a Petersen coil, in lieu of, or in combination with, the NGR to drive the ground fault current to very low values. This is referred to as a resonance grounded system. The Petersen coil, connected between the system neutral and ground, is tuned according to the total system capacitance to drive an inductive current and compensate the system capacitive

charging current. This technique has been developed and implemented in Chinese coal mines for several years and most of the capacitive charging current can be compensated [Wang, 1999]. However, this type of grounding system still works imperfectly. With more and more automation and control systems being introduced into coal mines, power electronic devices also add unwanted harmonics into mine power systems. Harmonics also exist in the power transmission system and are delivered to mine distribution systems, although to a (generally) much smaller degree. Once a ground fault occurs, these harmonics will create non-negligible harmonic components in the ground fault current [Li, 2010]. Moreover, total power system distributed capacitance will vary in some cases, and thus the traditional Peterson Coil which usually has a fixed or manually adjustable inductance, will result in inaccurate compensation.

1.3. Scope of Work

The objective of this research is to design a novel grounding system which can solve the problems with the high-resistance grounding system used in the US, including capacitive charging currents exceeding the NGR current limit, loss of relay selectivity, and the residual harmonic component of ground fault current. Unfortunately, it is not possible to build a hardware prototype due to lack of funding. Consequently, the major design procedure will necessarily be software simulation. Power System CAD (PSCAD/EMTDC) is used in this research to investigate the problems associated with high resistance grounding as well as a novel solution.

The research is performed in the following steps:

1. A PSCAD simulation model of a simplified three-branch mine power system is developed to investigate problems associated with extensive distributed capacitance in high-voltage coal mine distribution systems employing high-resistance grounding. Fault conditions are analyzed by computing voltages and currents in different portions of the distribution system.

2. Harmonic sources are included on the load side of each branch to represent harmonics

created by real-world non-linear loads and control devices. The harmonic content produced will be based on recent research papers and the maximum order set to the thirty-first harmonic. Each order of the fault current (including fundamental) is computed and analyzed by using Fast Fourier Transform (FFT) to predict the harmonic components of the ground fault current.

3. The phase currents in each branch are determined by running the simulation model. The relationship between the faulted phase currents and the ground fault current is analyzed and derived by constructing a corresponding sequence network of the simulation model. Therefore, the fault current, including fundamental and harmonic components, can be predicted so that the magnitude and phase angle of the compensation currents can be determined.

4. A method for injecting compensation current to the system neutral point is developed by combining several power electronic devices to create desired compensating current waveform.

5. Two compensation systems are proposed and discussed based on different compensation strategies. Subsequently, each method is evaluated for potential application to mining. A discussion on fault location detection is also provided. A flowchart of the compensation system operation before and after a single line-to-ground fault is presented.

6. Results, conclusions, and recommendations for future research are provided.

1.4. Dissertation Format

Chapter 2 provides a literature review of topics relevant to this research. It includes the following: (1) a brief overview of the mine power distribution system; (2) different mine distribution system grounding methods and their characteristics; (3) traditional capacitive charging current measurement methods and Peterson coil tuning methods; (4) traditional fault

detection methods; (5) symmetrical component theory and sequence networks; and (6) harmonics in mine power systems.

Chapter 3 presents an analysis of the problems associated with high-resistance grounding as practiced at most US underground coal mines. Problems are demonstrated through simulation models in PSCAD/EMTDC.

Chapter 4 presents a novel method to predict the ground fault contents, including fundamental and harmonics. PSCAD/EMTDC simulation models are developed to verify the new approach.

Chapter 5 presents two current injecting compensation methods based on different grounding systems. PSCAD simulations are performed and results are analyzed to determine the more effective method. A fault identification approach is also introduced and verified by simulation results.

Chapter 6 provides conclusions and recommendations for future work.

CHAPTER 2

LITERATURE REVIEW

2.1. Mine Power Distribution System Overview

2.1.1. Basic Power Distribution System Arrangement

The basic power distribution system commonly used in industries include radial, expanded radial, primary selective, primary loop, secondary selective, and secondary spot network. The expanded radial system is the most commonly used arrangement in coal mine distribution systems [Morley, 1990]. Because of their relevance to this research, only radial and expanded radial systems will be discussed in the dissertation.

2.1.1.1. Radial System

A simple radial system consists of a substation, switchhouses, and mining equipment loads, as shown in Figure 2.1. In this system, electricity is supplied by a single source, usually between 24,000 and 138,000 V, and transformed to the utilization voltage level of 1,000 V or less by the substation to supply the mining equipment loads. Switchhouses are located between the substation and loads to permit branching and protection of the outgoing circuits. Each load is connected to the main bus through a switchhouse, and the main bus in turn is connected to the substation through one or more switchhouses [Anon, 1993; Morley, 1990; Tripathi, 2007].

Radial systems are the least expensive to install because there is no duplication of equipment, and they can be easily expanded by extending the primary feeders. However, due to its simplicity, the entire system could be de-energized if a primary component fails [Morley, 1990].

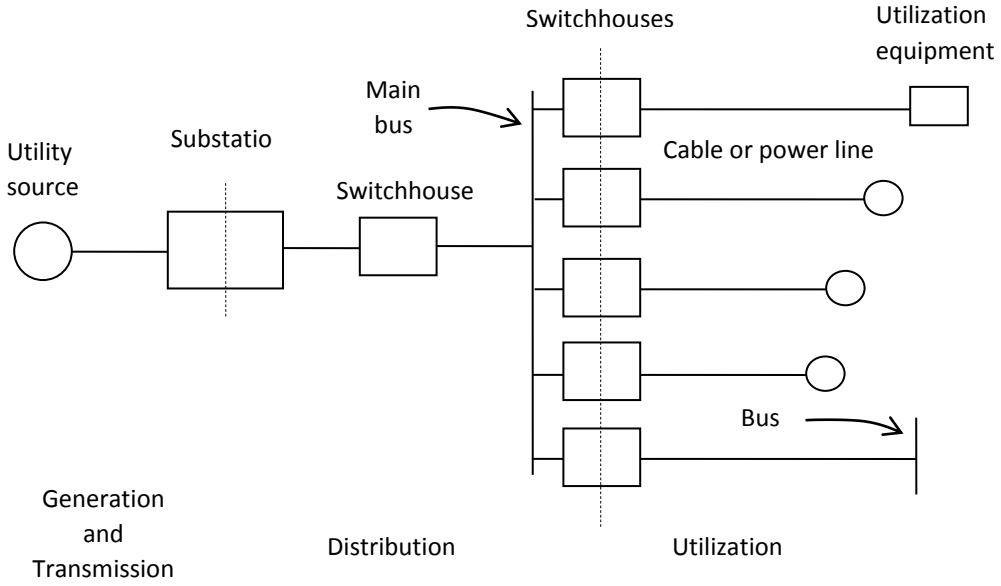

Figure 2.1. Simple radial distribution system [Morley, 1990].

2.1.1.2. Expanded Radial System

An expanded radial system is illustrated in Figure 2.2. In this system, the power source supplies power to each piece of mining equipment load through a substation, one or more switchhouses, and a load center. Power from the utility is transformed to distribution voltages of (commonly) 7,200 V, 12,470 V, 13,200 V, 13,800 V, or 14,400 V and then converted to the utilization level (typically 1,000 V or less) by load centers. Load centers are usually located as close as possible to the mining equipment to minimize voltage drop and losses [Anon, 1993; Morley, 1990; Tripathi, 2007].

In addition to the advantages of simple radial system, the use of an expanded radial system will reduce power loss because of the higher distribution voltage levels. This characteristic also permits the use of smaller power conductors for distribution. However, the cost of an expanded radial system is higher compared with the simple radial system [Morley, 1990].

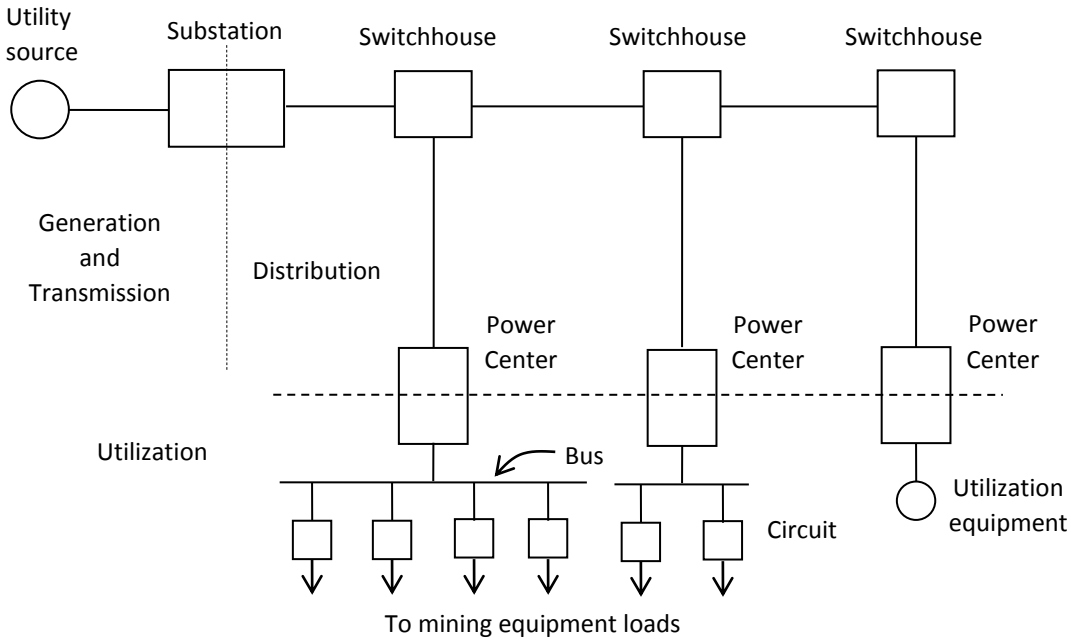

Figure 2.2. Expanded radial distribution system [Morley, 1990].

2.1.2. Mine Power System Components

The major mine power system components are the main substation, switchhouses, power (or load) centers, and power and grounding conductors. Power generation is generally not considered part of a mine power system [Morley, 1990; Sottile and Novak, 2001]. A simplified one-line diagram of a typical underground coal mine power system is illustrated in Figure 2.3.

2.1.2.1. Substation

The primary purposes of the substation are to receive power from the utility and reduce the utility voltage to the distribution voltage level, establish the grounding system, and provide protection for outgoing circuits. The substation also contains equipment for metering and power factor correction. Generally, the voltage level of the power supplied by the utility ranges from 24,000 to 138,000 V, which is transformed to the distribution level of (typically) 7,200

V, 12,470 V, 13,200 V, 13,800 V and 14,400 V. The number and location of substations are determined by the nature of mining operation and total power consumption [Morley, 1990; Tripathi, 2007].

2.1.2.2. Switchhouse

Switchhouses allow branching of the distribution system and provide protection to the outgoing circuits. Switchhouses are usually skid-mounted, metal-clad enclosures. A typical switchhouse consists of disconnect switches, vacuum circuit breakers, surge arresters, and protective relays. Each of the branching circuits has a complete set of protective devices in the switchhouse. A feedthrough circuit without protective devices may also be included in the switchhouse [Morley, 1990].

2.1.2.3. Power Center

Power centers, also termed load centers, are located at the outermost distribution points of a mine power system. They convert the mine distribution voltage level to utilization levels and provide protective circuitry for each outgoing circuit. The typical utilization voltage levels are 480 V, 600 V, 995 V, 1040 V, 2400 V, and 4160 V. The major components of a power center include a power transformer (with fused primary and surge protection), input and output receptacles, disconnect switches, circuit breakers, and protective relays. These components are usually housed in a heavy-duty steel enclosure which are tire, skid or track mounted [Morley, 1990].

2.1.2.4. Other Distribution Components

Other major distribution components consist of overhead power lines, cables, cable couplers, and (rarely) trolley lines used to deliver electricity and maintain grounding throughout the system. Distribution cables are generally called mine power feeder, or feeder, cables, while utilization cables are called portable or trailing cables. Cables are usually considered to be the

weakest (or, at least, the most vulnerable) part of a mine power system as they are subjected to various stresses when the mining equipment advances and retreats with the extraction of rocks/minerals [Morley, 1990].

2.1.3. Example of an Underground Coal Mine Power System

A simplified one-line diagram of an underground coal mine power system is shown in Figure 2.3. 115 kV power from utility is transformed to the 13.8 kV distribution voltage by the main substation transformer. The vacuum circuit breaker (used in 1000V or higher system) located at the substation transformer secondary protects the distribution circuit in case of an overload or fault. A fuse is used to protect the transformer. Surge arresters are located at both transformer primary and secondary to divert transient overvoltages to ground. Visible disconnect switches are used to provide visual assurance when the circuit is disconnected from the source. The substation transformer is delta-wye and the secondary neutral is connected to the safety ground bed through a neutral grounding resistance (NGR). All metal frames within the substation are connected to the station ground bed, while all mining equipment metal frames are connected to the safety ground bed to keep them at, or close to, ground potential during normal or abnormal conditions. Power enters unground by means of a borehole cables and switchhouses permit the system to branch. The power center transformer reduces the 13.8 kV distribution voltage to 995 V utilization voltage and supplies power to the mining equipment. Each outgoing circuit is protected by a circuit breaker. A typical mine power system typically has multiple switchhouses and power centers [Sottile and Novak, 2001].

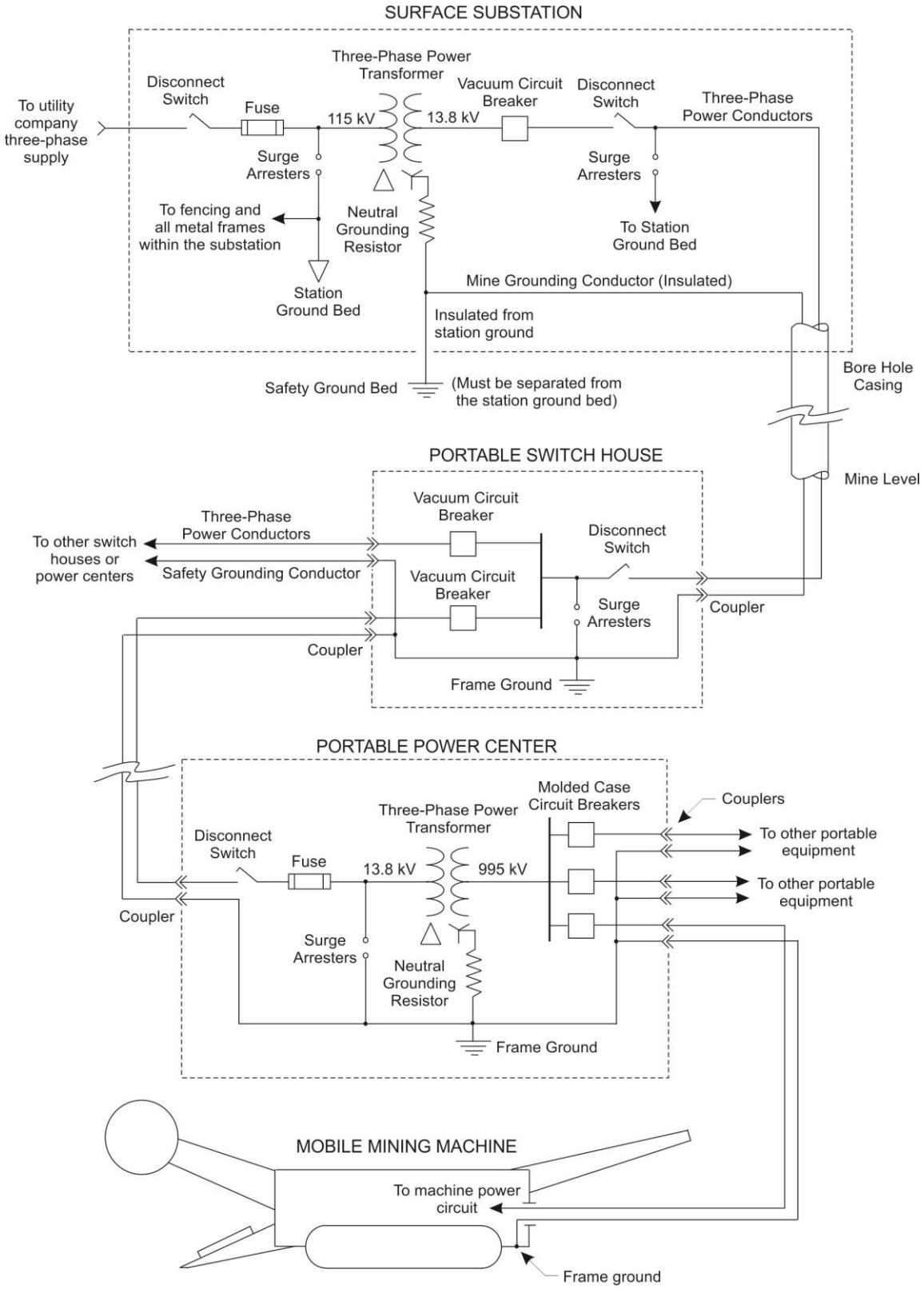

Figure 2.3. Simplified underground coal mine power system [Sottile and Novak, 2001].

2.2. System Grounding

2.2.1. Faults

Several different types of faults that can occur in mine power system include single-line-to-ground, line-to-line, double-line-to-ground, three-phase, and three-phase-to-ground. Power system faults can cause abnormally high current flow with the magnitude depending upon the circuit impedance between source and fault location. For instance, the fault current magnitude will be larger for a fault near the source compared with a fault near a load [Morley, 1990; Nasar and Trutt, 1999].

Faults involving ground are termed ground faults, such as single and double line-to-ground faults. The single-line-to-ground fault occurs most frequently and will be the emphasis of this dissertation. Ground faults can have a wide range of current magnitude and originate in several different ways such as insulation integrity deterioration due to moisture and atmospheric contamination, insulation physical damage due to mechanical stresses, and excessive transient or steady-state voltage stress on insulation. Good installation and maintenance practices ensure proper circuit connection and insulation integrity of cable and equipment, which can significantly reduce the possibility of ground faults occurrence [Amoh, 2006; Anon, 2001; Tripathi, 2007].

2.2.2. Purpose of Grounding

Properly installed, a grounding system can protect personnel from hazard and machinery from damage associated with ground faults and transients [Morley, 1990; Sottile and Novak, 2001]. The major purposes of grounding are listed below:

- **Limit potential gradients and transient overvoltages**

  Metal frames of all electrical mining equipment loads are connected to a common ground to keep them at or near ground potential and minimize the potential gradients between machine frames and ground. In most cases of ground faults, a power conductor comes in contact with the equipment frame, which causes the voltage of the

equipment frame to be equal to the voltage of the faulted power conductor. If a person touches the machine frame while being in contact with the ground, the body potential can be elevated and equal to the equipment frame which is likely to be lethal. When fault currents can flow from the equipment frame back to the source through the low impedance path created by the connection of ground conductors to the equipment frames, the shock hazard is reduced. Moreover, the current rating of the cable conductors, transformer windings, and other power system components may be exceeded due to transient phenomena, including lightning strikes, switching transients, and arcing faults. Stresses by repeated overvoltage exposure may cause deterioration of power system components. Effects of these transient overvoltage phenomena can be reduced by proper grounding of the power system [Amoh, 2006; Morley, 1990; Tripathi, 2007, Yu et al., 1998].

- **Limit energy available at the fault location**

  Large ground fault currents can cause arcing and sparking, which can ignite nearby combustible material or injure personnel close to the fault. The air near the fault can be ionized to carry significant amount of current. Conductors, circuit breakers, and switchgear can melt because of the high fault current, and protective enclosures may be blown apart with explosive force. Controlling the maximum allowable fault current by intentionally inserting an impedance between the ground conductor and the source can eliminate most of the problems mentioned above [Amoh, 2006; Morley, 1990; Tripathi, 2007].

- **Stabilize system voltage**

  Transient phenomena can produce surge voltages several times higher than the normal system voltage if the system is ungrounded. Connecting the distribution system neutral point to ground helps divert the transient overvoltages safely to earth. It can also minimize the effect of unbalanced system voltage conditions [Morley, 1990; Tripathi, 2007].

- **Minimize power disruption by selective relaying**

  A grounding system should be able to isolate the faulted section of a distribution system through selective relaying. Protective circuitry must have sufficient sensitivity and a reliable method of isolating the faulted portion of the power system to clear the fault as soon as possible. In most expanded radial power systems, relay coordination is achieved by using overcurrent relays and time delays to isolate the fault. Improper coordination of the relays can cause nuisance tripping or cause unnecessary removal of power from a large portion of the mine [Amoh, 2006; Morley, 1990; Tripathi, 2007]. As will be described later, the effect of capacitance charging current during a ground fault in a high-resistance grounded system can cause loss of relay coordination.

2.2.3. Types of Grounding Systems

The major types of power system grounding include ungrounded, solidly grounded, resistance grounded, and resonance grounded systems. Variations of these schemes, such as corner-delta grounded and midpoint delta grounded, also exist but are not common. Currently, U.S. coal mines are required to use resistance grounded systems; however, other methods are commonly found in other mining industries.

2.2.3.1. Ungrounded System

In an ungrounded system, no intentional connection exists between any part of the electrical system and ground, as shown in Figure 2.4, except for ground-fault monitoring equipment. However, a completely ungrounded system does not truly exist because each line of the system is actually coupled to ground through the inherent per-phase capacitance of transformer windings, motor windings, and cables. This capacitance is distributed throughout the entire system; however, it is represented as lumped capacitors connected between each power conductor and ground as shown in Figure 2.4. The magnitude of the system capacitance depends on the size of the power system, particularly the length and the type of cable used. For

instance, shielded power cables have much higher values of capacitance compared with unshielded cables. Thus, each power system has its own system capacitance values; even within a given system, the inherent capacitance changes when components are connected or disconnected [Morley, 1990; Sottile and Novak, 2001].

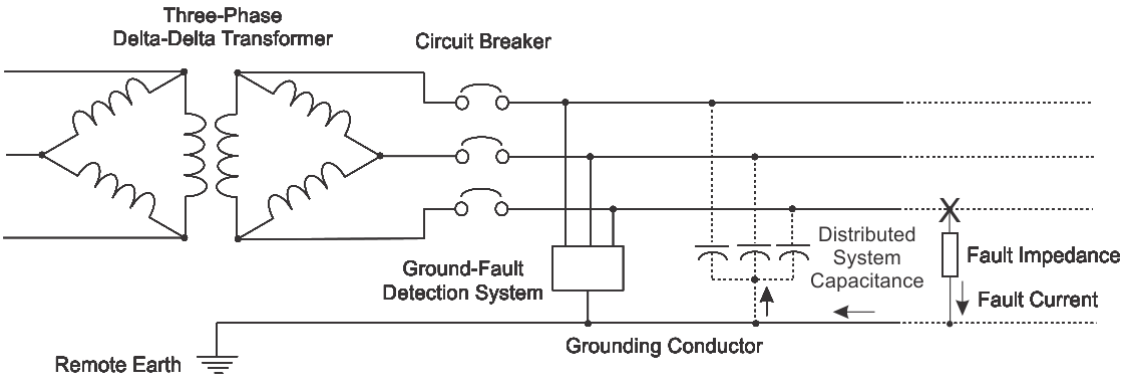

Figure 2.4. Ungrounded system with a line-to-ground fault [Sottile and Novak, 2001].

In an ungrounded system, once a line-to-ground fault occurs, the fault current does not have an intentional return path. As a result, the fault current will flow back to the source (three-phase power transformer), but its magnitude can be very small, such that the system can maintain normal operation without power interruption. However, it is difficult to detect the occurrence of the first ground fault and have automatic tripping of circuit breakers. Therefore, with a single-line-to-round fault, line-to-line voltage is developed between each line and ground. In addition, the second fault (on a different line) will cause significant hazards such as large current flow and arcing damage to the system and equipment. Additionally, the ungrounded system is also subject to insulation failures and shock hazards from transient overvoltages from physical contact with a higher voltage system, switching surges, or intermittent ground faults. The line-to-ground voltage may rise to several times the rated value under the abnormal conditions [Morley, 1990; Sottile and Novak, 2001].

Because capacitance is distributed throughout the entire system and it can be relatively small and variable, the use of ground fault current measurement as a means of ground fault detection is unreliable. Therefore, a ground fault detection unit (shown in Figure 2.4) is typically used to monitor the phase unbalance conditions [Morley, 1990; Sottile and Novak, 2001].

2.2.3.2. Solidly Grounded System

A solidly grounded system is shown in Figure 2.5. The system neutral point is connected to the ground bed without any intentional impedance. With a line-to-ground fault, the fault current will have a large value, and can be easily detected by a relay or circuit breaker. In this case, the system capacitance is essentially shorted by the low-impedance path to the transformer neutral point. However, the large value of ground fault current can result in significant damage to equipment or injury to personnel from arc and flash hazards. Exposed flesh and eyes may be seriously damaged by high temperature and ultraviolet radiation. Secondary injuries, such as cuts, abrasions and hearing loss, can be caused by rapidly increased pressure and loud noise [Morley, 1990; Sottile and Novak, 2001].

In case of a line-to-ground fault, circuit-breaker tripping must be initiated instantaneously that precludes an orderly shutdown of equipment. The equipment frame potential can become elevated by the high current in the grounding conductors creating shock hazards to personnel. However, if the fault impedance is relatively large, the fault will remain undetected unless sensitive ground-fault relaying is added to the normal overcurrent protection [Morley, 1990; Nelson, 2002].

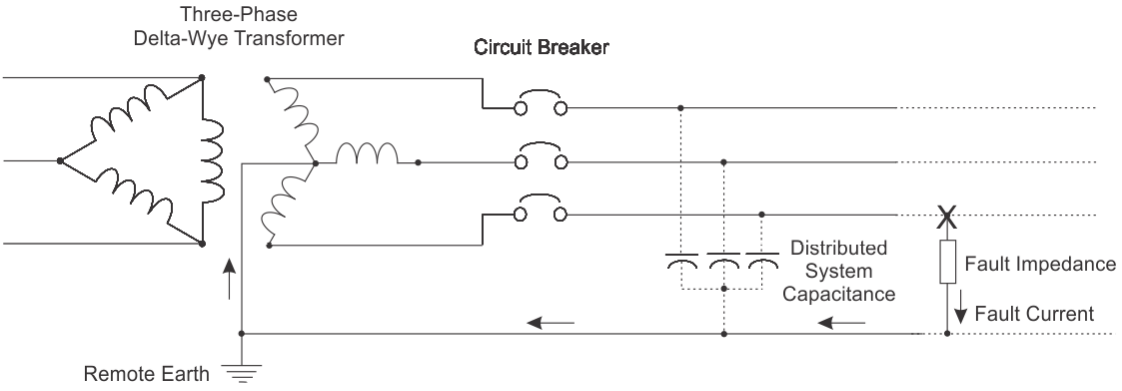

Figure 2.5. Solidly grounded system with a line-to-ground fault [Morley, 1990; Sottile and Novak, 2001].

The solidly grounded system has two major advantages compared with the ungrounded system. Firstly, overvoltages can be controlled because the system is solidly referenced to ground. Secondly, the system is designed to provide automatic ground-fault tripping by the same devices used for line-to-line fault tripping. Sensitive ground-fault relays can be used for low-level arcing ground-fault protection. The main disadvantage of a solidly grounded system is very large ground fault current [Sottile and Novak, 2001].

2.2.3.3. Resistance Grounded System

As described above, a problem associated with a solidly grounded system is the large ground fault current. To protect personnel from injury and equipment from damage, the ground fault current should be limited to low values. Some major reasons for limiting ground-fault current are to [Novak 2001]:

- Reduce electric-shock hazards to personnel caused by elevated frame potentials during a ground fault,
- Reduce the arc blast or flash hazard to personnel who may have accidentally caused, or who happen to be in close proximity to, the ground fault,
- Reduce burning and melting in faulted electric equipment, such as switchgear, transformers, cables, and rotating machines,
- Reduce thermal stress in circuits and devices conducting fault currents,
- Control overvoltages, and
- Reduce the momentary line-voltage dip caused by the occurrence and clearing of a ground fault [Sottile and Novak, 2001; Zipse, 2001].

One of the methods to limit ground fault currents is to use a resistance grounded system. In this type of system, a resistor, generally referred to as a neutral grounding resistor, is inserted between the system neutral point and the grounding conductor, as shown in Figure 2.6.

Two categories of resistance grounding are defined: low-resistance and high-resistance grounding. Low-resistance grounded systems generally limit the maximum ground-fault current to values ranging from 100 A to 1000 A. Due to the connection to earth, overvoltages are controlled and ample fault current is available to activate protective devices. However, personnel can be injured and equipment can be damaged by current within the range mentioned above, although the flash hazard is not as serious as in the solidly grounded system. The least sensitive ground relay has to respond at 10% of maximum ground fault current, which can be fairly high, to limit damage [Morley, 1990].

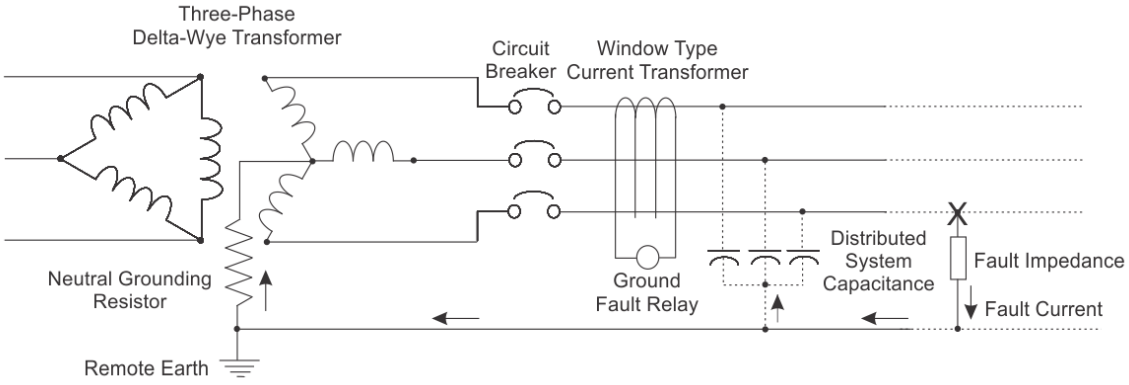

Figure 2.6. Resistance grounded system with a line-to-ground fault [Sottile and Novak, 2001].

In the coal mining industry, high resistance grounded systems generally limit the ground-fault current to 25 A or less. (However, this is actually a misnomer, because it is not truly a ground fault limit. Because ground fault current can also flow back to the source through the system capacitance the NGR current limit is not truly the ground fault limit.) Therefore, not only the amplitude of overvoltage is limited by the ground connection, arcing and flashover danger is reduced by the lower fault current. However, the ground-fault current should not be limited to a value less than the system capacitive charging current; otherwise the system starts to behave like an ungrounded system and acquires some of the undesirable characteristics of an ungrounded system [Novak, 1999; Novak 2001].

In high-resistance grounded systems, the ground-fault current is limited to a value significantly below the pickup setting of the short-circuit protection; therefore, separate ground-fault relaying is required. Zero-sequence relaying is commonly used for ground-fault current detection, as shown in Figure 2.6. The system consists of a single window-type current

transformer (CT) and ground-trip relay. Three power conductors pass through the current transformer window and the resulting current in the CT winding is the vector sum of the three line currents (reduced by the turn's ratio). Under normal conditions, the three line currents are equal in magnitude and 120 °out of phase with each other, which makes the sum of the currents equal to zero (according to Kirchhoff's current law). During a ground fault, the sum of the three line currents is no longer zero, and this resultant current activates the ground-trip relay, which in turn trips the circuit breaker [Trutt and Morley, 1988; Coyle, 2002].

2.2.3.4. Resonance Grounded System

Resonance grounded systems are widely used by utilities in some other countries. In a resonance grounded system, the neutral grounding resistor is replaced by an inductive reactance, typically an inductor, to connect the system neutral point to ground. The inductor is tuned such that its reactance is equal to the absolute value of the capacitive reactance of the system distributed capacitance. With a properly tuned inductor, ground fault current can be driven to a very low value.

A resonance grounded system is shown in Figure 2.7. The variable inductor is generally referred to as a Petersen coil, an arc-suppression coil, or ground-fault neutralizer. (The term Petersen coil will be used for uniformity.) The Petersen coil is most frequently implemented by utilizing a moving-core reactor. In case of a ground fault in the system, the Petersen coil can provide an inductive current with a proper magnitude and angle to compensate the capacitive charging current. If the Petersen coil is properly tuned, the ground fault current, which is the vector sum of the system capacitive charging current and the inductive current provided by the Petersen coil, can be limited to a fairly small magnitude that reduces the arcing possibility and thermal damage at the fault location.

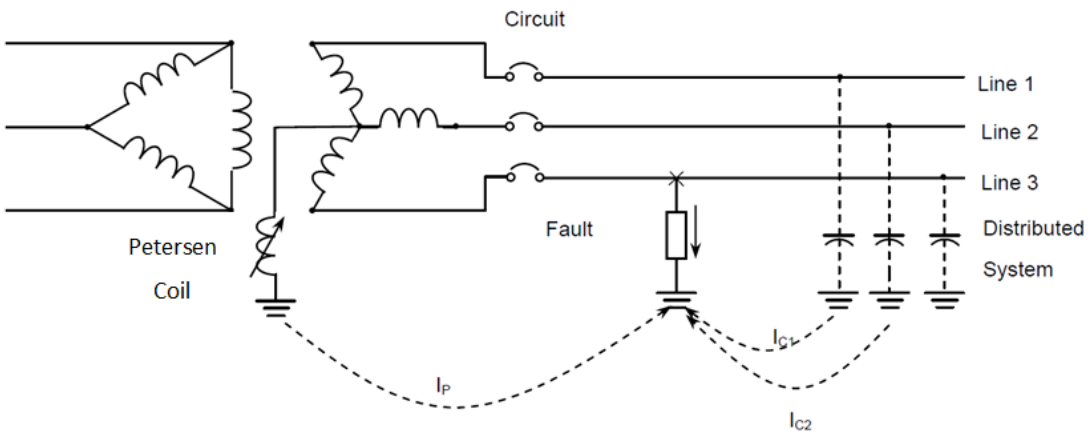

Figure 2.7. Resonance grounded system with a line-to-ground fault [Roberts et al., 2001].

A resonance grounded system has two major advantages compared with other types of system grounding. Firstly, it is able to provide self-extinction of an arc during a ground fault because the transient recovery voltage is limited during the current zero crossing. Another advantage of a resonance grounded system is that it is able to maintain power system operation during a sustained single-line-to-ground fault. Therefore, resonance grounded systems have been widely used in 10kV, or higher, systems in other countries.

As mentioned, resonance grounded systems have some unique and distinct advantages. However, maintaining proper tuning and fault isolation are not straightforward to implement. There are two primary difficulties with this system: (1) the system must be able to automatically measure system capacitance to tune the reactor and (2) fault isolation is difficult because the ground fault is driven to very low values.

In recent years, some variations of resonance grounded systems have been used in the mining industry of other countries, especially in China. Several different system connection methods have been explored and tested. For instance, the use of a Petersen coil connected in parallel with the grounding resistor has the potential to reduce or even eliminate the problems associated with these systems.

2.3. Peterson Coil Tuning

The most important aspect of a resonance grounded system is proper tuning of the Petersen coil to effectively compensate for the capacitance charging current. Several methods have been adopted to implement Petersen coil tuning, including the resonance method (extremum method), the phase angle method, the indirect measuring method, and the additional source method [Du, 2003].

2.3.1. Resonance Method

The principle of the resonance method is to seek the maximum value of the neutral point displacement voltage and calculate the system capacitive current in order to establish the proper tuning point of the Petersen coil. The system neutral point displacement voltage $\dot{V}_0$ can be expressed as [Mu and Meng, 2003; Yao, 2001; Chen et al., 2005]

$$\dot{V}_0 = -\frac{\dot{K}_c \dot{V}_\emptyset}{v - jd} \tag{2.1}$$

with its magnitude

$$\left|\dot{V}_0\right| = \frac{\left|\dot{K}_c\right|\left|\dot{V}_\emptyset\right|}{\sqrt{v^2 + d^2}} \tag{2.2}$$

Where $\dot{V}_\emptyset$ is the source line to neutral voltage at zero degrees (i.e., the reference),

d is the system damping coefficient,

v is the resonance deviation,

$\dot{K}_c$ is the three-phase asymmetry coefficient,

$j = \sqrt{-1} = 1.0\underline{/90°}$

The resonance deviation v and damping coefficient d can be calculated by

$$v = \frac{I_C - I_L}{I_C} \tag{2.3}$$

Where I_C is system capacitive current,

I_L is the system inductive current.

The system damping coefficient d can be expressed as

$$d = \frac{G_g + G_L}{\omega C} \tag{2.4}$$

Where G_g is the total line-to-ground conductance,

G_L is the Petersen coil conductance,

C is the system total distributed line-to-ground capacitance.

The three-phase asymmetry coefficient $\dot{K_c}$ can be calculated by

$$\dot{K_c} = \frac{C_A + a^2 C_B + a C_C}{C_A + C_B + C_C} \tag{2.5}$$

where $a = 1\underline{/120°}$ and C_A , C_B , C_C are the per-phase capacitance values to earth, for each phase (*A*, *B*, and *C*). The magnitude of the three-phase asymmetry coefficient $|\dot{K_c}|$ is determined by the feeder type. In mine power systems, all feeders are cables, which makes $|\dot{K_c}|$ within a range of 0.2%-0.5%. According to EQ 2.1, if a power system has a constant value of $|\dot{K_c}|$ and d, the value of V_0 is determined only by the resonance deviation v. When $v = 0$, $\dot{V}_0$ reaches its maximum value, which is the resonance voltage during full compensation [Yao, 2001].

The resonance deviation v can be calculated as

$$v = \frac{I_C - I_L}{I_C} = \frac{|\dot{V}_\emptyset|/X_C - |\dot{V}_\emptyset|/X_L}{|\dot{V}_\emptyset|/X_C} \tag{2.6}$$

where X_C is the total system capacitive reactance and X_L is the reactance of the Petersen coil. Continuously tuning the Petersen coil, the resonance deviation, v, is equal (or close) to zero when the neutral point displacement voltage $\dot{V}_0$ reaches its maximum value, which means $|X_C| = |X_L|$. The value of system capacitive current can be calculated by $|\dot{V}_\emptyset|/X_C$ [Yao, 2001].

Theoretically, the resonance method is reasonable; however, it has some problems that cannot be ignored. During normal power system operation, because of the low voltage across the

Petersen coil, the measured results will be much different from the fault condition (high voltage across the Petersen coil). Moreover, tuning the Petersen coil to full compensation can result in a high resonance voltages that may cause system damage. Therefore, resonance method is only suitable for small power systems with a low level of unbalance [Du, 2003].

2.3.2. Phase Angle Method

The principle of the phase angle method is to analyze the relationship between the angle of the neutral point displacement voltage θ and the resonance deviation v to achieve Petersen coil tuning. Choose phase A to ground voltage $\dot{V}_A$ as reference. Assuming the three-phase asymmetry confident $\dot{K}_c$ is a real number, then $\dot{V}_A$ can be calculated as [Mu and Meng, 2003]

$$\dot{V}_A = \dot{V}_{\emptyset} + \dot{V}_0 = \frac{v - jd - K_c}{v - jd}\dot{V}_{\emptyset A} \tag{2.7}$$

$$\frac{\dot{V}_0}{\dot{V}_A} = \frac{K_c(K_c - v - jd)}{(v - K_c)^2 + d^2} \tag{2.8}$$

Where $\dot{V}_{\emptyset}$ is the source line to neutral voltage at zero degrees,

$\dot{V}_0$ is the system neutral point displacement voltage.

The angle that $\dot{V}_0$ lags $\dot{V}_A$ is

$$\theta = \arctan\left(\frac{d}{K_c - v}\right) \tag{2.9}$$

Thus, when $v = 0$, the Petersen coil is in full compensation, the lag angle is

$$\theta_1 = \arctan\left(\frac{d}{K_c}\right) \tag{2.10}$$

If $v < 0$, the Petersen coil is in over compensation, $\theta < \theta_1$; if $v > 0$, the Petersen coil is in under compensation, $\theta > \theta_1$. When v is small, the relationship between θ and v can be considered as linear, which means the Petersen coil can be tuned according to the angle of neutral point displacement voltage. However, for an actual power system, even if the capacitive current is not changing, the angle θ still varies significantly to cause errors in Petersen coil

tuning. In order to fix this problem, it is required to have an additional capacitor installed with its value and location determined by the characteristics of the power system. Moreover, this additional capacitor will also increase the asymmetry of the power system, so that the phase angle method is limited in many practical situations [Li, 1993]

2.3.3. Indirect Measuring Method

The indirect measuring method is to tune the Petersen coil by calculating the system capacitive current in an indirect way. By changing the inductance of the Petersen coil, the voltage across it will change, as well as the current. The value and angle of the voltage and current can be measured, and the capacitive current can be indirectly calculated to achieve Petersen coil tuning [Du, 2003].

According to EQ 2.6,

$$v = \frac{|\dot{V}_{\emptyset}|/X_C - |\dot{V}_{\emptyset}|/X_L}{|\dot{V}_{\emptyset}|/X_C} = \frac{I_C - I_L}{I_C} = \frac{X_L - X_C}{X_L} \tag{2.11}$$

In EQ 2.11, the Petersen coil reactance X_L is known, but X_C is unknown; therefore the resonance deviation cannot be calculated directly. However, it can be indirectly calculated by using the relationship between the zero-sequence impedance triangle and the current angle. The equivalent circuit and the impedance triangle are shown in Figure 2.8. Ignoring the system damping coefficient, a neutral grounding resistor R_N is added in series with the Petersen coil. Assuming the Petersen coil has two taps T_1 and T_2, when the tap is in the T_1 position, the reactance of the Petersen coil is X_{L1}, the current is $\dot{I}_{01}$, and the impedance is $\dot{Z}_1 = \dot{V}_{ub}/\dot{I}_{01}$ ($\dot{V}_{ub}$ is the inherent unbalanced voltage of the power system); when the tap is in T_2 position, the reactance is X_{L2}, the current is $\dot{I}_{02}$, and the impedance is $\dot{Z}_2 = \dot{V}_{ub}/\dot{I}_{02}$.

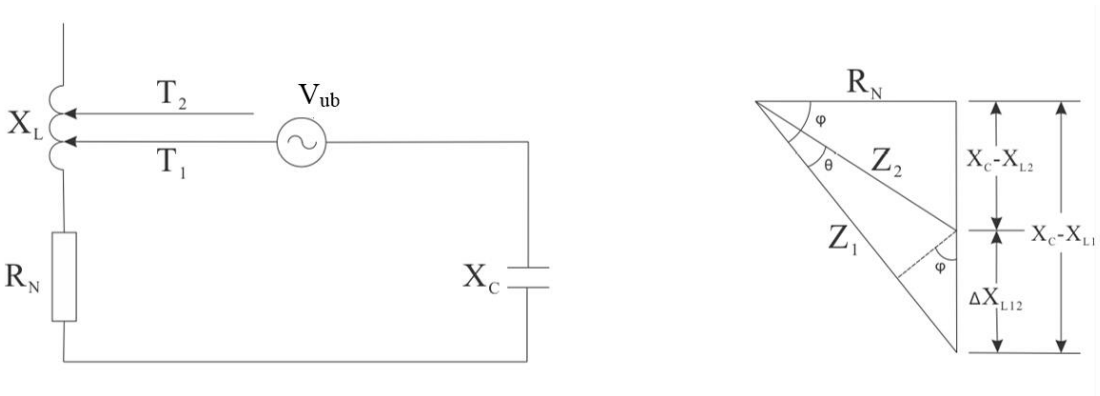

Figure 2.8. The equivalent circuit and impedance triangle of the indirect measuring method [Mu and Meng, 2003].

According to Figure 2.8, the cosine of angle φ can be calculated as

$$cos\varphi = \frac{Z_2}{\Delta X_{L12}} sin\theta \tag{2.12}$$

$$cos\varphi = \frac{R_N}{Z_1} \tag{2.13}$$

multiplying EQ 2.12 and EQ 2.13

$$cos^2\varphi = \frac{Z_2 R_N}{\Delta X_{L12} Z_1} sin\theta = \frac{I_{01} R_N}{\Delta X_{L12} I_{02}} sin\theta \tag{2.14}$$

The angle φ can be calculated by EQ 2.14 after measuring the reactance difference ΔX_{L12} and the angle difference of current I_{01} and I_{02}. From the impedance triangle, it is easy to get

$$X_C - X_{L1} = R_N tan\varphi \tag{2.15}$$

so that

$$v = \frac{X_L - X_C}{X_L} = -\frac{R_N}{X_{L1}} tan\varphi \tag{2.16}$$

Assuming v_1 is the resonance deviation when the Petersen coil tap stays at T_1 position, it can be calculated by EQ 2.16. Compared with the default setting v_0, if $|v_1 - v_0| \leq \varepsilon$ (ε is the allowed resonance deviation error), the Petersen coil tap does not need adjustment; if

$|v_1 - v_0| > \varepsilon$, the tap needs to be adjusted according to the sign of $v_1 - v_0$ [Mu and Meng, 2003].

According to the analysis presented above, the system damping coefficient is ignored so that it is necessary to consider the system conditions before using this method. Meanwhile, the reactance at each tap point needs to be measured, so it is also necessary to consider the Petersen coil distortion problem when its terminal voltage is quite low [Mu and Meng, 2003].

2.3.4. Additional Source Method

As the name implies, this method involves the addition of an additional source into the Petersen coil through a transformer to indirectly reflect the impedance changes of the system zero sequence circuit. The additional source method is divided into two major types: additional voltage source and addition current source [Mu and Meng, 2003].

2.3.4.1. Additional voltage source method

The principle of this method is to use an additional voltage source to generate a zero sequence voltage and current; and the Petersen coil can be tuned by measuring the phase angle between the generated voltage and current. The system schematic is shown in Figure 2.9. *V* is the additional voltage source and *I* is its current. T is the grounding transformer which is used in some systems to derive a system neutral point, and L is the inductance of the Petersen coil. R and C are the lumped resistance and capacitance of the distributed system.

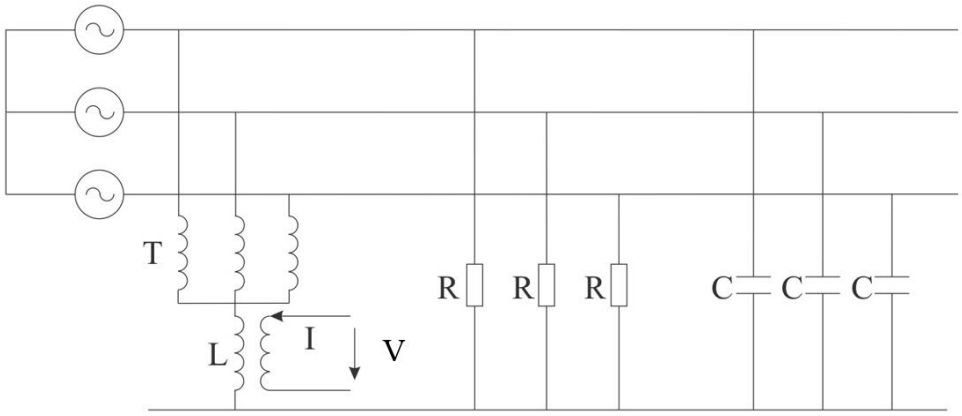

Figure 2.9. The additional voltage source method system schematic [Mu and Meng, 2003].

The voltage source generates a voltage V' on the Petersen coil; it can be treated as a zero sequence voltage and creates the zero sequence current I_0. Ignoring the leakage reactance of the Petersen coil primary and secondary windings, the equivalent circuit can be represented as shown in Figure 2.10.

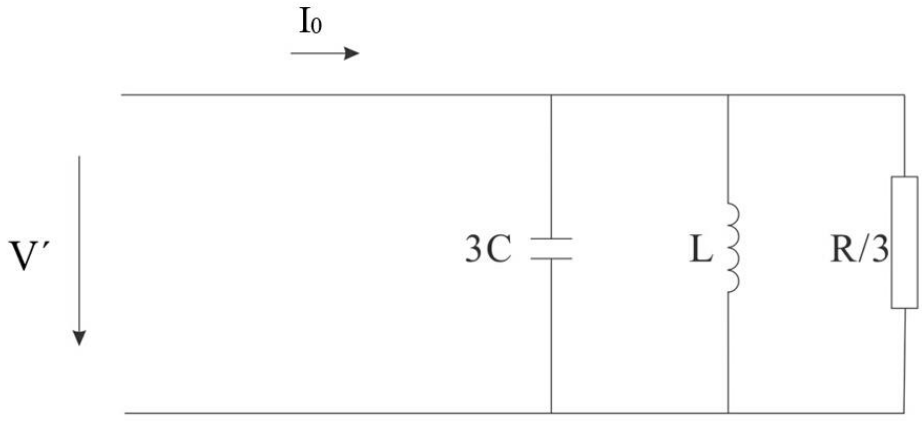

Figure 2.10. The additional voltage source method equivalent circuit [Mu and Meng, 2003].

According to the equivalent circuit above, the current I_0 has the same angle as the voltage V' when $\omega L = 1/(3\omega C)$. In this case, the circuit is in the condition of parallel resonance and the Petersen coil is in full compensation. When $\omega L < 1/(3\omega C)$, the current I_0 lags the voltage V',

and the Petersen coil is over compensating. When $\omega L > 1/(3\omega C)$, the current I_0 leads the voltage V', and the Petersen coil is under compensating. Therefore, if the angle between the voltage and current can be limited to within a certain range by adjusting the inductance of the Petersen coil, Petersen coil tuning can be achieved [Mu and Meng, 2003].

However, this method also has some disadvantages. A major one is that the system asymmetry may affect the Petersen coil adjustment accuracy. According to the previous analysis, the neutral point displacement voltage $\dot{V}_0$ will be large if the Petersen coil is connected between the system neutral and ground (as calculated by EQ 2.1 and EQ 2.2. Therefore, the measured zero sequence current I_0 becomes the result of both the neutral point displacement voltage $\dot{V}_0$ and the voltage source V'. In order to minimize the influence of $\dot{V}_0$, V' must be much higher than $\dot{V}_0$ on the Petersen coil. But a very large value V' will cause asymmetry of the voltage on each phase. Although it would not affect the power supply to each load, it still has some effect on the system and equipment insulation, and can even result in false tripping of protective devices. These issues have to be considered before using this method [Mu and Meng, 2003].

2.3.4.2. Additional current source method

As the name implies, this method uses a current source instead of a voltage source. A current with a variable frequency (30~65 Hz) is injected into the system through a zero sequence potential transformer as part of the Petersen coil, and the feedback signal is received by the Petersen coil tuning controller. When the Petersen coil and the system capacitance are in resonance at a certain injecting current frequency, the resonance deviation v and the system capacitive current can be calculated. The schematic of the additional current source method is shown in Figure 2.11, where I_{if} is the additional current source, and C and R are the per-phase system ground capacitance and resistance, respectively (assuming three-phase-symmetry). Figure 2.12 shows the system equivalent circuit, where X_1 and X_2 are the leakage reactance at the primary and secondary windings of the potential transformer, and R_L represents the resistance of the Petersen coil [Mu and Meng, 2003].

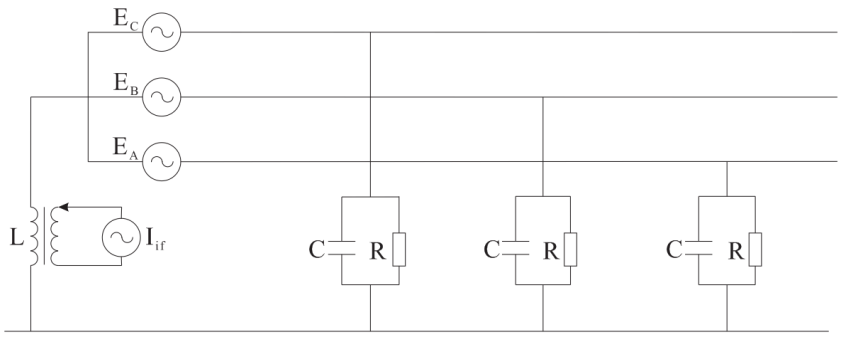

Figure 2.11. The additional current source method schematic [Mu and Meng, 2003].

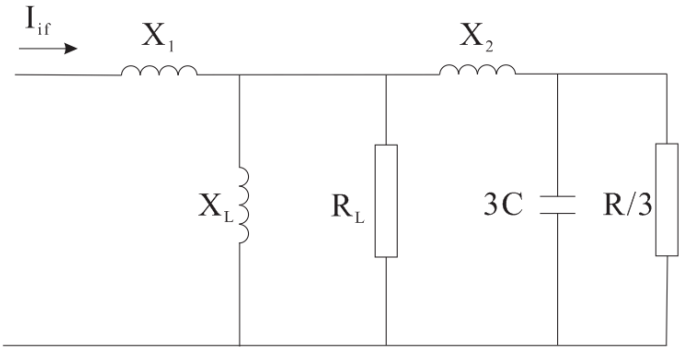

Figure 2.12. The additional current source method equivalent circuit [Mu and Meng, 2003].

In the system equivalent circuit, X_2 is very small and can be neglected; X_1 can also be neglected because it does not affect the measurements; R_L and $R/3$ only have a damping effect on the circuit. Thus, the equivalent circuit can be simplified to the Petersen coil inductive reactance, X_L, in parallel with system three-phase ground capacitance $3C$ [Mu and Meng, 2003].

By continuously changing the injected current frequency until the system is in resonance, the system resonant frequency, f_0, can be determined and the system capacitance can be determined as:

$$3C = \frac{1}{\omega_0^2 L} \tag{2.17}$$

where the system resonance angular frequency is $\omega_0 = 2\pi f_0$. The system capacitive current can be calculated as

$$I_C = 3V_{\emptyset}\omega C = \frac{\omega}{\omega_0^2 L}V_{\emptyset} \tag{2.18}$$

where the system angular frequency $\omega = 2\pi f$ and f is the system frequency; $V_{\emptyset}$ is the phase voltage. According to EQ 2.3, the resonance deviation can be calculated as

$$v = \frac{I_C - I_L}{I_C} = \frac{\frac{\omega}{\omega_0^2 L} - \frac{1}{\omega L}}{\frac{\omega}{\omega_0^2 L}} = 1 - \left(\frac{\omega_0}{\omega}\right)^2 = 1 - \left(\frac{f_0}{f}\right)^2 \tag{2.19}$$

Generally, this method applies to power systems with a low asymmetry coefficient. However, the accuracy of the Petersen coil tuning depends highly on the injecting signal accuracy. And, when the injecting frequency is close to the system frequency, it becomes difficult to achieve accurate Petersen coil tuning [Mu and Meng, 2003].

2.4. Fault Location Detection in Resonance Grounded System

When a line-to-ground fault occurs, it is expected that the faulted section can be detected and removed correctly and quickly. Inaccurate fault location detection will cause improper relay pickup which can remove several unfaulted branches or maintain a faulted branch in the system. In resonance grounded systems, several different types of fault detection methods are currently used, including fifth-order harmonic method, signal injection method, and active component method.

2.4.1. Fifth-Order Harmonic Method

In a resonance grounded system, once a line-to-ground fault occurs, zero-sequence currents which are generated by zero-sequence voltage, have several high order harmonics and the major component is the fifth-order harmonic. It has the same distribution as fundamental of the zero-sequence current in the system. Assume the system ground capacitance remains constant, according to the equation $X_C = 1/(2\pi f C)$, the capacitive reactance is inversely

proportional to the order of harmonics. Because the fifth-order harmonic frequency is five times the fundamental, the capacitive reactance becomes one fifth of that for the fundamental frequency; meanwhile the fifth-order harmonic component of the capacitive current becomes five times the fundamental frequency. In contrast, according to $X_L = 2\pi fL$, the inductive reactance is proportional to the order of harmonics, which makes the fifth-order harmonic component of the compensated inductive current one fifth of that for the fundamental. Thus, for the fifth-order harmonic component, the compensated inductive current is twenty-five times less than the capacitive current and can be neglected. Therefore, the faulted branch can be determined by the value of the fifth-order harmonic component of the zero-sequence current [Hao and Zhan, 2010]

However, the fifth-order harmonic component is a small portion of the entire zero-sequence current; and it may be affected by the current transformer asymmetric currents, some transition resistors, and some rectifying devices. In this case, both faulted branches and unfaulted branches will have harmonic currents that may cause incorrect fault detection [Ai, 2011].

2.4.2. Signal Injection Method

Instead of using the feedback signal of the faulted branch, the signal injection method is actively injecting a current signal through the Petersen coil and tracking and measuring its feedback in order to achieve fault detection. When a line-to-ground fault occurs, the injected current only flows through the faulted branch and goes to ground at the fault location. Early application of this method used a constant frequency current signal, but it caused some incorrect detection in situations where the ground fault resistance was high. Subsequently, a new model of this method has been developed. Instead of injecting a constant frequency signal, variable frequency signals are used to improve the detection accuracy. Two signals of different frequency are injected into the system through the Petersen coil or the grounding transformers (each phase is connected to ground through a potential transformer) on the faulted phase which is determined depending on the value of the neutral point displacement voltage. Signal receivers are installed in each branch to monitor and measure the factors of the zero-sequence current signal, including phase angle and damping coefficient variation. After comparing the

damping coefficient of each branch and considering the factor of feeder moisture and aging, the fault location and can be obtained by analysis [Fu and Wan, 2002; Xue et al., 2007].

Several issues have to be considered when the signal injection method is applied. If the power of the injected signal is small, the signal converted to the transformer secondary winding will be too weak to be monitored and measured. Moreover, the signal generating device is expensive and difficult to maintain [Fu and Wan, 2002].

2.4.3. Active Component Method

During a line-to ground fault, the fault current will have an active component and a reactive component. Generally, the active component is generated by the system ground conductance and the Petersen coil resistance. The current in the unfaulted branches and the Petersen coil will flow in the same direction, while the current on the faulted branch has a larger value and flows in the opposite direction. Thus, based on the zero-sequence voltages and currents, the faulted branch can be determined by calculating and comparing the zero-sequence real power of each branch. Another application of this method is to determine the faulted branch by calculating the zero-sequence conductance. For unfaulted branches, the calculated conductance is the inherent leakage conductance; while the faulted branch conductance has negative polarity and larger value than its inherent leakage conductance [Xue et al., 2007].

However, in some situations, the measurements may not be sufficient to detect the ground fault. Accuracy is affected by current transformer asymmetry, feeder distance and the value of transition resistors [Mu, 1999].

Besides the three most popular methods mentioned above, some other methods also exist, including the current increment method, first half-wave method, traveling wave method, energy function method, and intelligence method. Each of these methods has its own characteristics and application environment and it is significant to choose a proper method based on system conditions [Xue et al., 2007].

2.5. Symmetrical Components and Sequence Networks

2.5.1. Introduction

When dealing with power system fault problems, balanced faults, such as three-phase or three-phase to ground faults, can be analyzed by using single-phase equivalent circuits. However, unbalanced systems caused by unsymmetrical faults such as line-to-line or single-line-to ground faults cannot be solved by a per phase basis due to the loss of system symmetry. Under this circumstance, a method termed symmetrical components is commonly used to deal with unbalanced polyphase circuits. This theory, developed by C.L. Fortesque in 1918 [Fortesque, 1918], proves that a three-phase unbalanced system can be resolved into three systems of balanced phasors, named the symmetrical components of the original phasors, and the system can be represented by three single-phase equivalent sequence network [Granger and Stevenson, 1994]. Thus, the fault and unbalanced condition of a three phase power system can be represented by connecting the sequence networks in a particular manner in order to perform system voltage and current calculations [Nasar and Trutt, 1999; Stevenson, 1982].

The method of symmetrical components, seen as the language of relay engineer or technician, plays a significant role in power system analysis and protection. It is very useful to have a good understanding of this theory because it is not only an invaluable tool in power system protection, but it also provides a convenient way to visualize and analyze system unbalances using system parameters [Tripathi, 2007, Blackburn, 1993, 1997].

2.5.2. Conversion Between Unsymmetrical Phasors and Symmetrical Components

According to the symmetrical component theory, any set of three unbalanced phasors in a three-phase power system can be resolved into three sets of balanced phasors, identified as follows:

- Positive-sequence components: three phasors have an identical magnitude and are displaced from each other by 120 º, and the phase sequence follows the original phasors (i.e., a-b-c);

- Negative-sequence components: three phasors have an identical magnitude and are displaced from each other by 120 º, and the phase sequence is opposite to that of the original phasors (i.e., a-c-b);

- Zero-sequence components: three phasors have an identical magnitude, the phase displacement from each other is zero.

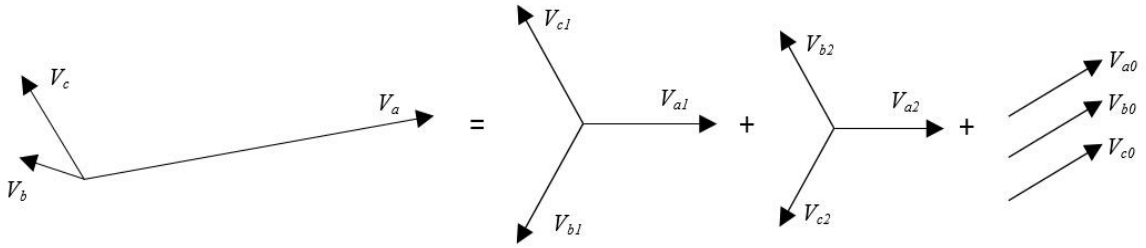

Figure 2.13. Unbalanced phasors and three sets of symmetrical components [Nasar and Trutt, 1999].

Figure 2.13 shows an unbalanced three-phase system and three sets of symmetrical components [Nasar and Trutt, 1999]. The components with subscript 1, 2 and 0 represent the sets of positive-sequence, negative-sequence and zero-sequence components, respectively. The synthesis of three unsymmetrical phasors from three sets of symmetrical phasors is shown in Figure 2.14 [Nasar and Trutt, 1999; Stevenson, 1982].

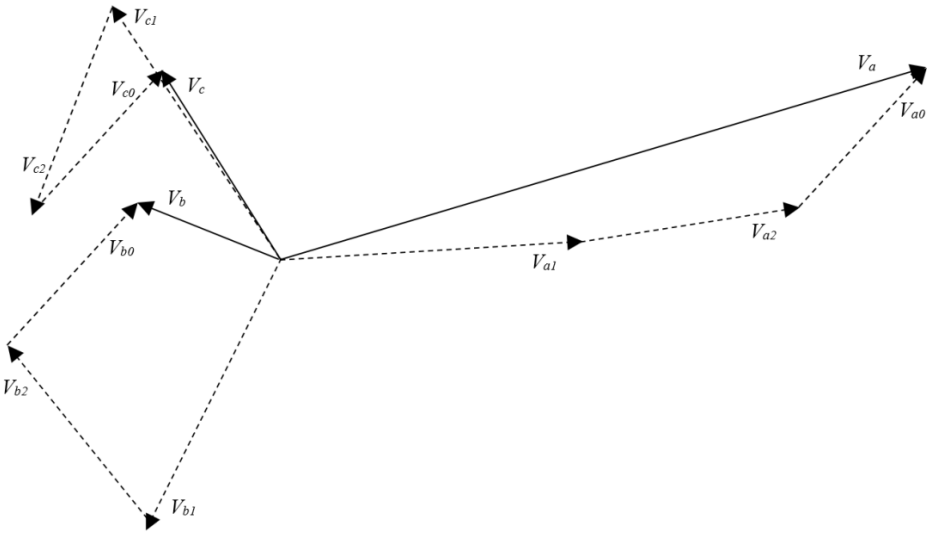

Figure 2.14. Graphical addition of the symmetrical components to obtain the three-phase unbalanced voltage phasors [Nasar and Trutt, 1999].

It is observed in Figure 2.14 that each of the original unbalanced phasors is the summation of its sequence components; thus, the original phasors can be expressed in terms of their sequence components as follows:

$$\begin{aligned} V_a &= V_{a0} + V_{a1} + V_{a2} \\ V_b &= V_{b0} + V_{b1} + V_{b2} \\ V_c &= V_{c0} + V_{c1} + V_{c2} \end{aligned} \tag{2.20}$$

In a perfect three-phase balanced system, three phasors A, B and C are composed of only positive sequence components with equal magnitude and 120 °phase displacement. Negative sequence components in a power system reflect the level of system unbalance. Power system faults and unbalances involving neutral or ground are indicated by zero-sequence components. For instance, currents flow through neutral to ground are directly related to zero-sequence currents [Nasar and Trutt, 1999].

To reduce the number of unknown quantities in EQ 2.20, V_b and V_c can be expressed as a product of a component of V_a and some function of the operator $a = \underline{1/120°}$, which causes a

counterclockwise rotation of a phasor by 120 º[Miller and Malinowski, 1994; Grainger and Stevenson, 1994]. Reference to Figure 2.13 verifies the following equations:

$$V_{b0} = V_{a0} \qquad V_{c0} = V_{a0}$$

$$V_{b1} = a^2 V_{a1} \qquad V_{c1} = aV_{a1} \tag{2.21}$$

$$V_{b2} = aV_{a2} \qquad V_{c2} = a^2 V_{a2}$$

Substituting EQ 2.21 into EQ 2.20, the equations become as follows:

$$\begin{aligned} V_a &= V_{a0} + V_{a1} + V_{a2} \\ \mathrm{V_b} &= \mathrm{V_{a0}} + \mathrm{a^2 V_{a1}} + \mathrm{a V_{a2}} \\ \mathrm{V_c} &= \mathrm{V_{a0}} + \mathrm{a V_{a1}} + \mathrm{a^2 V_{a2}} \end{aligned} \tag{2.22}$$

or in matrix form as:

$$\begin{bmatrix} V_a \\ V_b \\ V_c \end{bmatrix} = \begin{bmatrix} 1 & 1 & 1 \\ 1 & a^2 & a \\ 1 & a & a^2 \end{bmatrix} \begin{bmatrix} V_{a0} \\ V_{a1} \\ V_{a2} \end{bmatrix} \tag{2.23}$$

Similarly, the relationship between current phasors and their symmetrical components can be obtained as:

$$\begin{bmatrix} I_a \\ I_b \\ I_c \end{bmatrix} = \begin{bmatrix} 1 & 1 & 1 \\ 1 & a^2 & a \\ 1 & a & a^2 \end{bmatrix} \begin{bmatrix} I_{a0} \\ I_{a1} \\ I_{a2} \end{bmatrix} \tag{2.24}$$

The sequence components can be extracted from the phasors as follows:

$$\begin{bmatrix} V_{a0} \\ V_{a1} \\ V_{a2} \end{bmatrix} = \left(\frac{1}{3}\right) \begin{bmatrix} 1 & 1 & 1 \\ 1 & a & a^2 \\ 1 & a^2 & a \end{bmatrix} \begin{bmatrix} V_a \\ V_b \\ V_c \end{bmatrix} \tag{2.25}$$

$$\begin{bmatrix} I_{a0} \\ I_{a1} \\ I_{a2} \end{bmatrix} = \left(\frac{1}{3}\right) \begin{bmatrix} 1 & 1 & 1 \\ 1 & a & a^2 \\ 1 & a^2 & a \end{bmatrix} \begin{bmatrix} I_a \\ I_b \\ I_c \end{bmatrix} \tag{2.26}$$

2.5.3. Sequence Impedances

In power system analysis, the symmetrical component theory not only involves currents and voltages, but also impedance. In any part of a circuit, the relationship between currents and voltages of a certain sequence depends upon the related impedance of the same sequence. For different current sequence components, the system impedance could be different. The impedance which positive-sequence currents flow though is called positive-sequence impedance; similarly, impedance which negative-sequence and zero-sequence currents flow through are called negative-sequence and zero-sequence impedance, respectively [Nasar and Trutt, 1999; Stevenson, 1982].

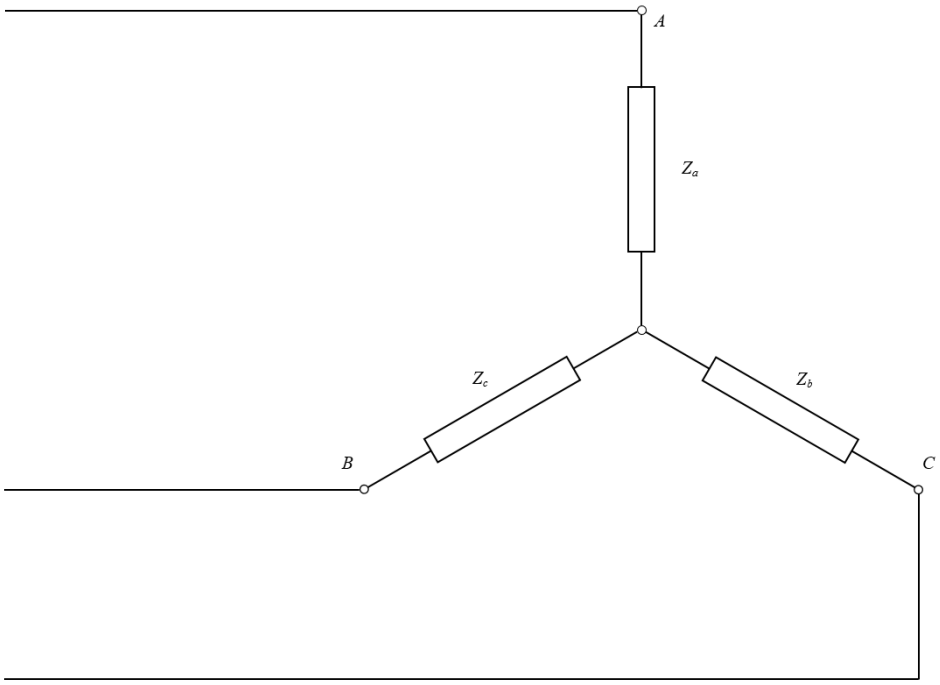

Figure 2.15. General wye-connected three-phase circuit [Stevenson, 1982].

Figure 2.15 shows a typical three-phase load with three impedance Z_a, Z_b and Z_c connected in wye. Phase A impedance Z_a has three components Z_{a0}, Z_{a1} and Z_{a2} which represent zero-sequence, positive sequence and negative sequence impedance, respectively. Similar quantities can be obtained for phase B and C. According to the principle mentioned above, relationships between the voltage, current and impedance of each sequence can be indicated by the following equations:

$$V_a = Z_{a0} \times I_{a0} + Z_{a1} \times I_{a1} + Z_{a2} \times I_{a2}$$

$$V_b = Z_{b0} \times I_{b0} + Z_{b1} \times I_{b1} + Z_{b2} \times I_{b2} \quad (2.27)$$

$$V_c = Z_{c0} \times I_{c0} + Z_{c1} \times I_{c1} + Z_{c2} \times I_{c2}$$

As EQ 2.21 also applies to currents, then the relationships above become as:

$$V_a = Z_{a0} \times I_{a0} + Z_{a1} \times I_{a1} + Z_{a2} \times I_{a2}$$

$$V_b = Z_{b0} \times I_{a0} + a^2 Z_{b1} \times I_{a1} + aZ_{b2} \times I_{a2} \quad (2.28)$$

$$V_c = Z_{c0} \times I_{a0} + aZ_{c1} \times I_{a1} + a^2 Z_{c2} \times I_{a2}$$

substituting EQ 2.22, we get

$$V_{a0} + V_{a1} + V_{a2} = Z_{a0} \times I_{a0} + Z_{a1} \times I_{a1} + Z_{a2} \times I_{a2}$$

$$\mathrm{V_{a0}} + \mathrm{a^2 V_{a1}} + \mathrm{a V_{a2}} = Z_{b0} \times I_{a0} + a^2 Z_{b1} \times I_{a1} + aZ_{b2} \times I_{a2} \quad (2.29)$$

$$\mathrm{V_{a0}} + \mathrm{a V_{a1}} + \mathrm{a^2 V_{a2}} = Z_{c0} \times I_{a0} + aZ_{c1} \times I_{a1} + a^2 Z_{c2} \times I_{a2}$$

or in matrix as:

$$\begin{bmatrix} 1 & 1 & 1 \\ 1 & a^2 & a \\ 1 & a & a^2 \end{bmatrix} \times \begin{bmatrix} V_{a0} \\ V_{a1} \\ V_{a2} \end{bmatrix} = \begin{bmatrix} Z_{a0} & Z_{a1} & Z_{a2} \\ Z_{b0} & a^2 Z_{b1} & aZ_{b2} \\ Z_{c0} & aZ_{c1} & a^2 Z_{c2} \end{bmatrix} \times \begin{bmatrix} I_{a0} \\ I_{a1} \\ I_{a2} \end{bmatrix} \quad (2.30)$$

So that

$$\begin{bmatrix} V_{a0} \\ V_{a1} \\ V_{a2} \end{bmatrix} = \frac{\begin{bmatrix} Z_{a0} & Z_{a1} & Z_{a2} \\ Z_{b0} & a^2 Z_{b1} & aZ_{b2} \\ Z_{c0} & aZ_{c1} & a^2 Z_{c2} \end{bmatrix}}{\begin{bmatrix} 1 & 1 & 1 \\ 1 & a^2 & a \\ 1 & a & a^2 \end{bmatrix}} \times \begin{bmatrix} I_{a0} \\ I_{a1} \\ I_{a2} \end{bmatrix} \quad (2.31)$$

or, using a parameter δ to simplify the equation as:

$$\begin{bmatrix} V_{a0} \\ V_{a1} \\ V_{a2} \end{bmatrix} = \begin{bmatrix} \delta_{00} & \delta_{21} & \delta_{12} \\ \delta_{10} & \delta_{01} & \delta_{22} \\ \delta_{20} & \delta_{11} & \delta_{02} \end{bmatrix} \times \begin{bmatrix} I_{a0} \\ I_{a1} \\ I_{a2} \end{bmatrix} \tag{2.32}$$

or in equation form as:

$$\begin{aligned} V_{a0} &= \delta_{00} \times I_{a0} + \delta_{21} \times I_{a1} + \delta_{12} \times I_{a2} \\ V_{a1} &= \delta_{10} \times I_{a0} + \delta_{01} \times I_{a1} + \delta_{22} \times I_{a2} \\ V_{a2} &= \delta_{20} \times I_{a0} + \delta_{11} \times I_{a1} + \delta_{02} \times I_{a2} \end{aligned} \tag{2.33}$$

where

$$\delta_{00} = \frac{Z_{a0} + Z_{b0} + Z_{c0}}{3} \quad \delta_{21} = \frac{Z_{a1} + a^2 Z_{b1} + a Z_{c1}}{3} \quad \delta_{12} = \frac{Z_{a2} + a Z_{b2} + a^2 Z_{c2}}{3}$$

$$\delta_{10} = \frac{Z_{a0} + a Z_{b0} + a^2 Z_{c0}}{3} \quad \delta_{01} = \frac{Z_{a1} + Z_{b1} + Z_{c1}}{3} \quad \delta_{22} = \frac{Z_{a2} + a^2 Z_{b2} + a Z_{c2}}{3} \tag{2.34}$$

$$\delta_{20} = \frac{Z_{a0} + a^2 Z_{b0} + a Z_{c0}}{3} \quad \delta_{11} = \frac{Z_{a1} + a Z_{b1} + a^2 Z_{c1}}{3} \quad \delta_{02} = \frac{Z_{a2} + Z_{b2} + Z_{c2}}{3}$$

A symmetrical, three-phase rotating machine has balanced impedances, but a different impedance to each sequence component of current, as:

$$\begin{aligned} Z_{a0} = Z_{b0} = Z_{c0} = Z_0 = \delta_{00} \\ Z_{a1} = Z_{b1} = Z_{c1} = Z_1 = \delta_{01} \\ Z_{a2} = Z_{b2} = Z_{c2} = Z_2 = \delta_{02} \end{aligned} \tag{2.35}$$

Thus, we get

$$\begin{bmatrix} V_{a0} \\ V_{a1} \\ V_{a2} \end{bmatrix} = \begin{bmatrix} \delta_{00} & 0 & 0 \\ 0 & \delta_{01} & 0 \\ 0 & 0 & \delta_{02} \end{bmatrix} \times \begin{bmatrix} I_{a0} \\ I_{a1} \\ I_{a2} \end{bmatrix} \tag{2.36}$$

or,

$$\begin{bmatrix} V_{a0} \\ V_{a1} \\ V_{a2} \end{bmatrix} = \begin{bmatrix} Z_0 & 0 & 0 \\ 0 & Z_1 & 0 \\ 0 & 0 & Z_2 \end{bmatrix} \times \begin{bmatrix} I_{a0} \\ I_{a1} \\ I_{a2} \end{bmatrix} \tag{2.37}$$

Thus, it is shown that the sequence components are independent of each other in this case.

2.5.4. Sequence Network of an Unloaded Three-phase Voltage Source

A circuit diagram of an unloaded three-phase voltage source is shown in Figure 2.16. The source neutral is grounded through an impedance Z_n, and the generated voltage is in positive sequence only since it supplies balanced three-phase voltages. Therefore, the positive sequence network consists of the positive-sequence voltage source in series with the positive-sequence impedance, while negative and zero sequence networks only contain negative-sequence and zero-sequence impedances, respectively, but without voltage sources [Nasar and Trutt, 1999].

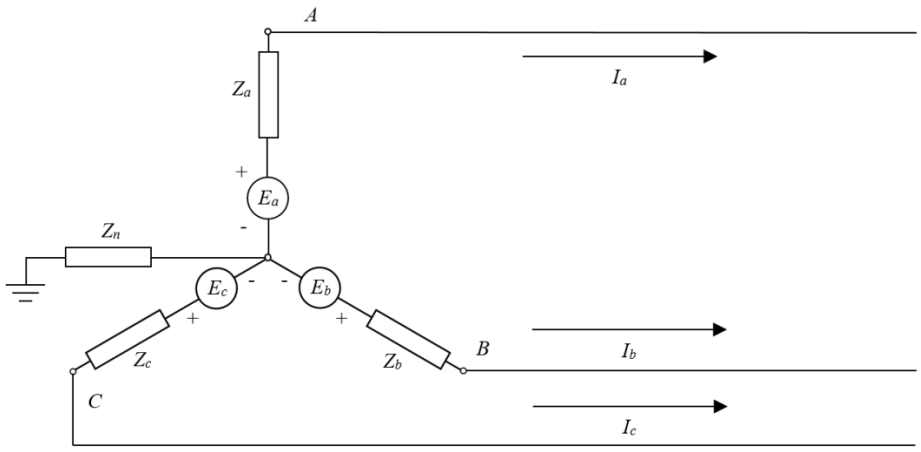

Figure 2.16. Circuit Diagram of an unloaded three-phase voltage source grounded through an impedance [Stevenson, 1982].

Figure 2.17 demonstrates the paths for each sequence current through the impedances of its own sequence; the sequence networks are shown in Figure 2.18.

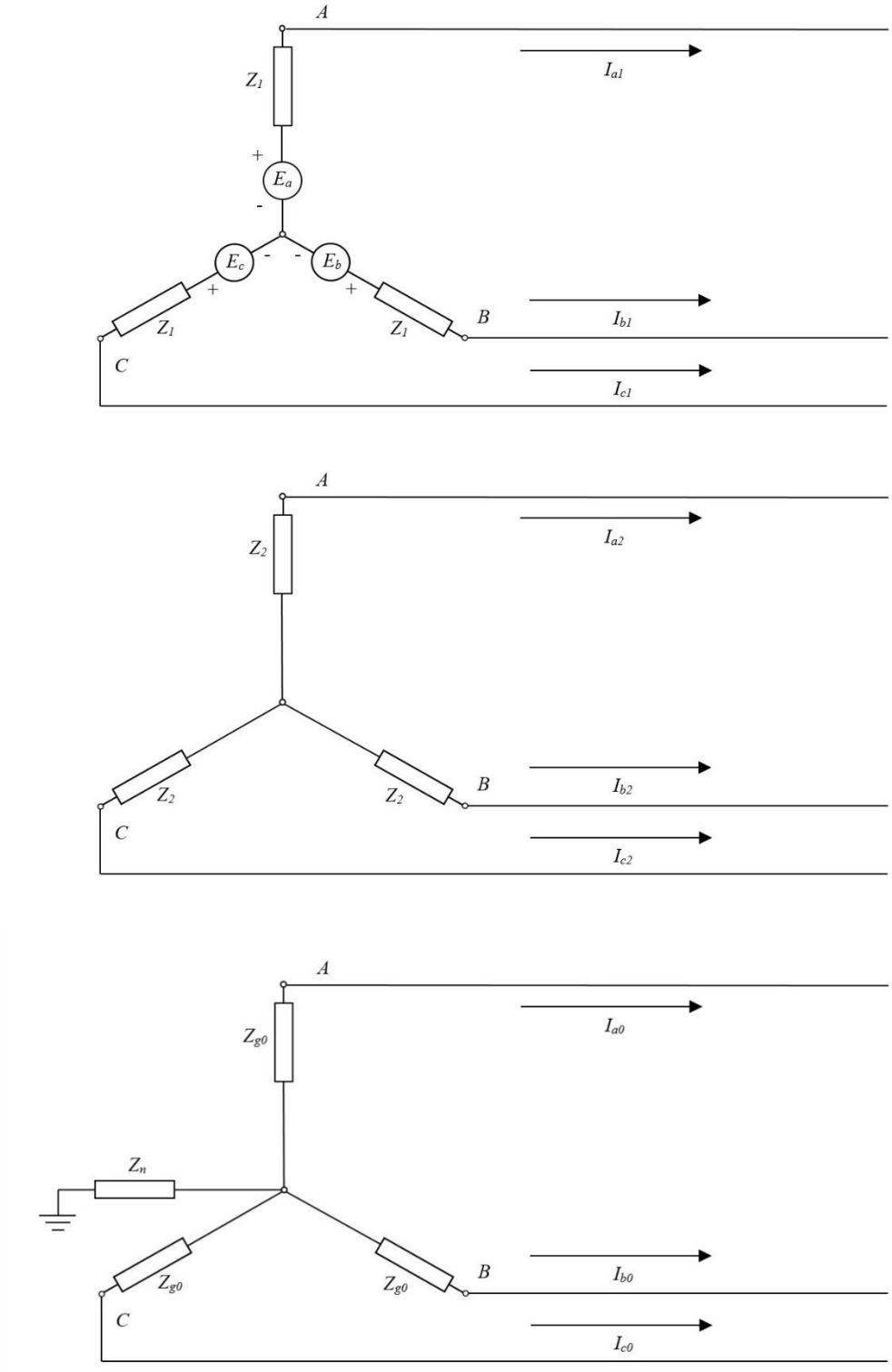

Figure 2.17. Path for sequence components of currents in an unloaded three-phase voltage source with a neutral- ground impedance [Stevenson, 1982].

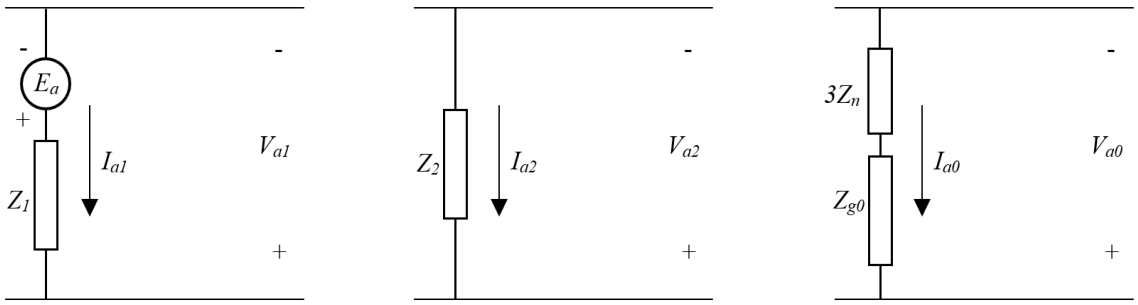

Figure 2.18. Positive, negative and zero sequence networks for an unloaded three-phase voltage source with a neutral- ground impedance [Stevenson, 1982].

The zero-sequence current through Z_n is

$$I_{a0} + I_{b0} + I_{c0} = 3I_{a0} \tag{2.38}$$

Inspection of Figure 2.18 can be used to develop the following relationships between sequence voltages and currents:

$$\begin{aligned} V_{a0} &= -I_{a0} \times Z_{g0} - 3I_{a0} \times Z_n = -I_{a0} \times \left(Z_{g0} + 3Z_n\right) \\ &= -I_{a0} \times Z_0 \end{aligned} \tag{2.39}$$

and

$$Z_0 = Z_{g0} + 3Z_n \tag{2.40}$$

$$\begin{aligned} V_{a1} &= E_a - I_{a1} \times Z_1 \\ \mathrm{V_{a2}} &= -I_{a2} \times Z_2 \\ \mathrm{V_{a0}} &= -I_{a0} \times Z_0 \end{aligned} \tag{2.41}$$

or in matrix form as:

$$\begin{bmatrix} V_{a0} \\ V_{a1} \\ V_{a2} \end{bmatrix} = \begin{bmatrix} 0 \\ E_a \\ 0 \end{bmatrix} - \begin{bmatrix} Z_0 & 0 & 0 \\ 0 & Z_1 & 0 \\ 0 & 0 & Z_2 \end{bmatrix} \times \begin{bmatrix} I_{a0} \\ I_{a1} \\ I_{a2} \end{bmatrix} \tag{2.42}$$

Since a particular voltage sequence produces current of that sequence only, no mutual coupling exists between the sequence networks [Nasar and Trutt, 1999; Stevenson, 1982]. In the next section, the sequence network of the same voltage source with a line-to-ground fault will be developed.

2.5.5. Sequence Network of the Unloaded Voltage Source with a Single Line-to-Ground Fault

Figure 2.19 shows a circuit diagram for an unloaded three-phase wye-connected voltage source with single line-to-ground fault occurring on phase A.

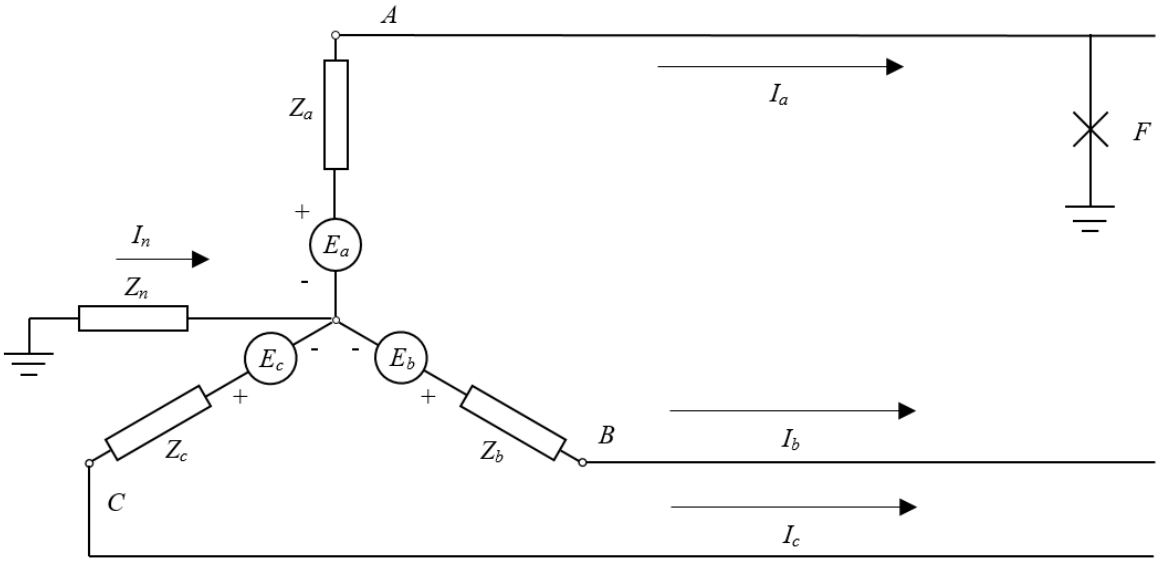

Figure 2.19. An unloaded three-phase voltage source with a single line-to-ground fault [Stevenson, 1982].

Since the fault is occurring on phase A, the conditions of non-load and short circuit can be expressed as:

$$I_b = I_c = 0 \tag{2.43}$$

$$\mathrm{V_a} = 0 \tag{2.44}$$

Thus,

$$\begin{aligned} I_{a0} &= \frac{1}{3}(I_a + I_b + I_c) = \frac{1}{3}I_a \\ \mathrm{I_{a1}} &= \frac{1}{3}(I_a + aI_b + a^2I_c) = \frac{1}{3}I_a \\ \mathrm{I_{a2}} &= \frac{1}{3}(I_a + a^2I_b + aI_c) = \frac{1}{3}I_a \end{aligned} \tag{2.45}$$

so that

$$I_{a0} = \mathrm{I_{a1}} = \mathrm{I_{a2}} = \frac{1}{3}I_a \tag{2.46}$$

Substituting in EQ 2.42, we get

$$\begin{bmatrix} V_{a0} \\ V_{a1} \\ V_{a2} \end{bmatrix} = \begin{bmatrix} 0 \\ E_a \\ 0 \end{bmatrix} - \begin{bmatrix} Z_0 & 0 & 0 \\ 0 & Z_1 & 0 \\ 0 & 0 & Z_2 \end{bmatrix} \times \begin{bmatrix} I_{a1} \\ I_{a1} \\ I_{a1} \end{bmatrix} \tag{2.47}$$

or

$$V_{a0} + V_{a1} + V_{a2} = E_a - I_{a1}(Z_0 + Z_1 + Z_2) \tag{2.48}$$

According to EQ 2.44,

$$V_{a0} + V_{a1} + V_{a2} = V_a = 0 \tag{2.49}$$

Thus, we have

$$I_{a1} = \frac{1}{3} I_a = \frac{E_a}{Z_1 + Z_2 + Z_0} \tag{2.50}$$

The connection of three sequence networks in series is shown in Figure 2.20, shown as below.

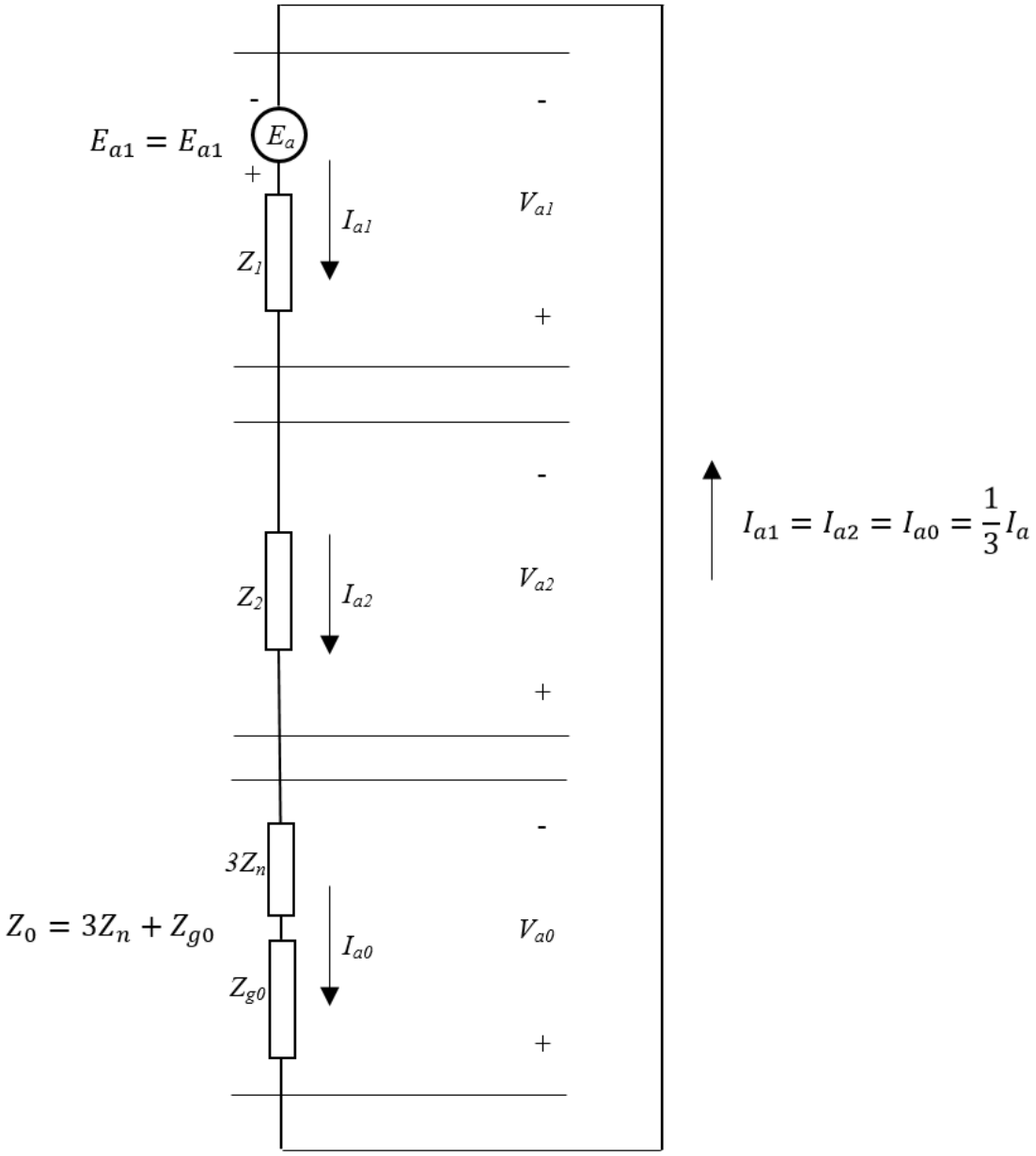

Figure 2.20. Sequence network connection for an unloaded voltage source with a single-line-to-ground fault on phase A [Stevenson, 1982].

2.5.6. Sequence Network for a Loaded Three-Phase Voltage Source with a Single Line-to-Ground Fault

The procedure of constructing the sequence network connection for a loaded three-phase voltage source is very similar to that for an unloaded voltage source. However, some notice must be kept in mind while drawing the zero-sequence network. If ungrounded wye connections exist, they present infinite impedance to zero-sequence current. Also, when the neutral points of wye connections are grounded through an impedance Z_n, $3Z_n$ must be placed between the neutral point and ground. Moreover, an infinite impedance is offered to the zero-sequence line current by a delta connection [Blackburn, 1993].

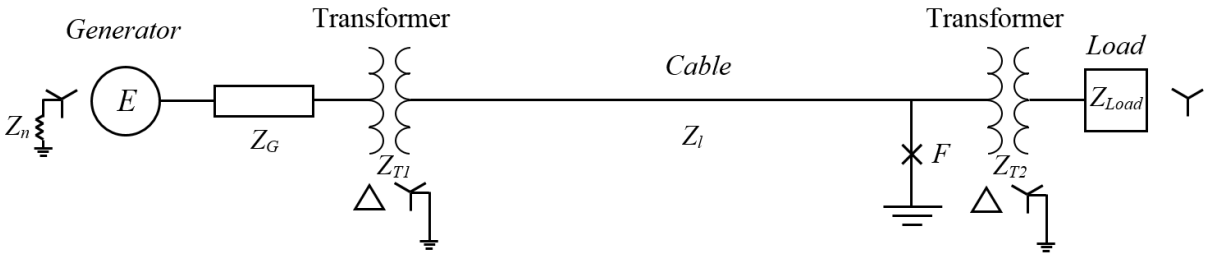

Figure 2.21. One-line diagram of a simplified power system with a single line-to-ground fault.

A one-line diagram of a simplified power system with a single line-to ground fault is shown in Figure 2.21. The generator supplies power to the load through two transformers and a cable. The generator has an internal impedance Z_g and its neutral point is grounded through an impedance Z_n. The primary sides of the transformers are connected as delta and the secondary sides are connected as wye and solidly grounded. The load is connected in wye and the neutral point is ungrounded. The generator and cable offer different impedances to different sequence components of current, while the impedances of different sequence components of current

offered by load and transformer are the same. The fault, represents by the letter F, occurs on phase A at the end of the cable. All impedances shown above are in per unit.

Figure 2.22 shows the sequence networks connected in series at the fault point F which describes the system condition in Figure 2.21.

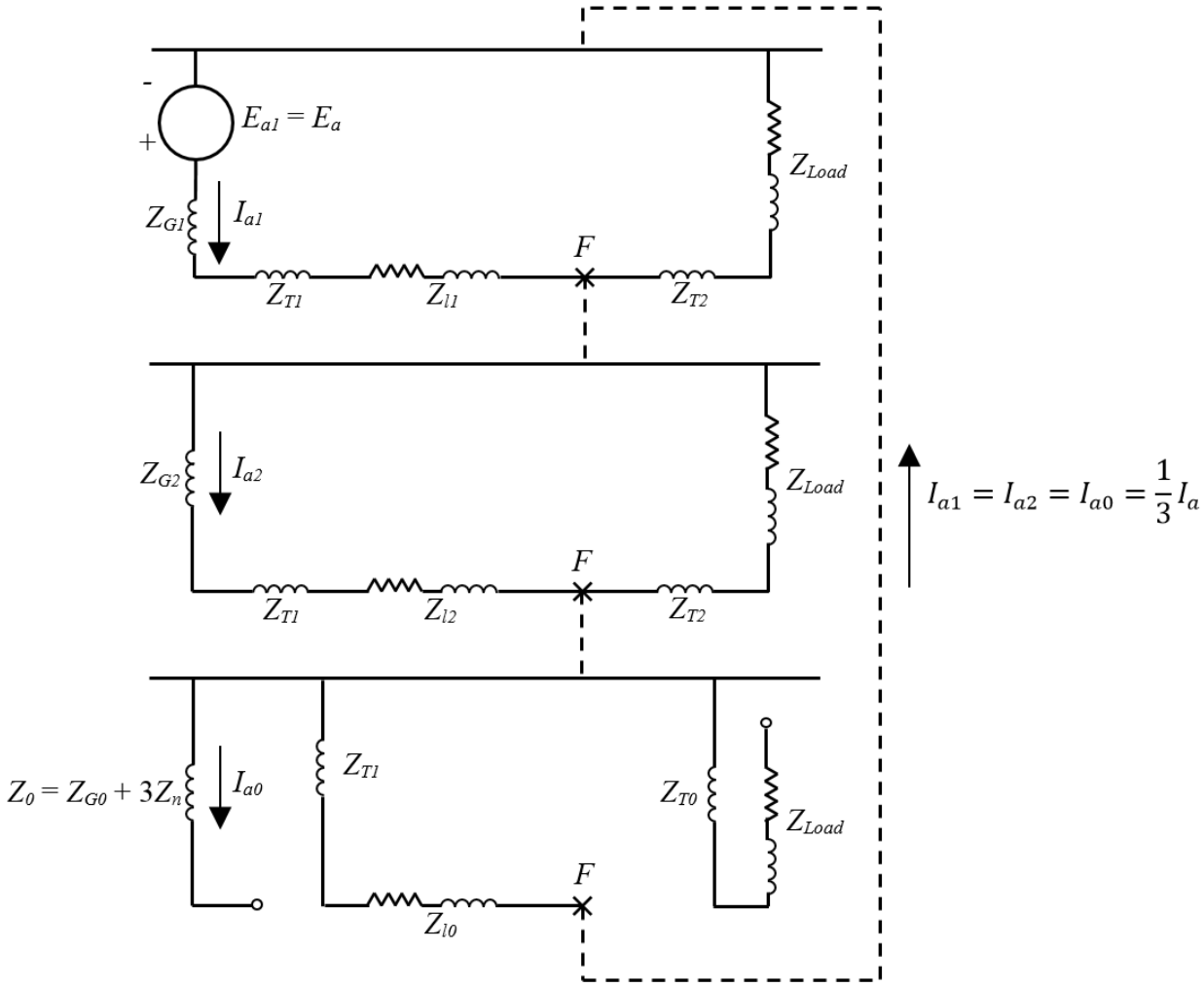

Figure 2.22. Sequence network connection of a simplified power system with a single line-to-ground fault.

The method of symmetrical components is a very convenient method for power system analysis during unsymmetrical faults or unbalanced conditions. (It is noted that the sequence components are not fictitious quantities; they can be measured and used for protective relaying.)

Sequence networks can be constructed for each particular type of fault and analyzed for establishing fault currents and voltages. These values can be used for establishing protective relay settings with a high degree of accuracy.

2.6. Harmonics in Mine Power System

In power distribution systems, both voltage and current waveforms should be purely sinusoidal. When a sinusoidal voltage is applied to a linear component, its voltage and current will also be sinusoidal. However, if the voltage is applied on a non-linear component, its current will be non-sinusoidal and no longer proportional to the voltage. According to Fourier theory, the non-sinusoidal voltages and currents can be decomposed into a Fourier series as the fundamental component and the integer multiples of the fundamental wave. The fundamental component has the same frequency as the operating (i.e., supply) frequency, while other components are integer multiples of the fundamental frequency and are defined as harmonics [Yang et al., 2010; Chen, 2011]. In order to represent steady-state waveform with equal positive and negative half-cycles, the Fourier series can be expressed as follows [Yang et al., 2010]:

$$f(t) = \sum_{n=1}^{\infty} A_n \times \sin(n\Pi t/T) \tag{2.51}$$

where

f(t) is the time domain function,

n is the order of harmonic,

A_n is the amplitude of the n*th* harmonic component,

T is the length of one period in seconds

Therefore, the Fourier series expressions for the voltage and current can be derived as:

$$V(t) = \sum_{n=1}^{\infty} \sqrt{2} V_n \times \sin(n\omega t + \varphi_n) \tag{2.52}$$

$$I(t) = \sum_{n=1}^{\infty} \sqrt{2} I_n \times \sin(n\omega t + \varphi_n) \tag{2.53}$$

where

ω is the fundamental angular frequency,

φ_n is the initial phase angle of the n*th* harmonic component,

According to EQ 2.52 and EQ 2.53, a non-sinusoidal periodical voltage or current waveform can be decomposed into an infinite number of sinusoidal waveforms with different amplitudes, frequencies, and initial phase angles. For example, the fundamental frequency of US power systems is 60 Hz, and the 2nd order harmonic is 120 Hz, the 3rd order harmonic is 180 Hz, and so on. To describe the level of distortion of the sinusoidal waveform deviation, two factors termed total harmonic distortion (THD) and harmonic ratio (HR) are commonly used and identified as follows:

THD for voltages:

$$THD(V) = \frac{\sqrt{\sum_{n=1}^{\infty} V_n{}^2}}{V_1} \times 100\% \tag{2.54}$$

THD for currents:

$$THD(I) = \frac{\sqrt{\sum_{n=1}^{\infty} I_n{}^2}}{I_1} \times 100\% \tag{2.55}$$

HR for voltages:

$$HR(V) = \frac{V_n}{V_1} \times 100\% \tag{2.56}$$

HR for currents:

$$HR(I) = \frac{I_n}{I_1} \times 100\% \tag{2.57}$$

In traditional mine power systems, zero-sequence harmonics are mainly caused by the nonlinear characteristics of the transformer core and only a few odd harmonics, such as the third, fifth and seventh order exist in ground fault currents. However, with an increasing number of power electronic devices and nonlinear loads being used in modern coal mine power systems, new harmonic sources are created, and harmonics of higher amplitude and frequency are produced. Thus, even when ground fault currents (at the supply frequency) are fully compensated by the Peterson coil, the residual current at the fault point can still be large enough to cause personnel injuries and equipment damage because of the harmonics [Li, 2010].

2.7. Chapter Summary

The expanded radial system is the most commonly used distribution arrangement in underground coal mines. A typical mine power system is comprised of a substation to convert voltage from utility voltage to distribution voltage, several switchhouses to branch and protect outgoing circuits, power centers to transform distribution voltage to utilization voltage (and supply mining equipment), and distribution cables to conduct current.

The occurrence of a fault in a mine power system results in abnormal current in phase conductors, the ground conductor(s), or both. The faulted section must be detected and isolated as quickly and selectively as possible to prevent personnel injuries and equipment damage. Faults involving ground are termed ground faults, e.g., single line-to-ground fault and double line-to-ground faults.

System grounding is the connection of the power system to earth. Grounding systems protect personnel and machinery from hazards associated with ground faults and equipment failure.

The major types of mine power system grounding are (1) an ungrounded system, (2) the solidly grounded system, (3) the resistance grounded system, and (4) the resonant grounded system. Although US coal mines are required to use a high-resistance grounded system, it is believed that the resonant grounded system, which is already widely used in certain other countries, can solve most of the problems associated with a high-resistance grounded system.

In a resonant grounded system, the Peterson coil must be properly tuned to effectively compensate the capacitive charging current. Some commonly used tuning methods include the resonance method (extremum method), the phase angle method, the indirect measuring method, and the additional source method. These methods have specific advantages and disadvantages, depending on the power system characteristics.

Several fault location detection methods are applied to resonant grounded systems, such as the fifth-order harmonic method, the signal injection method, and the active component method. Each of these methods has specific advantages and disadvantages, and it is important to choose the proper method based on system conditions.

Power system faults consist of symmetrical and unsymmetrical faults. Symmetrical faults such as a three-phase fault can be analyzed on a per-phase basis, while unsymmetrical faults such as line-to-ground faults are analyzed by the theory of symmetrical components. Unbalanced voltages and currents can be resolved into their symmetrical components and each set of symmetrical components can be treated and superimposed separately. A good understanding of symmetrical component theory can be very useful in power system protective relay operation.

A harmonic of a signal is a component frequency of the signal that is an integer multiple of the fundamental frequency. Harmonic voltages and currents are a result of non-linear electric loads and they are a frequent cause of power quality problems. In modern mine power systems, harmonics generated by power electronic devices and nonlinear loads can cause a significant problem during a ground fault.

CHAPTER 3

ANALYSIS OF VERY HIGH-RESISTANCE GROUNDED SYSTEMS

3.1. Introduction

As mentioned in the previous chapter, U. S. coal mine distribution systems include a neutral grounding resistor (NGR) sized to limit the NGR current to 25 A during a ground fault. However, as coal mine power systems become more extensive, system distributed capacitance increases such that the charging current can be several times larger than the NGR current limit. This can lead to problems commonly associated with ungrounded power systems, i.e., overvoltages and loss of relay selectivity during ground faults. In this chapter, a three-branch system is modeled using PSCAD to analyze a high-resistance grounded coal mine power system as practiced in the U.S.

3.2. Distribution System Components Parameters Calculation

3.2.1. Introduction

A three-branch system model is used to represent a simplified mine power system (see Figure 3.1). This system contains a utility source, transformers, cables, and loads. The utility source represents the secondary side of the main substation transformer which provides power at the distribution voltage level, chosen to be 12,470 V. Two types of cable are used, 500 kcmil MP-GC cable is used for the borehole, and a 4/0 MP-GC cables is used in each branch.

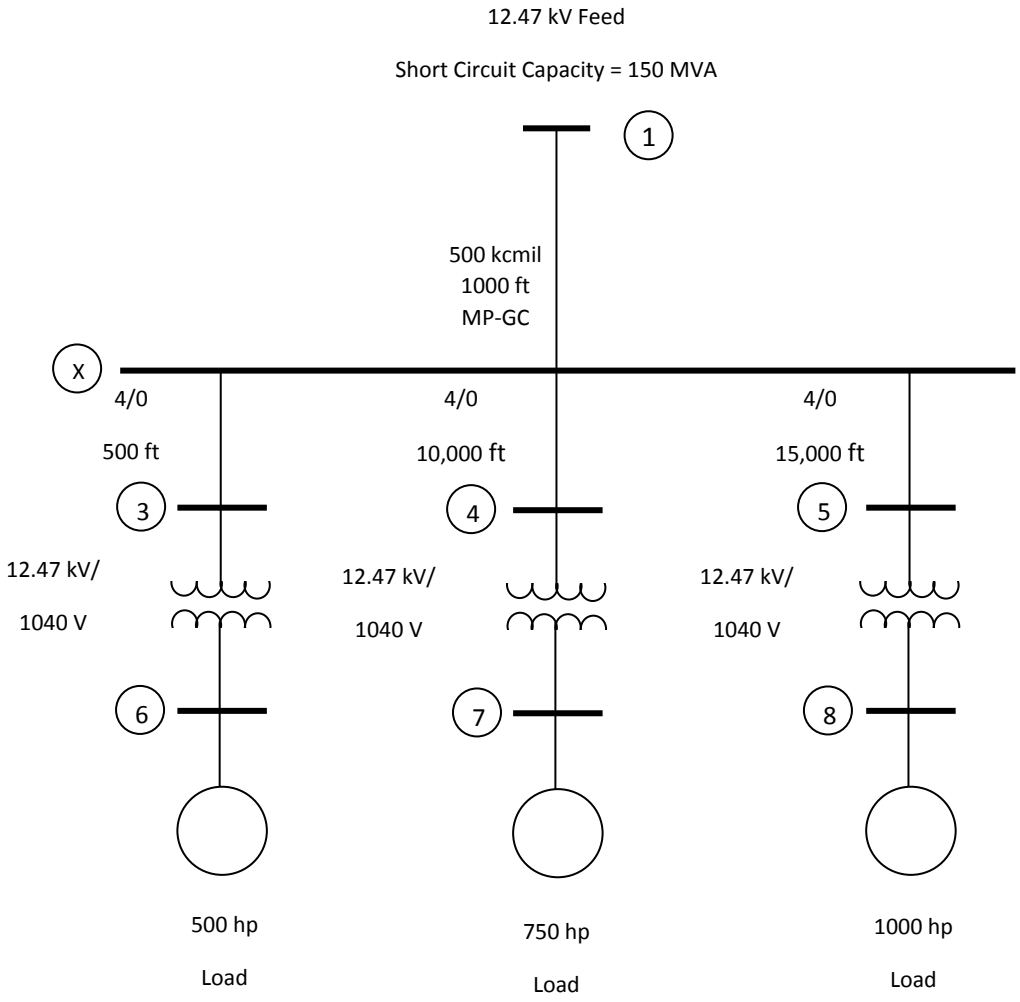

Figure 3.1. One line diagram of simplified mine power system.

Transformers on each branch represent power centers and step down the distribution voltage to utilization voltage, chosen to be 1040 V. Three loads: 500 hp, 750 hp, and 1000hp are used to represent mining equipment. The voltage level, cables and loads are chosen somewhat arbitrarily, but are representative of what would be found in a typical mine power system.

3.2.2. Utility

The secondary side of the main substation is simulated by a three-phase wye-connected voltage source. The magnitude of the output line-to-line voltage is 12,470 V and the frequency is 60 Hz. As the simulation is focusing on the entire system, the source is selected as ideal without source impedance. The wye-connection neutral point is grounded through a 288 ohm resistor which is typically used in the industry.

3.2.3. Transformer

The transformers are simulated as a resistance in series with a reactance in each phase. The impedance is selected to be 5% with 4/1 X/R ratio for all three power center transformers. The resistance and reactance can be calculated as shown below.

The phase angle of the impedance can be calculated as:

$$\theta = tan^{-1}\left(\frac{4}{1}\right) = 75.96°. \tag{3.1}$$

The impedance base of each transformer is calculated as:

$$Z_{1_{base}} = \frac{{V_{base}}^2}{S_{1_{base}}} = \frac{12470^2}{1000000} = 155.50\ \Omega. \tag{3.2}$$

$$Z_{2_{base}} = \frac{{V_{base}}^2}{S_{2_{base}}} = \frac{12470^2}{1250000} = 124.40\ \Omega. \tag{3.3}$$

$$Z_{3_{base}} = \frac{{V_{base}}^2}{S_{3_{base}}} = \frac{12470^2}{1500000} = 103.67\ \Omega. \tag{3.4}$$

The actual impedance of the transformers on each branch can be calculated as:

$$Z_{1_{actual}} = Z_{1_{pu}} \times Z_{1_{base}} = (0.05\angle 75.96°) \times 155.50 = 1.886 + j7.543\ \Omega. \quad (3.5)$$

$$Z_{2_{actual}} = Z_{2_{pu}} \times Z_{2_{base}} = (0.05\angle 75.96°) \times 124.40 = 1.509 + j6.034\ \Omega. \quad (3.6)$$

$$Z_{3_{actual}} = Z_{3_{pu}} \times Z_{3_{base}} = (0.05\angle 75.96°) \times 103.67 = 1.257 + j5.029\ \Omega. \quad (3.7)$$

The inductance of each transformer can be calculated from the reactance at 60 Hz as:

$$L_1 = \frac{X_{L_1}}{\omega} = \frac{7.543}{2 \times \pi \times 60} = 0.0200\ H. \quad (3.8)$$

$$L_2 = \frac{X_{L_2}}{\omega} = \frac{6.034}{2 \times \pi \times 60} = 0.0160\ H. \quad (3.9)$$

$$L_3 = \frac{X_{L_3}}{\omega} = \frac{5.029}{2 \times \pi \times 60} = 0.0133\ H. \quad (3.10)$$

3.2.4. Cables

There is no assembled multi-conductor cable component in PSCAD. Therefore, cables are represented by lumped parameters connected in a π configuration in the simulation model. Power and ground conductor resistance and reactance values are determined by the typical 90˚ C resistance and 60 Hz reactance values for 15 kV mine power cables. The selected brand and types of cable used is AmerCable TB2-604 Type MP-GC, 3/C, 15kV. The size of 500 kcmil and 4/0 AWG are used for the borehole and mine power feeders, respectively; and their general characteristics are shown in Table 3.1 and Table 3.2.

Table 3.1. Mine power feeder resistance and reactance values [Anon, 1976; Anon, 2005].

Power Conductor			Ground Conductor	
Size	**R/1000 ft.**	**X_L/1000 ft.**	**Size**	**R/1000 ft.**
500 kcmil	0.027	0.031	4/0	0.063
4/0 AWG	0.063	0.035	1	0.160

Table 3.2. Mine power feeder dimensions and insulation [Anon, 2005].

Power Conductor		Insulation				Extruded Strand Shield Thickness
Size	**Strand Diameter**	**Material**	**Thickness**	**SIC (max)**	**SIC (typical)**	
500 kcmil	0.789 in.	EPR	175 mils	4.0	3.2	0.022 in.
4/0 AWG	0.512 in.	EPR	175 mils	4.0	3.2	0.022 in.

3.2.4.1. Cable Series Resistance and Reactance

3.2.4.1.1. Borehole Cable Series Resistance and Inductance

As mentioned above, the 1000-foot borehole cable is modeled using three, 500 kcmil power conductors. The resistance and reactance of the power conductors can be calculated as:

$$R = \frac{0.027\ \Omega}{1000\ ft} \times 1000\ ft = 0.027\ \Omega. \tag{3.11}$$

$$X_L = \frac{0.031\ \Omega}{1000\ ft} \times 1000\ ft = 0.031\ \Omega. \tag{3.12}$$

Thus, the inductance of each power conductor can be calculated as:

$$L = \frac{X_L}{2\,\pi\,\times 60} = 8.223\,\times\,10^{-5}\,H. \tag{3.13}$$

A single ground conductor has a resistance of:

$$R_g = \frac{0.063\,\Omega}{1000\,ft} \times 1000\,ft = 0.063\,\Omega. \tag{3.14}$$

For two parallel ground conductors, the equivalent resistance can be calculated as:

$$R_g{}' = \frac{0.063^2}{0.063 + 0.063} = 0.0315\,\Omega. \tag{3.15}$$

The inductance of the ground conductor is assumed to be equal to the power conductor inductance value, since the ground conductor reactance is not available. Thus, for a 1000-ft, 500 kcmil cable, the inductance of ground conductor is 0.08223 mH.

3.2.4.1.2. Mine Power Feeder Series Resistance and Inductance

The cables used in the remainder of the distribution system are 4/0 AWG, with lengths of 500 feet (branch 1), 10,000 feet (branch 2) and 15,000 feet (branch 3), respectively. The 500 ft length branch was selected to represent a branch with very little capacitance, while the 10,000 and 15,000 ft branches represent typical lengths in an underground coal mine distribution system. The resistance and reactance for branch 1 are calculated as:

$$R_1 = \frac{0.063\,\Omega}{1000\,ft} \times 500\,ft = 0.0315\,\Omega. \tag{3.16}$$

$$X_{L_1} = \frac{0.035\,\Omega}{1000\,ft} \times 500\,ft = 0.0175\,\Omega. \tag{3.17}$$

Thus, the inductance of branch 1 can be calculated as:

$$L_1 = \frac{X_L}{2\,\pi\,\times 60} = 4.642\,\times\,10^{-5}\,H. \tag{3.18}$$

A single ground conductor resistance of the 500 feet 4/0 AWG cable is:

$$R_{g_1} = \frac{0.16\,\Omega}{1000\,ft} \times 500\,ft = 0.08\,\Omega. \tag{3.19}$$

For two parallel ground conductors, the equivalent resistance can be calculated as:

$$R_{g_1}{}' = \frac{0.08^2}{0.08 + 0.08} = 0.04\,\Omega. \tag{3.20}$$

The same calculations were performed to obtain the conductor resistance, inductance, and ground conductor resistance for branches 2 and 3 and the results are given below.

$$R_2 = 0.63\,\Omega \qquad L_2 = 9.284\times\,10^{-4}\,H \qquad R_{g_2}{}' = 0.8\,\Omega$$

$$R_3 = 0.95\,\Omega \qquad L_3 = 1.393\,\times\,10^{-3}\,H \qquad R_{g_3}{}' = 1.2\,\Omega$$

The inductance of the ground conductor in each branch is also assumed to be equal to the power conductor inductance value, which are 0.04642 mH, 0.9284 mH, and 1.3926 mH, for branches 1, 2, and 3, respectively.

3.2.4.2. Distributed Capacitance to Ground

The distributed capacitance to ground (in pF per foot) can be determined as [Anon., 1976]:

$$C_{\frac{pF}{ft}} = \frac{7.354\varepsilon}{\lg(1 + \frac{2t}{d})}, \quad (3.21)$$

where

ε = dielectric constant of the cable insulation (SIC),

t = thickness of the conductor insulation, and

d = diameter under the insulation or the conductor diameter.

Table 3.2 gives the strand diameter extruded strand shield and diameter under the insulation for MP-GC cable type, and the typical SIC value of 3.2 is selected to calculated the distributed capacitance.

3.2.4.2.1. Borehole Cable Distributed Capacitance to Ground

The parameters of the borehole cable are shown below:

Cable type:	MP-GC 3/C 15 kV
Conductor size:	500 kcmil
Length:	1000 feet
Strand diameter:	0.789 inches
Extruded strand shield:	0.044 inches (0.022 inches thick)
Insulation thickness:	0.175 inches

There is 2% reduction in strand diameter when the extruded strand shield is applied, thus the diameter under the insulation is calculated as:

$$d = 0.789 \times (1 - 2\%) + 0.044 = 0.81722\ inches. \tag{3.22}$$

The capacitance of the borehole cable in pF per feet can be calculated as:

$$C_{\frac{pF}{ft}} = \frac{7.354\varepsilon}{\lg(1 + \frac{2t}{d})} = \frac{7.354 \times 3.2}{\lg(1 + \frac{2 \times 0.175}{0.81722})} = 152.007\ \frac{pF}{ft}. \tag{3.23}$$

For 1,000 feet cable length, the total capacitance is:

$$C = C_{\frac{pF}{ft}} \times 1000\ ft = 0.152\ \mu F. \tag{3.24}$$

The lumped capacitance at each end of a π-configured cable can be obtained from:

$$C_{per-leg} = 0.152\ \mu F \div 2 = 0.076\ \mu F. \tag{3.25}$$

3.2.4.2.2. Mine Power Feeder Distributed Capacitance to Ground

The cable parameters of the mine power feeders are shown below:

	Branch 1	Branch 2	Branch 3
Cable type:	MP-GC 3/C 15 kV	MP-GC 3/C 15 kV	MP-GC 3/C 15 kV
Conductor size:	4/0 AWG	4/0 AWG	4/0 AWG
Length:	500 feet	10000 feet	15000 feet
Strand diameter:	0.512 inches	0.512 inches	0.512 inches

Extruded strand shield:	0.044 inches	0.044 inches	0.044 inches
Insulation thickness:	0.175 inches	0.175 inches	0.175 inches

The diameter under the insulation for all three branches is calculated as:

$$d = 0.512 \times (1 - 2\%) + 0.044 = 0.54576\ inches. \tag{3.26}$$

The per feet capacitance of the mine power feeders can be calculated as:

$$C_{brach\frac{pF}{ft}} = \frac{7.354\varepsilon}{\lg(1 + \frac{2t}{d})} = \frac{7.354 \times 3.2}{\lg(1 + \frac{2 \times 0.175}{0.54576})} = 109.3583\ \frac{pF}{ft}. \tag{3.27}$$

Using this value of capacitance, the lumped capacitance at each end of the π equivalent for each branch is given below:

$$C_{1_{per-leg}} = 0.0273\ \mu F$$
$$C_{2_{per-leg}} = 0.5468\ \mu F$$
$$C_{3_{per-leg}} = 0.8202\ \mu F$$

3.2.5. Loads

As the simulation is focusing on the entire system, the motor loads are modeled as constant impedance loads operating at a 0.90 lagging power factor. The load impedance is determined from the nominal system voltage and rated power.

For load 1 (500 hp), the per-phase real and reactive power values are calculated as:

$$P_{1/\emptyset} = \frac{P_1}{3} = \frac{500\ hp}{3} \times 0.7457\ \frac{kW}{hp} = 124.2833\ kW. \tag{3.28}$$

$$Q_{1/\emptyset} = P_{1/\emptyset} \times \tan[cos^{-1}(0.9)] = 60.1931\ kVAR. \tag{3.29}$$

The per-phase complex power is:

$$S_{1/\emptyset} = (124.2833 + j60.1931)\ kVA. \tag{3.30}$$

The per-phase impedance is:

$$Z_{1/\emptyset} = \frac{|V|^2}{S_{1/\emptyset}^*} = \frac{7200^2}{(124.2833 - j60.1931) \times 10^3} = 337.87 + j163.64\ \Omega. \tag{3.31}$$

The per-phase resistance is 337.87 Ω, and the per-phase inductance is 0.434 H.

Similar calculations were performed to obtain the per-phase resistance and inductance for load 2 (750 hp) and load 3 (1000 hp), and the results are given below.

$$R_{2/\emptyset} = 225.24\ \Omega \qquad L_{2/\emptyset} = 0.289\ H$$

$$R_{3/\emptyset} = 168.93\ \Omega \qquad L_{3/\emptyset} = 0.217\ H$$

Table 3.3 – Table 3.6 provides a summary of the relevant parameters of the model.

Table 3.3. Source parameters for the simulation model

Voltage (V_{LL})	**Frequency (Hz)**	**Neutral Grounding Resistor (Ω)**
12,470	60	288

Table 3.4. Transformer parameters for the simulation model

Voltage (V)	Capacity (kVA)	Z_{pu} (Ω)	X/R Ratio	Z_{base} (Ω)	θ (degrees)	R (Ω)	X_L (Ω)	L (H)
12,470	1,000	0.05	4	155.50	75.96	1.886	7.543	0.0200
12,470	1,250	0.05	4	124.40	75.96	1.509	6.034	0.0160
12,470	1,500	0.05	4	103.67	75.96	1.257	5.029	0.0133

Table 3.5. Cable parameters for the simulation model

Branch	Power Conductor			Grounding Conductor		Capacitance to ground (μF/leg)
	Length (ft)	R (Ω/ph)	L (mH/ph)	R (Ω)	L (mH)	
Borehole	1000	0.0270	0.0822	0.0315	0.0822	0.0760
1	500	0.0315	0.0464	0.0400	0.0464	0.0273
2	10,000	0.6300	0.9284	0.800	0.9284	0.5468
3	15,000	0.9450	1.3926	1.2000	1.3926	0.8202

Table 3.6. Load parameters for the simulation model

Location	hp	pf	R (Ω)	L (H)
Branch 1	500	0.90 lagging	337.866	0.434
Branch 2	750	0.90 lagging	225.240	0.289
Branch 3	1,000	0.90 lagging	168.930	0.217

3.3. PSCAD/EMTDC Simulation Model Development

3.3.1. PSCAD/EMTDC Description

PSCAD/EMTDC is widely used software for power system electromagnetic transient simulation. It is developed by the Manitoba HVDC Research Center of Canada which is one

of the world leaders in power system simulation innovation and applied services. PSCAD (**P**ower **S**ystem **C**omputer **A**ided **D**esign) is the graphical interface for the EMTDC (**E**lectro-**M**agnetic **T**ransient simulation including **DC**), briefly described below [Anon, 2010].

EMTDC is an electromagnetic transient simulation program that was first used to analyze DC transients. Its initial version was developed by Dr. Dennis Woodford in 1976 at the Manitoba Hydro-Electric Board. Since then, the program has been under continuous development and currently is widely used in many areas of power system analysis and simulation, including AC transmission and distribution, lightning transients, and power electronics. EMTDC was initially used on mainframe computers, and then migrated into UNIX machines, and later personal computers [Anon, 2010].

The initial version of PSCAD was used on Apollo workstations in 1988, and the second version was developed in 1995. In 1999, the PSCAD V3 began running on the Microsoft Windows OS and the current version is PSCAD V4. In this dissertation, a copy of PSCAD V4.2 is used, and the simulation step size is 50~100 μs and its frequency response accuracy can attain to 3000Hz [Anon, 2010].

PSCAD/EMTDC has a master library which consists of various power system elements and integrated modules. The classification of these elements and modules include passive elements, sources, transformers, machines, cable and transmission lines, breaker and faults, I/O devices, protection devices, data recorders and readers, power electronics, and so forth. These elements and modules can be invoked from the master library and used to assemble the simulated power system. Users can also create customized modules by combining required elements or data processors to represent large-scale models or perform complicated calculations. The simulation output formats include real-time waveforms, instantaneous values, RMS values, and phasors. PSCAD also contains processing and calculation modules, e.g., FFT and other CSM (Continuous System Model) functions, to perform required digital and analog calculations. The combination of the EMTDC algorithms and the PSCAD graphical interface produces a powerful, yet user-friendly, application for electromagnet transient analysis.

The distribution system simulation model was developed using the parameters calculated previously and its diagram is shown in Figure 3.2. The software requires a voltage ramp up

time and it is selected to be 0.05 second. The simulation is conducted for 2 seconds to avoid the voltage ramp-up transient period.

The distribution system simulation model was developed using the parameters calculated previously and its diagram is shown in Figure 3.2. The software requires a voltage ramp up time and it is selected to be 0.05 second. The simulation is conducted for 2 seconds.

3.3.2. Simulation Model Verification

To verify that the simulation model was assembled correctly, hand calculations for balanced operation at 60-Hz were compared with the results from the PSCAD model.

3.3.2.1. Hand Calculations of System Under Balanced Operation

For the system operating under balanced, steady-state conditions, it is relatively straightforward to determine voltages and currents using phasor analysis. Figure 3.3 shows the resulting circuit for the mine distribution system. Combining series and parallel branches, the equivalent 60-Hz impedance, with respect to the source is (81.9766 + j33.2404) Ω in parallel with the –j34,902.4 Ω shunt capacitance, as shown in Figure 3.4. From this, I_s can be determined from the equivalent impedance of the entire system (EQ 3.32) and I_1 can be determined from current division (EQ 3.33). (Note that I_1 can also be calculated as shown in (EQ 3.34), but current division is shown to illustrate the procedure for using current division in branches in which the voltage has not been calculated.)

$$I_s = \frac{7200\underline{/0^\circ}}{[(-j34{,}902.4)^{-1}+(81.9766+j33.2404)^{-1}]^{-1}} = (75.4281 - j30.3787)\ \text{A} \tag{3.32}$$

$$I_1 = (75.4281 - j30.3787)\left(\frac{[(-j34{,}902.4)^{-1}+(81.9766+j33.2404)^{-1}]^{-1}}{(81.9766+j33.2404)}\right) = (75.4281 - j30.5850)\ \text{A} \tag{3.33}$$

$$I_1 = \frac{7200\underline{/0^\circ}}{(81.9766 + \mathrm{j}33.2404)} = (75.4281 - j30.5850)\ \mathrm{A} \tag{3.34}$$

Three currents were selected for comparison with PSCAD/EMTDC: the line *a* charging current in branch 3, $I_{3c\_a\_1}$ and $I_{3c\_a\_2}$, and the line *a* branch current between the two legs of capacitance in branch 3, I_3 (shown in Figure 3.2 and Figure 3.3). Each of these was computed by repeated use of equivalence and current division. The results are shown below.

$$I_3 = 36.500\underline{/\text{-}23.98^\circ}\ \mathrm{A}$$

$$I_{3c\_a\_1} = 2.225\underline{/\text{-}90.01^\circ}\ \mathrm{A}$$

$$I_{3c\_a\_2} = 2.210\underline{/\text{-}90.04^\circ}\ \mathrm{A}$$

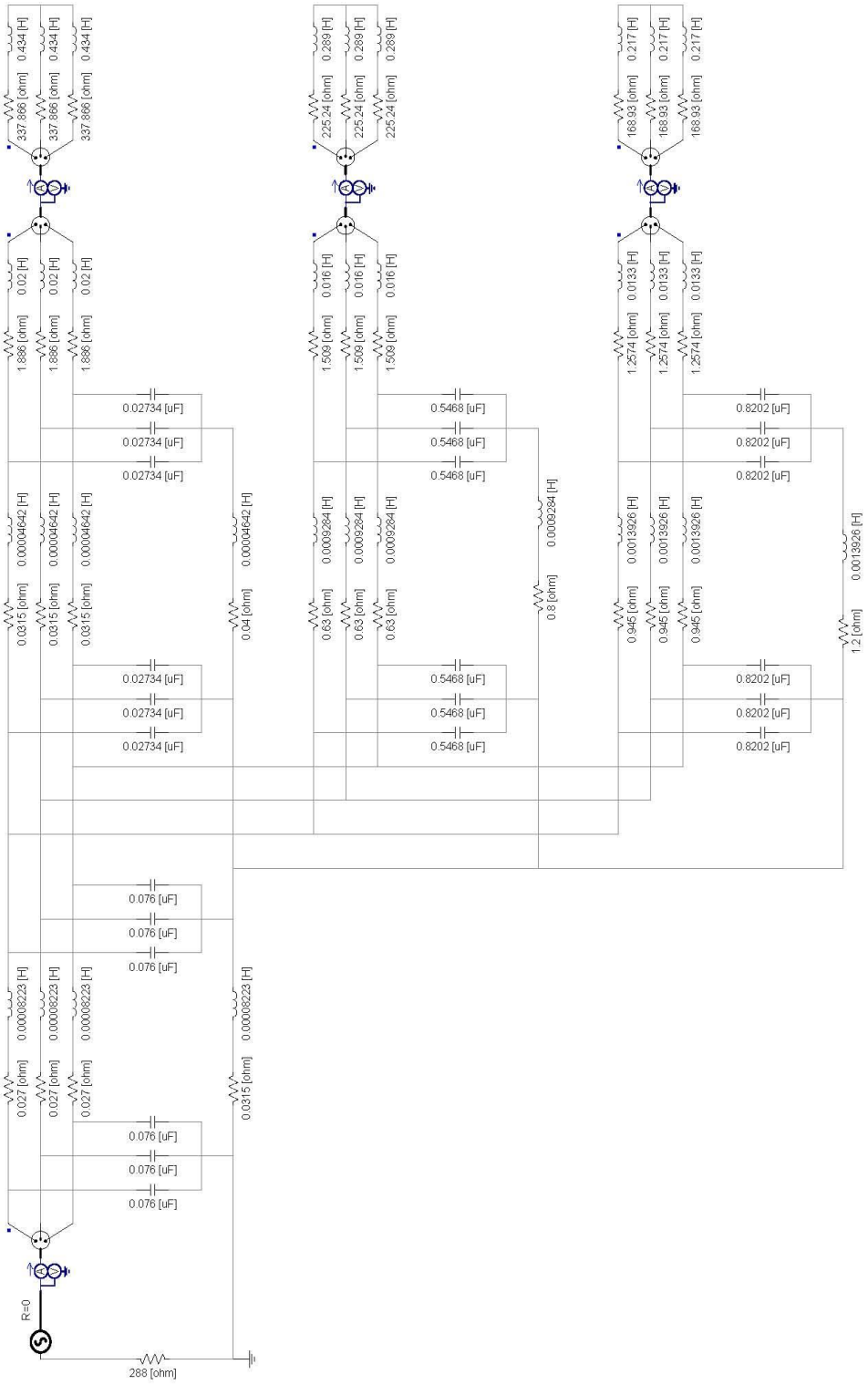

Figure 3.2. Simulation model diagram of the three-branch distribution system

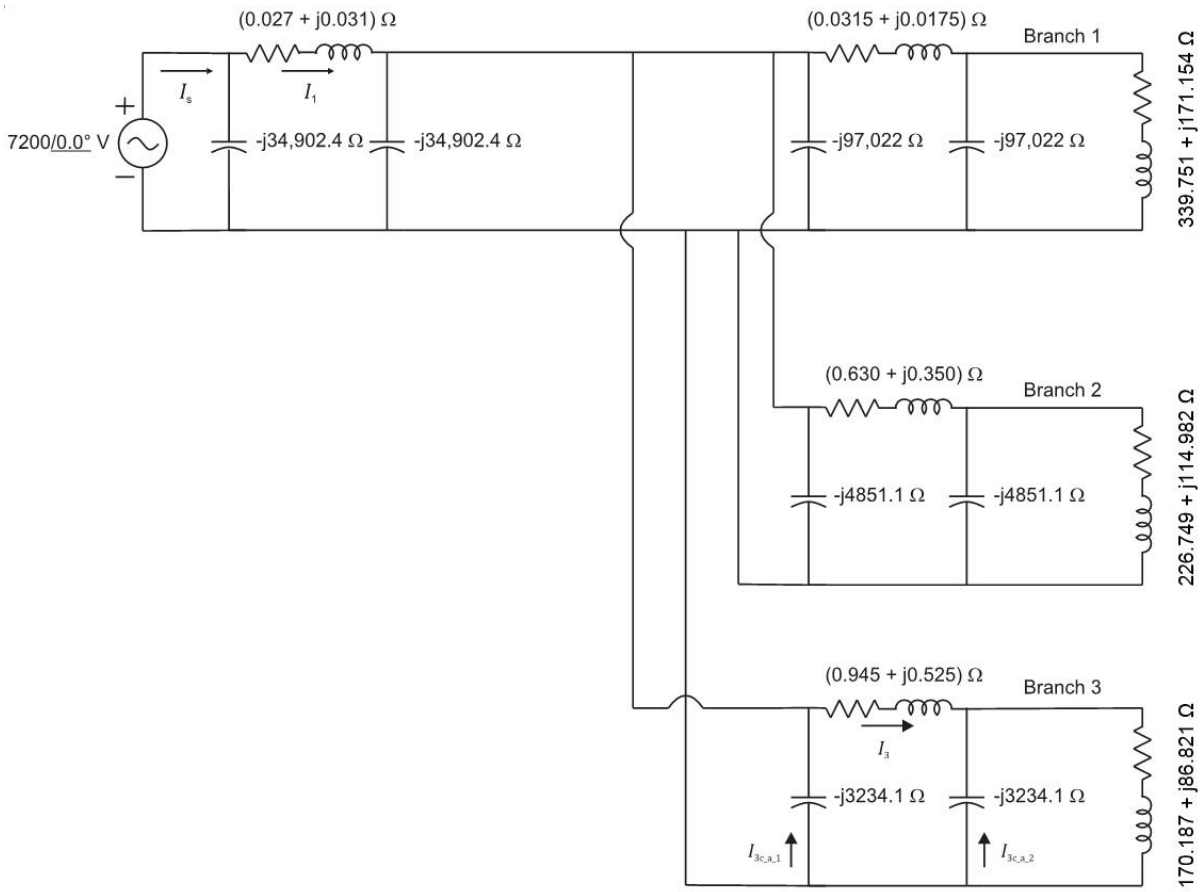

Figure 3.3. Per-phase, equivalent-wye model of distribution system.

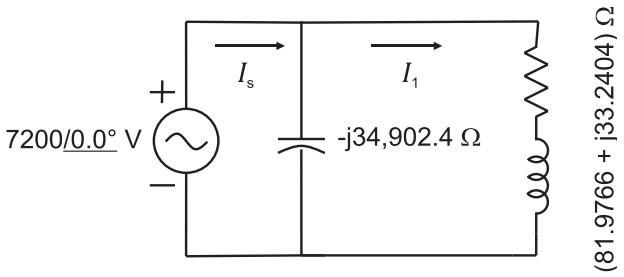

Figure 3.4. Reduced equivalent circuit for the mine distribution system under balanced operation.

3.3.2.2. PSCAD/EMTDC Results

For verification, the simulation model was run under the same balanced conditions as for the hand calculations to verify its construction. The first step was to verify balanced operation. Several voltage and current phasormeter plots are shown below in Figure 3.5 and Figure 3.6. Figure 3.5 shows that the three phase voltages have the same magnitude of approximately 7,200 V, with a phase shift of 120˚ (and phase sequence *a-b-c*), indicating balanced operation. Figure 3.6 shows currents of 81.308 A with a 120 ° phase shift between phases, indicating balanced operation.

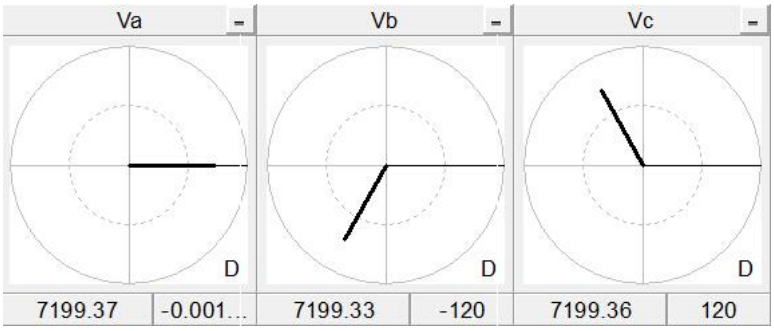

Figure 3.5. Source voltage phasormeter plot

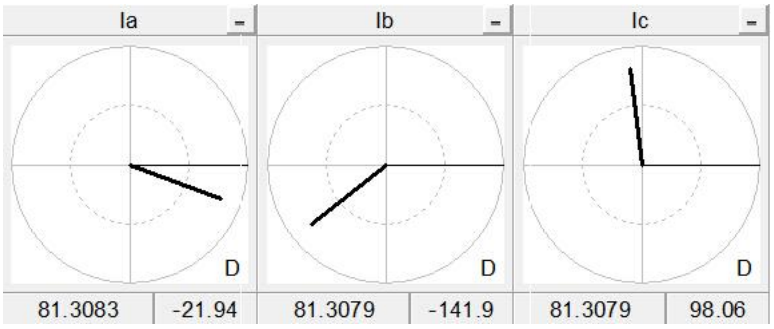

Figure 3.6. Source current phasormeter plot

Once it was determined that the system was balanced, ammeters were placed on branches 3, 3*c_a*_1, and 3*c_a*_2 and the results were compared with the hand calculaitons, as shown in Table 3.7. As expected, the results are in agreement. These results indicate that the

PSCAD/EMTDC model is an accurate representaiton of the distribution system, and can be used for simulating unbalanced conditions and harmonics during balanced and unbalanced conditions.

Table 3.7. Comparison of hand calculations with PSCAD/EMTDC for balanced operation

Branch Current	Hand Calculation	PSCAD/EMTDC
I_3	36.500/-23.98° A	36.500/-23.98° A
$I_{3c\_a\_1}$	2.225/-90.01° A	2.225/-90.01° A
$I_{3c\_a\_2}$	2.210/-90.04° A	2.210/-90.04° A

3.3.3. Simulation of Single Line-to-Ground Fault

A single-line-to-ground fault was next added to the model to simulate the system under fault conditions. The fault was located in phase *a* at the load end of branch 2, and is shown in Figure 3.7. The fault begins at 1.50 second and continues until the simulation ends at 2.00 seconds. Ammeters are added to each branch to measure the current during the fault, and voltages are determined by inserting voltmeters in each branch.

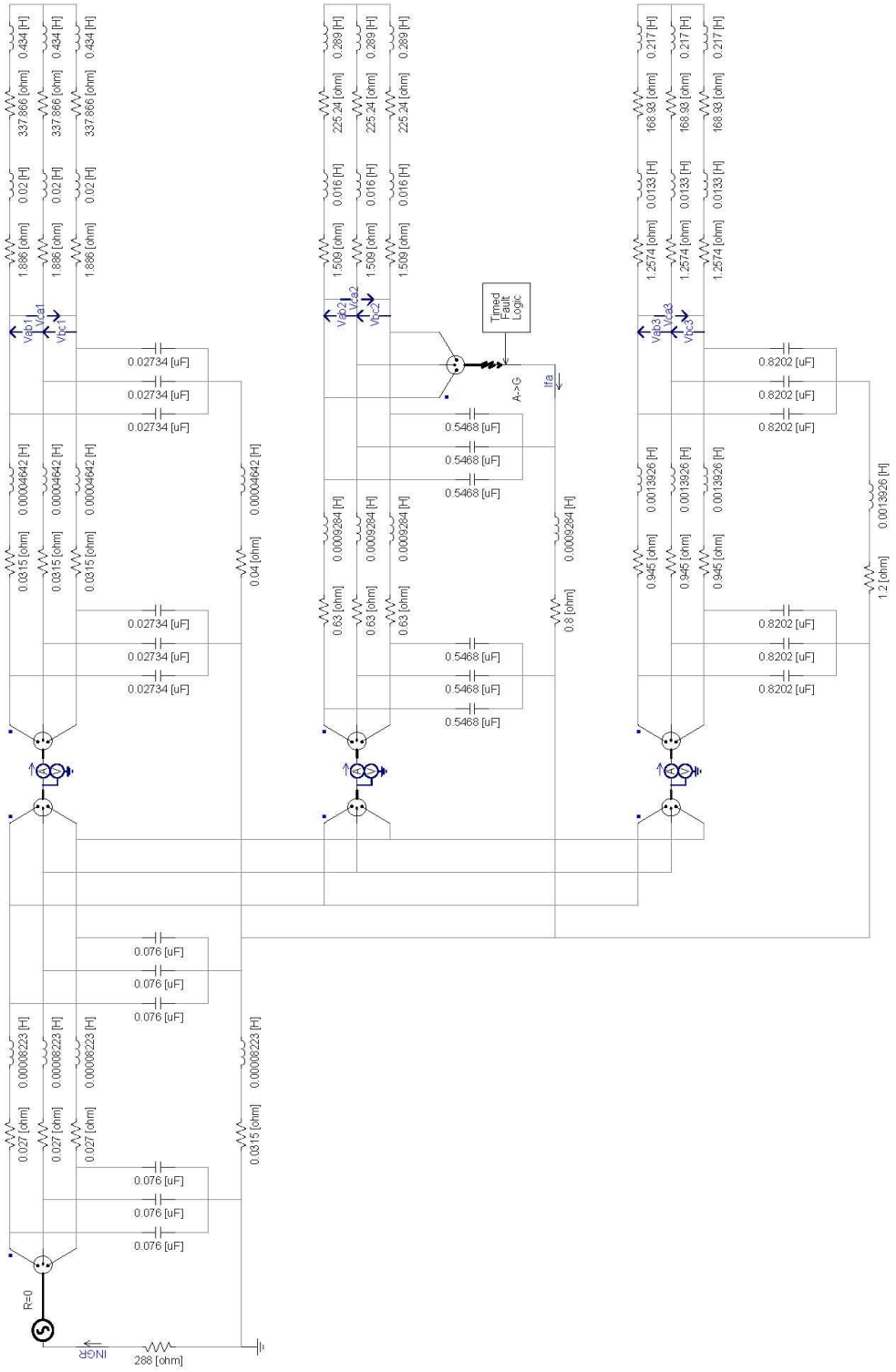

Figure 3.7. Simulation model diagram of the three-branch distribution system with a single-line-to-ground fault on branch 2.

Phase A is shorted to ground during the fault condition, which essentially grounds that line, i.e., zero volts. As a result, the line-to-ground voltages of phases B and C become equal to the unfaulted line-to-line voltage. However, the line-to-line voltages during the fault remain the same as before the fault, primarily because the fault current is limited by the NGR. Figure 3.8 shows the phasormeter plots (from PSCAD/EMTDC) of line-to-line voltages measured before the power center on each branch, and the voltage magnitude and angle remain the same before and after the fault. Therefore, induction motor loads supplied by line-to-line voltages are not significantly affected by a single-line-to-ground fault, provided that this fault current is limited by a NGR.

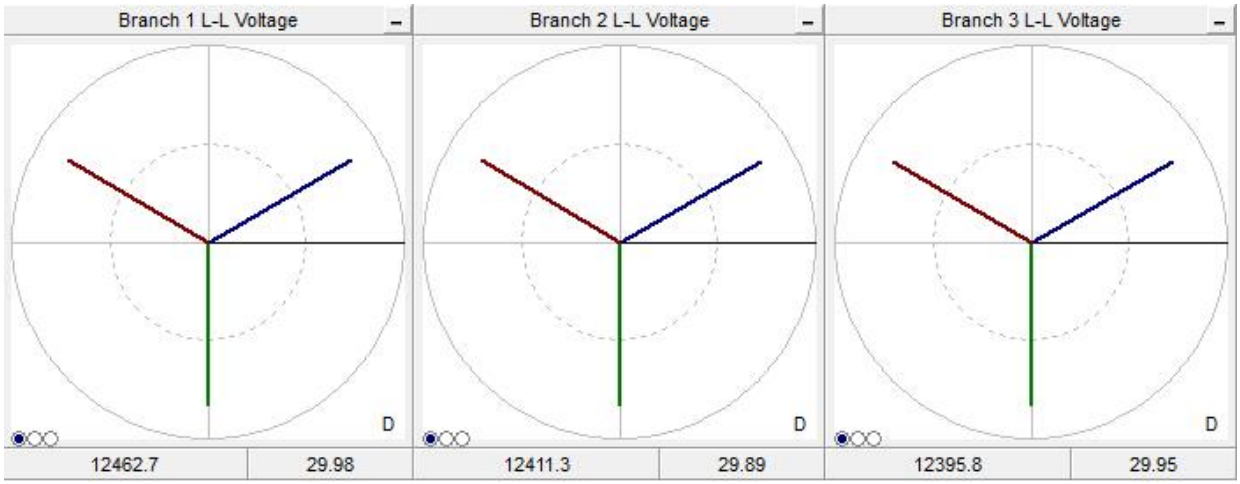

Figure 3.8. Line-to-line voltage measured on each branch during the fault condition.

Table 3.8 presents the simulation results obtained for the magnitudes of fault current, current flowing through the neutral grounding resistor, and zero-sequence current measured on each branch for the three faults. According to the simulation results, the current flowing though the fault point to ground is 34.4 A, which is significantly higher than the NGR limit of 25.0 A. This is because a significant portion of the fault current returns to the source through distributed capacitance rather than the 288 Ω NGR. Moreover, the obtained results in this table are based on a three-branch simplified coal mine power system, while a practical mine could have significantly higher total system capacitance that would cause an increase of the fault current (might be several times higher than the NGR current limit) [Tripathi, 2007]. The zero-sequence

currents flowing through a practical coal mine power system, on both faulted and unfaulted branches, will also be larger than the values shown in the table, and can cause loss of relay selectivity with the 10 A pickup level required for a 25 A limit [Tripathi, 2007]. For example, in this particular case, a fault on branch 1 will cause a trip signal to the circuit breaker on branch 3 because the zero-sequence current exceeds 10 A; likewise for a ground fault on branch 2 (both values highlighted in the table). In addition, a trip signal may also be sent to the circuit breaker protecting branch 2 because the zero-sequence current in branch 2 is very close to 10 A. Note that there would be no false tripping on branch 1 because of the low value of capacitance in that branch.

Table 3.8. Currents measured at different locations with fault occurs at different branches.

Fault location	**Fault current (A)**	**NGR Current (A)**	**Total Zero-sequence current, $3I_{a0}$ (A)**		
			Branch 1	**Branch 2**	**Branch 3**
Branch 1	34.60	24.98	33.43	8.97	**13.35**
Branch 2	34.40	24.84	0.45	29.01	**13.50**
Branch 3	34.24	24.73	0.46	9.13	27.02

3.4. Harmonic Analysis in a Single Line-to-Ground Fault Condition

As mentioned in Chapter 2, an increasing number of drives and non-linear loads produce more harmonics than previously experienced in underground coal mine distribution systems. Harmonic sources in a power system are mainly due to non-linear loads. Sinusoidal voltages applied to these non-linear loads can generate non-sinusoidal current signals at various frequencies. In balanced three-phase systems, the even harmonics generally cancel due to system symmetry so the odd harmonics are the primary content of harmonic distortion. During a single-line-to-ground fault, the fundamental component of the ground fault current can be limited to a very low value, passively, by a properly tuned Peterson coil; however, the ground

fault current can also contain a significant level of harmonics that could cause safety issues for personnel. In this section, a model of the three-branch distribution system with harmonics is developed, and simulations are performed to compare the results with and without the harmonics.

The line-to-line voltage has been shown to remain balanced during the ground fault; therefore, the voltage at the secondary side of a delta-wye transformer can be treated as steady. Thus, the harmonic current signals generated by non-linear loads can be treated as a stable current source. To represent these harmonic sources, integrated modules, connected in parallel with the loads, were used to generate harmonics of current. The simulation diagram is shown in Figure 3.9. Three customized modules, tagged as Harmonic 1, 2 and 3, are added to the previous faulted simulation model and placed at the load end of each branch to serve as harmonic sources. In practical situations, six-bridge and twelve-bridge control circuits are the typical types of non-linear loads; therefore, the frequencies of internal harmonic current generating components include 300, 420, 660, 780, 1020, 1140, 1380, 1500, 1740, and 1860 Hz to represent the 5^{th}, 7^{th}, 11^{th}, 13^{th}, 17^{th}, 19^{th}, 23^{rd}, 25^{th}, 29^{th}, and 31^{st} harmonic signals, respectively. According to recent research, the 5^{th}, 7^{th}, 11^{th} and 13^{th} harmonics play more significant roles than others, with the 5^{th} and 7^{th} harmonic signals being the largest and the 29^{th} and 31^{st} harmonic signals being the smallest [Chen, 2011]. The magnitudes of each harmonic signal are shown in Table 3.9, which is selected based on several surveys in practical situations [Li, 2010; Chen, 2011].

Table 3.9. Harmonic current generating components input parameters.

Harmonic order	5^{th}	7^{th}	11^{th}	13^{th}	17^{th}	19^{th}	23^{rd}	25^{th}	29^{th}	31^{st}
Frequency (Hz)	300	420	660	780	1020	1140	1380	1500	1740	1860
Magnitude (A)	12	12	10	10	3	3	2	2	1	1

The first analysis conducted was an inspection of the harmonics in the line currents in branch 2 before and after the ground fault. Comparison of Figure 3.10 (no fault) and Figure 3.11

(faulted) shows that in lines *b* and *c*, which are unfaulted, there is little change in the harmonics. However, in line *a*, which is the faulted line, it can be observed that there is a slight increase in the 5^{th} and 7^{th} harmonics, while there is a significant increase in the 17^{th} and 19^{th} harmonics. It is noted here that because of plotting limitations in the PSCAD/EMTDC, that the line *a* current had to be rescaled to keep the harmonics at the same scale as those shown in Figure 3.10. Table 3.10 provides a comparison of the harmonics in the faulted branch before and after the fault.

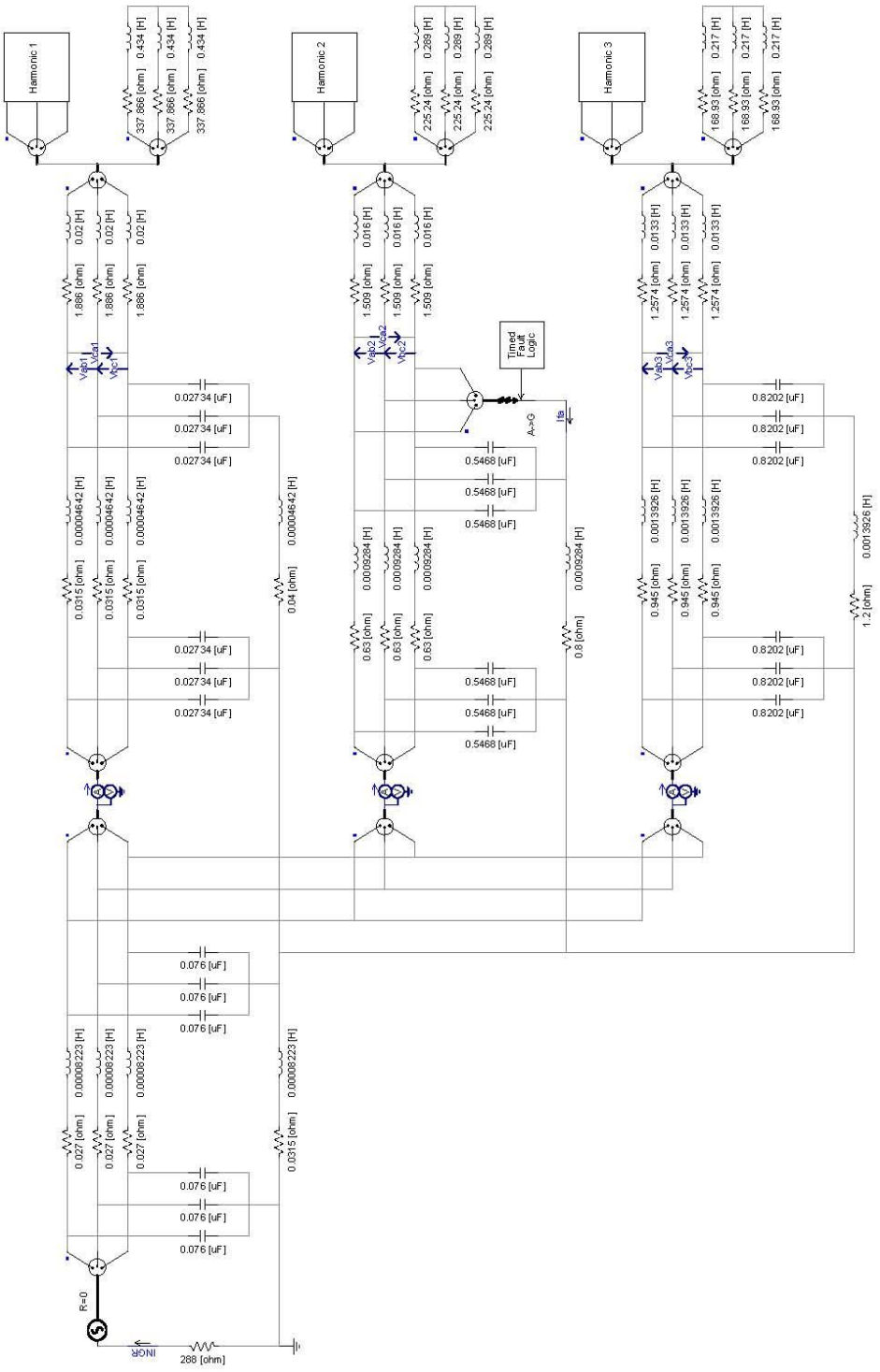

Figure 3.9. Simulation model with harmonic sources added at each branch under a single line-to-ground fault condition.

Figure 3.10. Amplitude spectra of the line currents in branch 2 without a ground fault.

Figure 3.11. Amplitude spectra of the line currents in branch 2 with a ground fault.

Table 3.10. Harmonics of line A of branch 2, before and after ground fault.

Harmonic of Line *a* Current	**Before Fault (A)**	**After Fault (A)**
5th	8.1	8.3
7th	8.1	8.6
9th	0.0	0.0
11th	0.7	1.0
13th	0.7	1.2
15th	0.0	0.0
17th	3.4	6.8
19th	3.4	10.3
21st	0.0	0.0
23rd	1.4	1.9
25th	1.4	0.8
27th	0.0	0.0
29th	0.7	0.1
31st	0.6	0.1

During the occurrence of a single-line-to-ground fault, these harmonic components will be present in the fault current. A Fast Fourier Transform (FFT) of the fault current was used to extract the harmonics, which are presented in Table 3.11.

Table 3.11. Magnitudes of ground fault current components at different frequencies.

Fault current	**Frequency (Hz)**	**Magnitude (A)**	**Fault current**	**Frequency (Hz)**	**Magnitude (A)**
1st	60	34.402	17th	1020	3.938
3rd	180	0.008	19th	1140	8.301
5th	300	0.337	21st	1260	0.004
7th	420	0.677	23rd	1380	3.170
9th	540	0.011	25th	1500	2.048
11th	660	0.369	27th	1620	0.006
13th	780	0.600	29th	1740	1.091
15th	900	0.001	31st	1860	0.892

From these results, it is clear that with harmonic sources in the distribution system, the ground fault current contains both the fundamental and harmonic components, and each order of harmonic signal has a different magnitude at the corresponding frequency. These magnitudes depend upon the injected harmonic signals and system characteristics. Their distribution is shown in Figure 3.12.

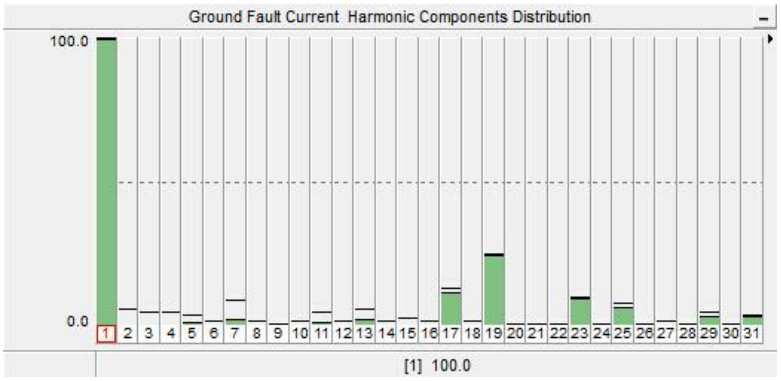

Figure 3.12. Individual harmonic components of ground fault current distribution.

According to Figure 3.12, the 7^{th}, 13^{th}, 17^{th}, 19^{th}, 23^{rd}, 25^{th}, 29^{th} and 31^{st} harmonics are the major components in the ground fault current, and even with the fundamental component fully compensated, these harmonic magnitudes are still large enough to injure personnel or cause nuisance tripping of unfaulted branches. A comparison chart of the ground fault current magnitudes measured in two simulation models (with/without harmonics) is shown below in Table 3.12. Due to the unchanged system distribution parameters, the ground fault current fundamental component in the simulation model with harmonics equals the total ground fault current in the model without harmonics. In the simulation model with harmonics, the total ground fault current reaches 49.1 A, with the harmonic sources being 14.7 A. The simulation results indicate that harmonic currents caused by non-linear loads flow through the entire system, and during a single line-to-ground fault, these currents will flow into the fault point and are part of the ground fault current.

Table 3.12. Ground fault current magnitudes comparison of simulation models with/without harmonics.

Ground fault current (A) (without harmonics)	**Ground fault current (A) (with harmonics)**		
Total	**Total**	**Fundamental**	**Harmonics**
34.4	49.1	34.4	14.7

As described in Chapter 2, the traditional methods commonly used for tuning the Petersen coil in a resonance grounded system are the resonance method, the phase angle method, the signal injection method, etc. With each of these methods, most of the fundamental component of the ground fault current can be neutralized. However, these traditional Peterson coil tuning methods do not account for the harmonic components of the ground fault current because they are all based on measuring the 60-Hz capacitive reactance in order to neutralize the capacitive ground fault current. In some applications, this strategy works perfectly well; however, with harmonics in the distribution system, this passive method cannot effectively neutralize the harmonics in the fault current because reactance is a function of frequency. So, although the value of capacitance will remain relatively constant once the coal mine power system has been established (unless there is a significant modification); the harmonics in the system, and the relevant harmonic impedances, will be variable. Therefore, in order to improve the traditional resonance grounded systems to give them the ability to compensate for both fundamental and harmonic components of ground fault currents during a single line-to-ground fault occurrence, the protection system should have the ability to measure, or predict, the harmonic signals in the fault current and produce the proper neutralizing current.

3.5. Chapter Summary

In this chapter, a simulation model of a high-resistance-grounded mine distribution system is developed and verified for balanced operation. Subsequently, analysis under a single-line-to-ground fault is conducted. The simulation results indicate that the fault current can be

significantly higher than the 25 A NGR current limit, and loss of relay selectivity is observed in unfaulted branches that have a charging current in excess of the 10 A pick-up setting presently used in coal mine distribution systems. Subsequently, a harmonic source is added at the load end of each branch, in parallel with each load, to simulate harmonics produced in modern coal mines. Simulations show that the harmonics of the fault current are not effectively neutralized by a traditional resonance-grounded system tuned for 60-Hz. To deal with these harmonics, a novel method to measure their real-time magnitudes and angles is required and will be developed in the next chapter.

CHAPTER 4

A NOVEL METHOD TO PREDICT HARMONIC COMPONENTS IN THE GROUND FAULT CURRENT

4.1. Introduction

As with typical power systems, coal mine power systems requires power supplies that provide reliability, safety, technical rationality, and economical efficiency. Harmonic distortion, appearing more and more frequently, is considered to have a significant impact on power supply quality. With the development of power electronics technology, an increasing number of nonlinear sources such as frequency conversion and rectifying devices are used in modern coal mining operations and activities, which generate a significant amount of harmonics in power systems. Meanwhile, the level of automation in coal mining is also increasing, especially the application of computers, modern control theory, and precision measurement technologies, which results in an increasing percentage of sensitive loads and much stricter requirements for power supply quality. In a coal mine distribution system, harmonics would not only impact the performance of the power system and equipment, but also increase hazards during system faults. It was shown in Chapter 3 that harmonics flow through the distribution system and appear in the ground fault current during a single-phase-to-ground fault. And, although most of the 60-Hz ground fault current fundamental can be neutralized by a resonance grounded system, the harmonic components could still be large enough to cause arcs and fire, and even injury.

As mentioned in the previous chapter, the method to measure the ground fault current fundamental cannot be used on harmonic components; therefore, measuring the harmonic

content of ground fault current becomes a significant challenge. In this chapter, a novel, real-time method to measure and monitor the harmonic signals is presented and simulation verification is performed.

4.2. A Novel Method to Provide Prediction of Harmonic Components in the Ground Fault Current

4.2.1. Introduction

As mentioned before, the major deficiency of traditional resonance grounded systems is the inability of providing measurement and monitoring of the harmonic components in the fault current. The principle of a typical resonance grounded system is to measure the total system capacitance during system normal operation in order to make predictions of the capacitive ground fault current and then use a Petersen coil to neutralize it. This method can be considered as passive, and due to the stability of the fundamental components it works fine regardless of the fault location. However, unlike the fundamental, harmonics are not stable and would vary for different fault conditions, so they cannot easily be predicted and passively neutralized. Thus, the only way to perform harmonic neutralization is to actively inject compensating signals with equal magnitude and opposite phase angles. To achieve this objective, a real-time measuring method of harmonic fault current during the fault occurrence is developed to provide required magnitudes and phase angle values for the injected signals.

4.2.2. Analysis of a Three-Branch System and its Sequence Network

In many power system analysis cases, symmetrical components theory is usually used to solve problems related to different fault conditions. According to the symmetrical components theory, as mentioned in Chapter 2, any set of unbalanced currents or voltages can be resolved into three sets of balanced phasors named positive, negative, and zero sequence components.

Under normal system operating conditions, only positive sequence components exist in the network, while zero and negative sequence components will appear during a fault condition. During the single phase-to-ground fault condition, the three-phase system can be solved using the sequence networks. In order to perform measurements and prediction of the ground fault current, both its fundamental and harmonic component will be analyzed.

4.2.2.1. Ground Fault Current Fundamental Component Prediction Analysis

Take the previous model as an example with a single-phase-to-ground fault in branch 2. The one-line diagram and equivalent three-phase circuit diagrams are shown in Figure 4.1 and Figure 4.2. The fundamental signal is analyzed first so the harmonics sources are removed from the ends of each branch temporarily for convenience. As before, a three-phase voltage source supplies power to three branches through π-equivalent representation of cables, and loads are represented by series resistance and inductance connected in wye in each phase. Load center transformers are represented by equivalent impedance. The source and load voltage are converted to the distribution voltage level and a NGR is placed between the source neutral point and ground. A single-to-ground fault, represented by the letter F, is located in the middle of branch 2.

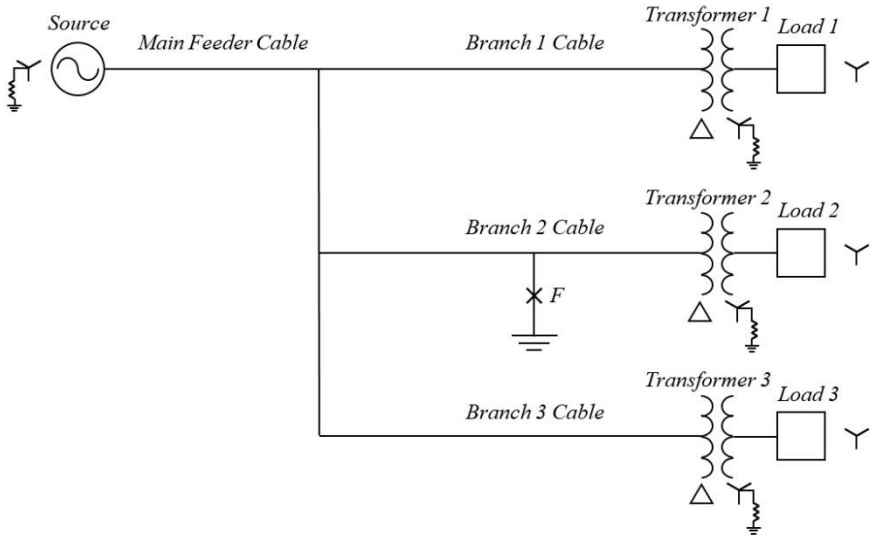

Figure 4.1. One-line diagram of a simplified 3-branch coal mine power system.

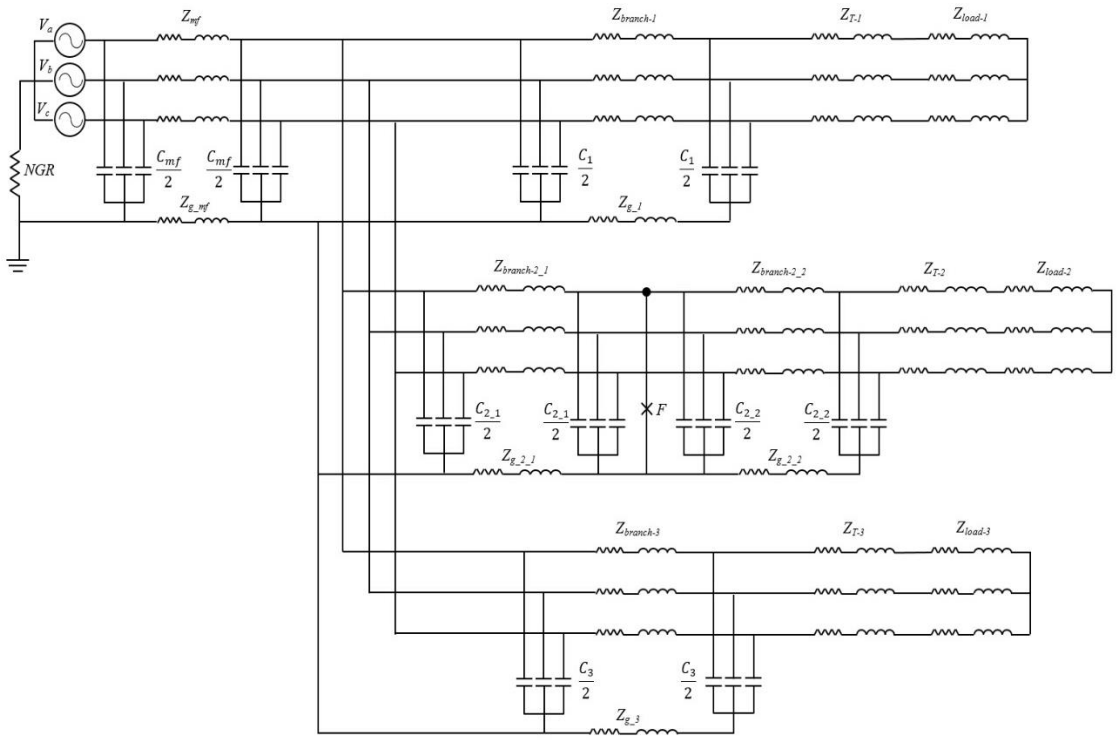

Figure 4.2. Three-phase circuit diagram of a simplified 3-branch coal mine power system.

According to the symmetrical components theory, the sequence network of this 3-branch system with a single-phase-to-ground fault can be drawn, demonstrated in Figure 4.3. In the zero-sequence current path, the load side is open circuited to represent infinite impedance provided by the delta connection of the transformer primary. Meanwhile, the impedance, Z_n, between the source neutral point and ground must be 3 times larger in the zero-sequence network (because $3I_{a0}$ flows through it).

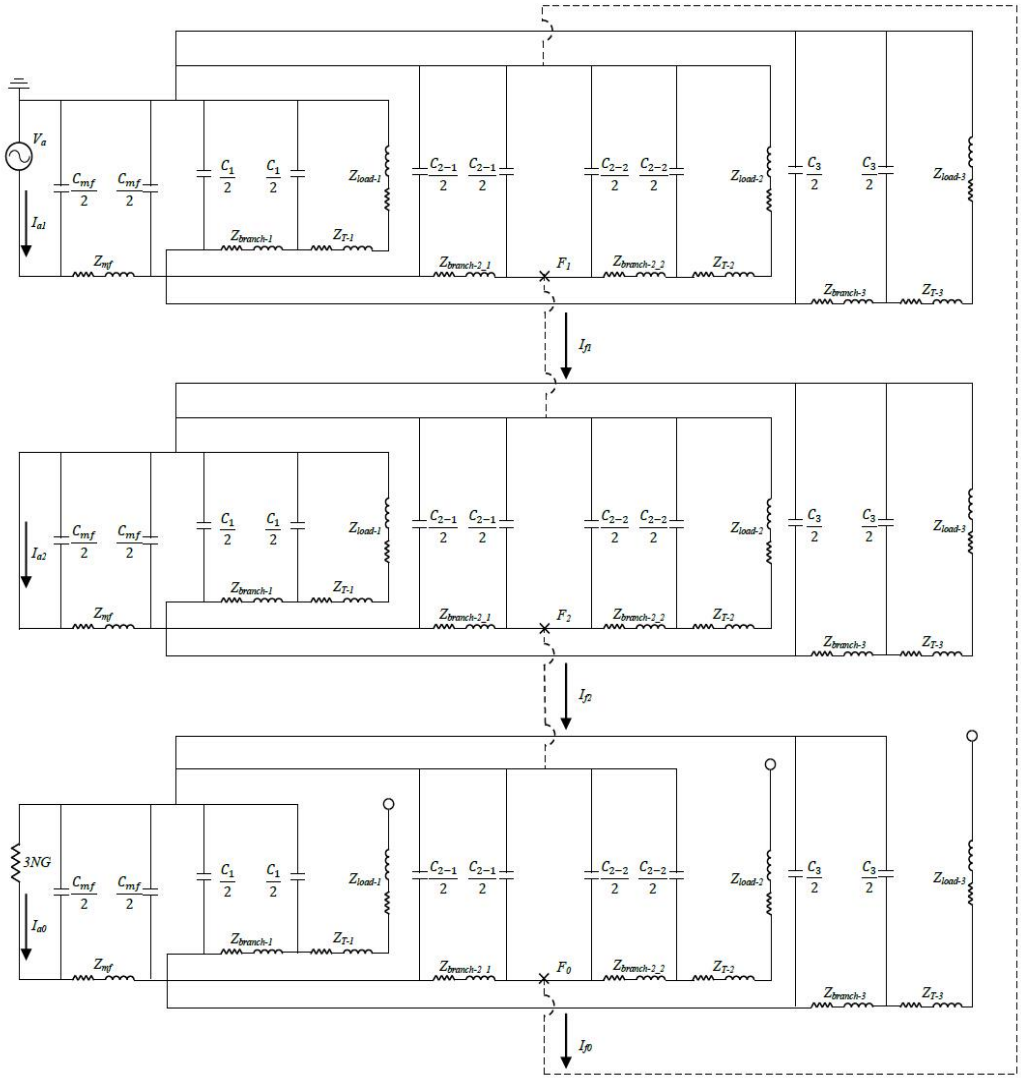

Figure 4.3. Sequence networks diagram of a simplified 3-branch coal mine power system.

Subsequently, both the three-phase model and the sequence network model are developed in PSCAD, shown in Figure 4.4 and Figure 4.5. The following data are used to construct the models:

Utility:

$V_{L\text{-}L}$ = 12470 V R_N = 288 Ω

Main feeder:

$C_{per\text{-}leg}$ = 0.076 μF $R_{per\text{-}phase}$ = 0.027 Ω $L_{per\text{-}phase}$ = 0.08223 mH

R_g = 0.0315 Ω L_g = 0.08223 mH

Branch 1 cable:

$C_{per\text{-}leg}$ = 0.02734 μF $R_{per\text{-}phase}$ = 0.0315 Ω $L_{per\text{-}phase}$ = 0.04642 mH

R_g = 0.04 Ω L_g = 0.04642 mH

Branch 2 cable:

$C_{per\text{-}leg}$ = 0.5468 μF $R_{per\text{-}phase}$ = 0.63 Ω $L_{per\text{-}phase}$ = 0.9284 mH

R_g = 0.8 Ω L_g = 0.9284 mH

Branch 3 cable:

$C_{per\text{-}leg}$ = 0.8202 μF $R_{per\text{-}phase}$ = 0.945 Ω $L_{per\text{-}phase}$ = 1.3926 mH

R_g = 1.2 Ω L_g = 1.3926 mH

Load:

R_1 = 337.866 Ω R_2 = 225.24 Ω R_3 = 168.93 Ω

L_1 = 0.434 H L_2 = 0.289 H L_3 = 0.217 H

Ammeters are placed at the both ends of each branch, and also on the borehole cable and ground wires to measure the instantaneous and RMS currents for each phase and sequence. Both simulation models are set to run 2 seconds and the fault starts at 0 second and remains until the simulation ends.

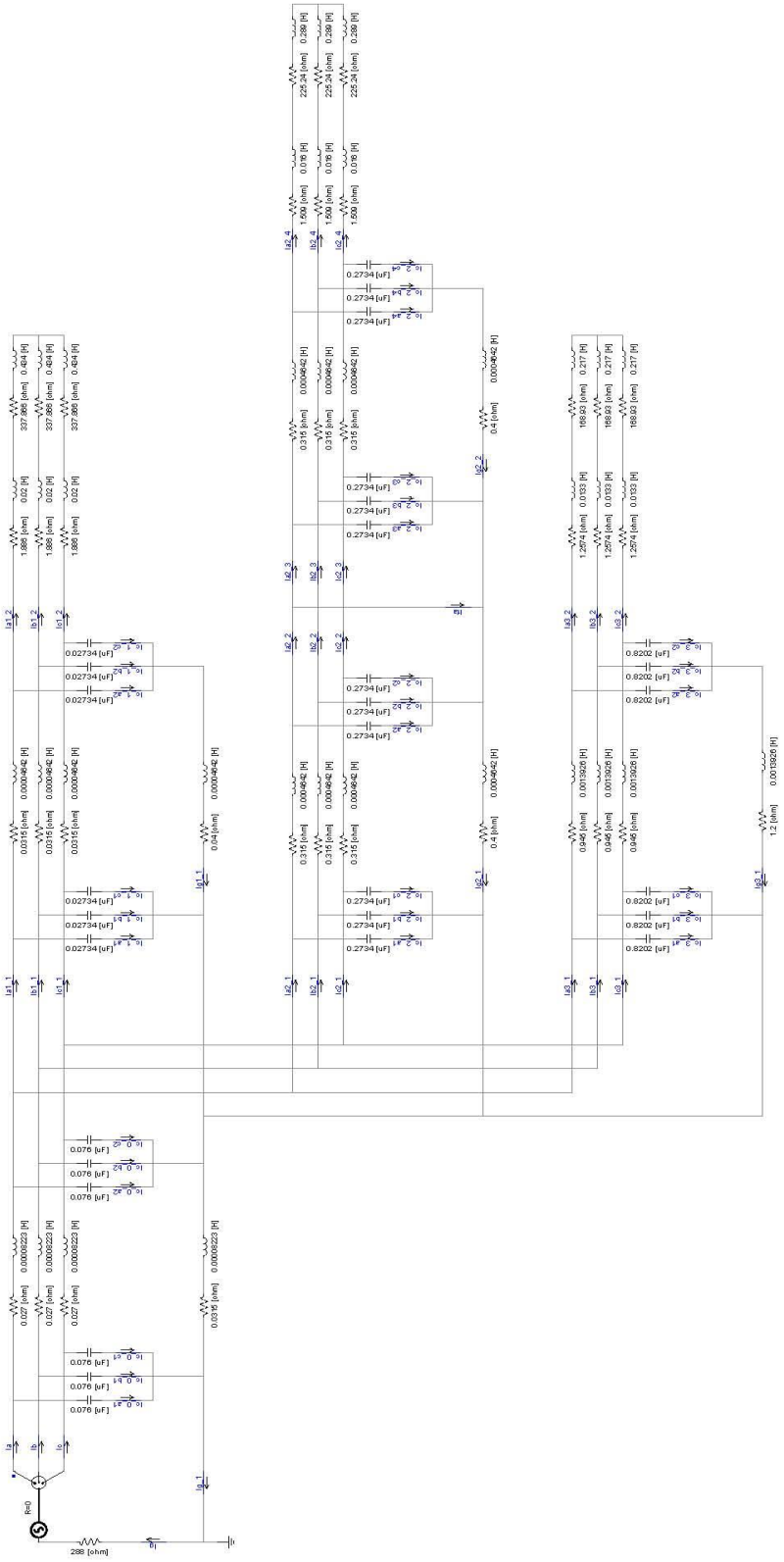

Figure 4.4. Three-phase network simulation model of the three-branch distribution system.

Figure 4.5. Sequence network simulation model of the three-branch distribution system.

A summary of the simulation results for both three-phase and sequence network models are shown in Table 4.1.

Table 4.1. Simulation results comparison between 3-Phase and sequence models.

Current Signal	3-Phase Model Value (A)	Sequence Model Value (A)
I_a	101.42∠-8.3 º	101.42∠-8.3 º
I_b	86.44∠-137.8 º	86.45∠-137.8 º
I_c	73.45∠98.9 º	73.46∠98.9 º
I_{a1}	18.91∠-26.8 º	18.92∠-26.8 º
I_{b1}	18.93∠-146.0 º	18.93∠-146.0 º
I_{c1}	18.70∠93.7 º	18.70∠93.7 º
I_{a2}	51.33∠12.3 º	51.33∠12.4 º
I_{b2}	28.95∠-136.7 º	28.95∠-136.7 º
I_{c2}	24.11∠99.8 º	24.11∠99.8 º
I_{a3}	37.45∠-27.1 º	37.45∠-27.1 º
I_{b3}	38.64∠-135.6 º	38.64∠-135.6 º
I_{c3}	31.30∠100.6 º	31.30∠100.6 º
$I_{c\_0\_a1}$	≈0	≈0
$I_{c\_0\_a2}$	≈0	≈0
$I_{c\_1\_a1}$	≈0	≈0
$I_{c\_1\_a2}$	≈0	≈0
$I_{c\_2\_a1}$	≈0	≈0
$I_{c\_2\_a2}$	≈0	≈0
$I_{c\_2\_a3}$	≈0	≈0
$I_{c\_2\_a4}$	≈0	≈0
$I_{c\_3\_a1}$	≈0	≈0
$I_{c\_3\_a2}$	≈0	≈0
I_{fa}	34.50∠43.6 º	34.50∠43.6 º
I_{g1}	0.22∠-90.2 º	0.22∠-90.2 º
$I_{g2\text{-}1}$	30.29∠-34.4 º	30.29∠-34.4 º
$I_{g2\text{-}2}$	2.22∠-90.1 º	2.22∠-90.1 º
I_{g3}	6.66∠-90.3 º	6.66∠-90.3 º
I_g	24.91∠-0.2 º	24.91∠-0.2 º

The current value of the three-phase model are measured by ammeters directly while the current results for the symmetrical network model are calculated by using standard symmetrical component equations. The currents I_a, I_b, and I_c represent the main feeder currents

on each phase, while the phase currents of each branch correspond to $I_{a(b)(c)1}$, $I_{a(b)(c)2}$, *and* $I_{a(b)(c)3}$. Due to the phase-A to ground fault, a short circuit at the fault point is created and all currents flow though phase A distributed capacitance are driven to zero. I_{fa} is the fault current which equals the summation of fault current components of each phasor, I_{fa0}, I_{fa1}, and I_{fa2}. I_g and $I_{g(x)}$ are the ground wire currents in the borehole cable and branches, respectively. Comparison of simulation results obtained from the three-phase and sequence network models have shown the correctness of these two simulation models.

In the sequence network shown in Figure 4.5, the ground fault current I_{fa} can be expressed according to the symmetrical components theory as:

$$I_{fa} = I_{fa\_p} + I_{fa\_n} + I_{fa\_z} \tag{4.1}$$

where I_{fa_p}, I_{fa_n}, and I_{fa_z} are the positive, negative and zero sequence components of I_{fa}, respectively.

Then the following equations can be obtained based on Kirchhoff's current law:

$$\begin{aligned} I_{fa\_p} &= I_{a22\_p} - I_{a23\_p} \\ I_{fa\_n} &= I_{a22\_n} - I_{a23\_n} \\ I_{fa\_z} &= I_{a22\_z} - I_{a23\_z} \end{aligned} \tag{4.2}$$

We can also get

$$\begin{aligned} I_{a22\_p} &= I_{a21\_p} + I_{c22\_p} + I_{c21\_p} \\ I_{a23\_p} &= I_{a24\_p} + I_{c23\_p} + I_{c24\_p} \\ I_{a22\_n} &= I_{a21\_n} + I_{c22\_n} + I_{c21\_n} \\ I_{a23\_n} &= I_{a24\_n} + I_{c23\_n} + I_{c24\_n} \\ I_{a22\_z} &= I_{a21\_z} + I_{c22\_z} + I_{c21\_z} \\ I_{a23\_z} &= I_{a24\_z} + I_{c23\_z} + I_{c24\_z} \end{aligned} \tag{4.3}$$

Here $I_{a21\_p(n)(z)}$ are the positive, negative and zero sequence components of the phase A current measured at the source side of branch-2 and $I_{a22\_p(n)(z)}$ are those measured at the load side of

branch-2. All the parameters starting with I_c represent currents flowing though each sequence of phase A capacitance, as shown in Figure 4.5. Thus, EQ 4.2 can be reformed by substituting EQ 4.3 as

$$\begin{aligned} I_{fa\_p} &= I_{a21\_p} + I_{a24\_p} + \sum I_{c\_p} \\ I_{fa\_n} &= I_{a21\_n} + I_{a24\_n} + \sum I_{c\_n} \\ I_{fa\_z} &= I_{a21\_z} + I_{a24\_z} + \sum I_{c\_z} \end{aligned} \tag{4.4}$$

Sequence components can be converted into phasors as:

$$\begin{aligned} I_{a21} &= I_{a21\_p} + I_{a21\_n} + I_{a21\_z} \\ I_{a24} &= I_{a24\_p} + I_{a24\_n} + I_{a24\_z} \\ I_{cn} &= I_{cn\_p} + I_{cn\_n} + I_{cn\_z} = 0 \end{aligned} \tag{4.5}$$

Finally, the ground fault current I_{fa} becomes

$$I_{fa} = I_{a21} - I_{a24} \tag{4.6}$$

The equation derivation makes the ground fault current I_{fa} expressed from unmeasurable sequence components to measurable phasor components. In a practical coal mine distribution system, current transformers can be installed at the source and load sides of each branch, and the magnitude and phase angle of I_{a21} and I_{a24} can be obtained. Table 4.2 shows the results taken from the three-phase simulation model and the difference of I_{a21} and I_{a24} is calculated, then EQ 4.6 is proved.

Table 4.2. Simulation results of the source and load sides of phase-A currents and the ground fault current of the three-phase system model.

$\boldsymbol{I_{a21}}$	$\boldsymbol{I_{a24}}$	$\boldsymbol{I_{a21} - I_{a24}}$	$\boldsymbol{I_{fa}}$
51.33∠12.3 º	28.23∠-27.0 º	34.50∠43.6 º	34.50∠43.6 º

4.2.2.2. Ground Fault Current Harmonic Component Prediction Analysis

The method of predicting the ground fault current has been shown for the fundamental signal in a typical three-phase distribution system simulation model with a single line-to-ground fault. In a practical coal mine power system, harmonic components will also be present in the ground fault current. These harmonics can be large enough to cause hazards and should be neutralized as well. Unlike the harmonics caused by system switching and transformers, the harmonic signals discussed here are generated by applying three-phase utilization voltage on non-linear loads and control devices. The utilization voltages are converted from the distribution voltages through load center transformers. During system normal operation, the three voltages on each phase at the transformer primary side are balanced, while under a single line-to-ground fault condition, the voltage of on faulted phase becomes zero and unfaulted phase voltage rise to the original line-to-line voltage. However, the line-to-line voltage balance will remain the same before and after the fault occurrence, which means the input voltage of the delta-wye connected load center transformer remains balanced. Therefore, the output phase voltage of the transformer secondary side will also be balanced, which generates stable harmonic currents from non-linear loads and control devices.

The previous three-phase distribution system simulation model is used with three additional harmonic sources added at the load side of each branch and in parallel with each load, as shown in Figure 4.6. Each harmonic source generates 5^{th}, 7^{th}, 11^{th}, 13^{th}, 17^{th}, 19^{th}, 23^{rd}, 25^{th}, 29^{th}, and 31^{st} harmonic signals with different magnitudes, shown in Table 4.3 below. Ammeters are placed at the sending and receiving ends of each distribution cable to measure the phase currents needed for the ground fault current prediction. The simulation model is set to run 1sec with the fault occurring at 0.5 sec and maintained until the end of the simulation.

Table 4.3. Frequency and magnitudes of each harmonic current generated by the harmonic sources.

Harmonic order	5^{th}	7^{th}	11^{th}	13^{th}	17^{th}	19^{th}	23^{rd}	25^{th}	29^{th}	31^{st}
Frequency (Hz)	300	420	660	780	1020	1140	1380	1500	1740	1860
magnitude (A)	12	12	10	10	5	5	2	2	1	1

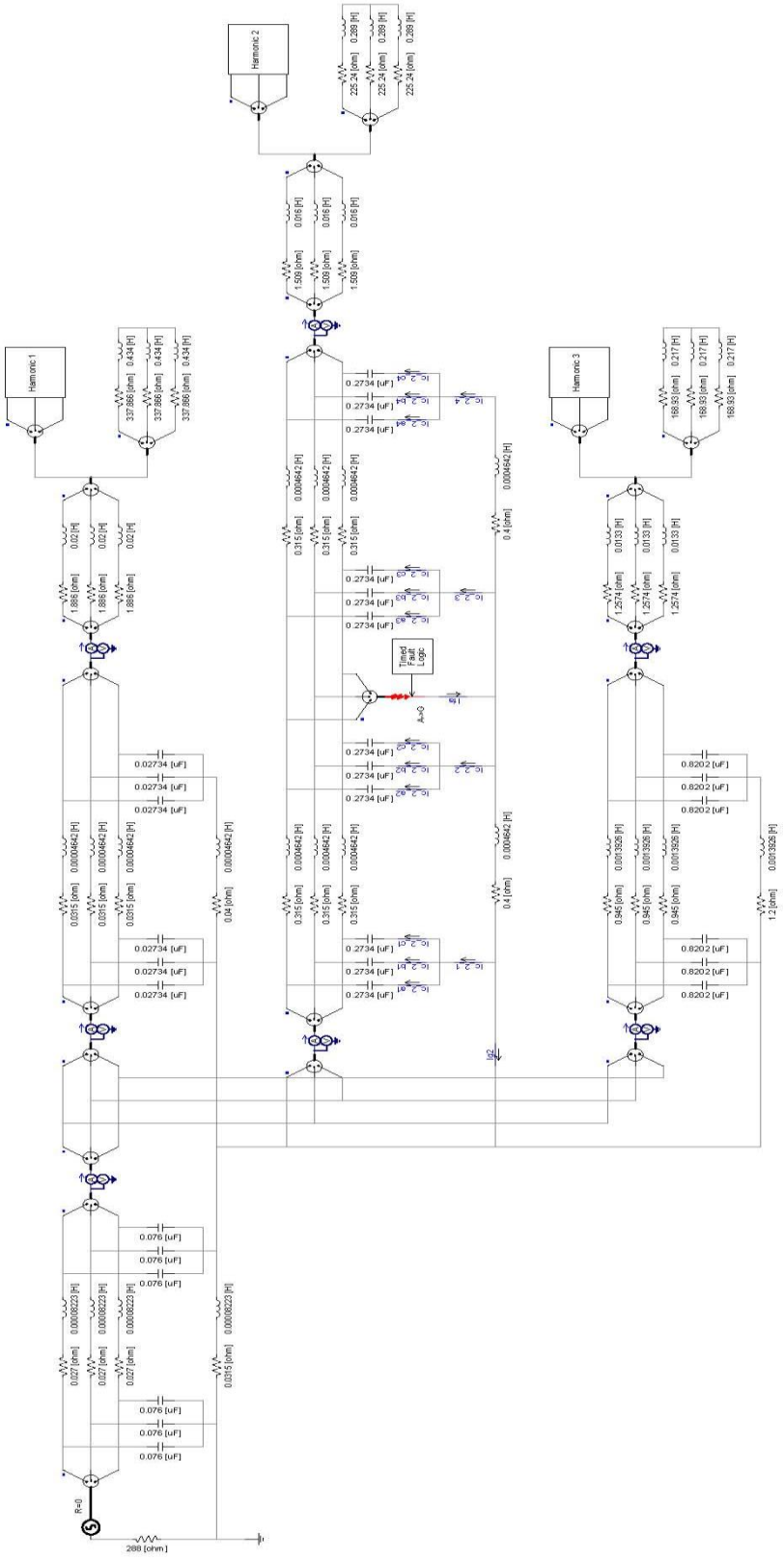

Figure 4.6. Three-phase network simulation model of the three-branch distribution system with harmonic sources.

The simulation results are shown in Table 4.4 where I_{21} and I_{22} are the phase A currents measured at the source and load ends of branch 2 and I_x is their subtraction.

Table 4.4. Simulation results of the measured currents and fault current prediction comparison.

	I_{21}	I_{22}	I_x	I_{fa}	$\lvert I_{fa} - I_x \rvert$
1st	51.38∠12.3 º	28.22∠-27.0 º	34.52∠43.6 º	34.51∠43.6 º	0.01
5th	8.23∠178.4 º	8.06∠179.0 º	0.19∠152.2 º	0.20∠149.6 º	0.01
7th	8.38∠173.2 º	8.02∠179.2 º	0.39∠156.9 º	0.38∠157.3 º	0.03
11th	7.48∠177.4 º	6.66∠179.2 º	0.86∠163.3 º	0.86∠163.4 º	0.00
13th	7.87∠176.8 º	6.64∠179.0 º	1.26∠165.1 º	1.26∠165.2 º	0.00
17th	4.59∠174.4 º	3.31∠178.2 º	1.31∠164.8 º	1.33∠164.6 º	0.01
19th	5.18∠172.3 º	3.30∠177.6 º	1.92∠163.2 º	1.94∠163.1 º	0.02
23rd	3.10∠162.6 º	1.29∠175.0 º	1.86∠154.0 º	1.89∠153.8 º	0.04
25th	4.58∠147.7 º	1.26∠173.7 º	3.49∠138.6 º	3.57∠138.4 º	0.08
29th	1.42∠33.7 º	0.58∠171.2 º	1.89∠21.7 º	1.95∠21.5 º	0.06
31st	0.52∠21.9 º	0.57∠172.9 º	1.05∠6.7 º	1.09∠6.6 º	0.04

The simulation results indicate that in each frequency, including fundamental and harmonics, the subtractions of I_{21} and I_{22} are very close to the ground fault current I_{fa}, with small errors existing in both the fundamental and harmonic components. During the single line-to-ground fault, the line-to-ground voltage of the faulted phase drops to zero which causes no current flow through the distributed capacitance of the faulted phase. However, harmonic currents are supplied by the harmonic sources from the load side and a small portion of these currents will flow through the distributed capacitance of the faulted phase. Compared with the ground fault current, the errors of fundamental and each harmonic are considered small enough to be negligible.

4.2.3. The Novel Ground Fault Current Prediction Method Verification for Different Fault Locations

In the previous simulation model shown in Figure 4.6, the single line-to-ground fault is simulated at the middle of the faulted branch. To further verify the novel ground fault current prediction method, two additional three-phase distribution system models are developed to simulate the conditions that faults located at different positions of the cable.

4.2.3.1. Ground Fault Occurrence at the Source Side of the Faulted Branch

Similar to the previous model shown in Figure 4.6, a three-phase distribution system is modeled with a single line-to-ground fault on phase A at branch 2. The fault is placed at the head of branch 2 in order to simulate the condition that there is a failure on the distribution cable close to the switchhouse. All input parameters and simulation settings remain the same as in the previous model. The simulation model is shown in Figure 4.7 and the results are demonstrated in Table 4.5.

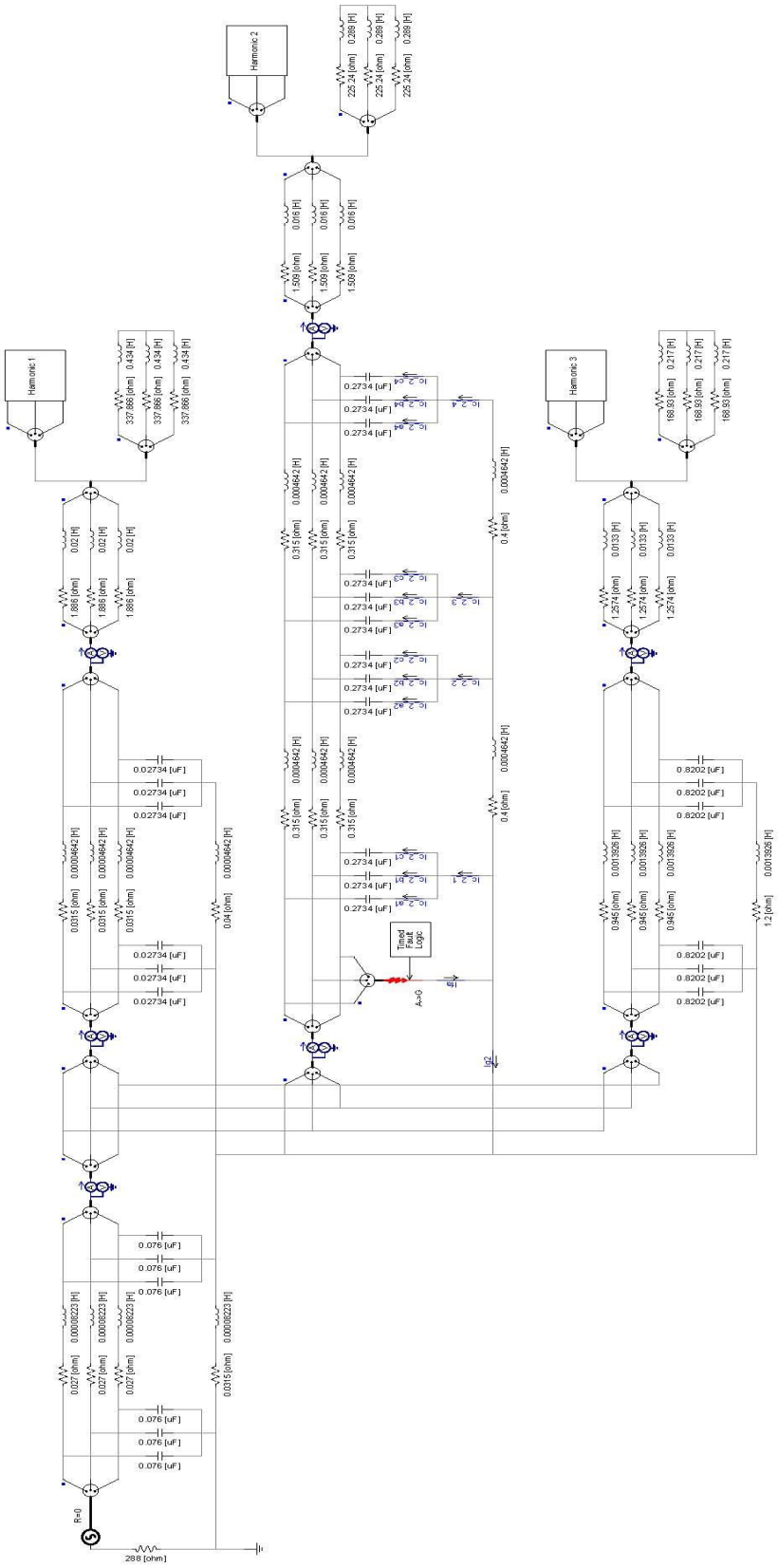

Figure 4.7. Three-phase simulation model with fault occurs at the head of branch 2.

Table 4.5. Simulation results and fault current prediction comparison with fault occurring at the source side of branch 2.

	I_{21}	I_{22}	I_x	I_{fa}	$\lvert I_{fa} - I_x \rvert$
1st	51.44∠12.5 º	28.23∠-26.9 º	34.62∠43.7 º	34.61∠43.7 º	0.01
5th	8.14∠178.8 º	8.06∠179.0 º	0.08∠158.3 º	0.07∠157.0 º	0.01
7th	8.18∠178.9 º	8.03∠179.2 º	0.15∠163.4 º	0.13∠163.6 º	0.02
11th	6.98∠178.7 º	6.66∠179.2 º	0.33∠168.4 º	0.27∠168.7 º	0.06
13th	7.11∠178.4 º	6.65∠179.0 º	0.46∠169.8 º	0.38∠170.1 º	0.08
17th	3.72∠177.4 º	3.31∠178.2 º	0.42∠171.0 º	0.35∠171.0 º	0.07
19th	3.84∠176.6 º	3.30∠177.5 º	0.54∠171.1 º	0.45∠170.9 º	0.09
23rd	1.64∠173.9 º	1.30∠175.1 º	0.34∠169.4 º	0.29∠169.0 º	0.05
25th	1.69∠172.0 º	1.27∠173.5 º	0.42∠167.5 º	0.37∠167.3 º	0.06
29th	0.90∠169.2 º	0.58∠171.5 º	0.32∠165.0 º	0.28∠164.5 º	0.04
31st	0.97∠168.5 º	0.57∠171.9 º	0.41∠163.8 º	0.37∠163.2 º	0.04

Compared with the first simulation model with the fault occurring in the middle of the branch, the ground fault current harmonic components drop to a lower magnitude. However, the subtractions of the measured phase A currents I_{21} and I_{22} are still very close to the fault currents at each harmonic frequency and the errors are small enough to be negligible.

4.2.3.2. Ground Fault Occurrence at the Load Side of the Faulted Branch

In this simulation model, the fault is placed at the load side of branch 2 to simulate ground fault at the load side of the distribution cable. The three-phase distribution system remains the same and all its input parameters and simulation settings remain the same as the previous model. Figure 4.8 demonstrates the structure of the simulation mode and the results are presented in Table 4.6.

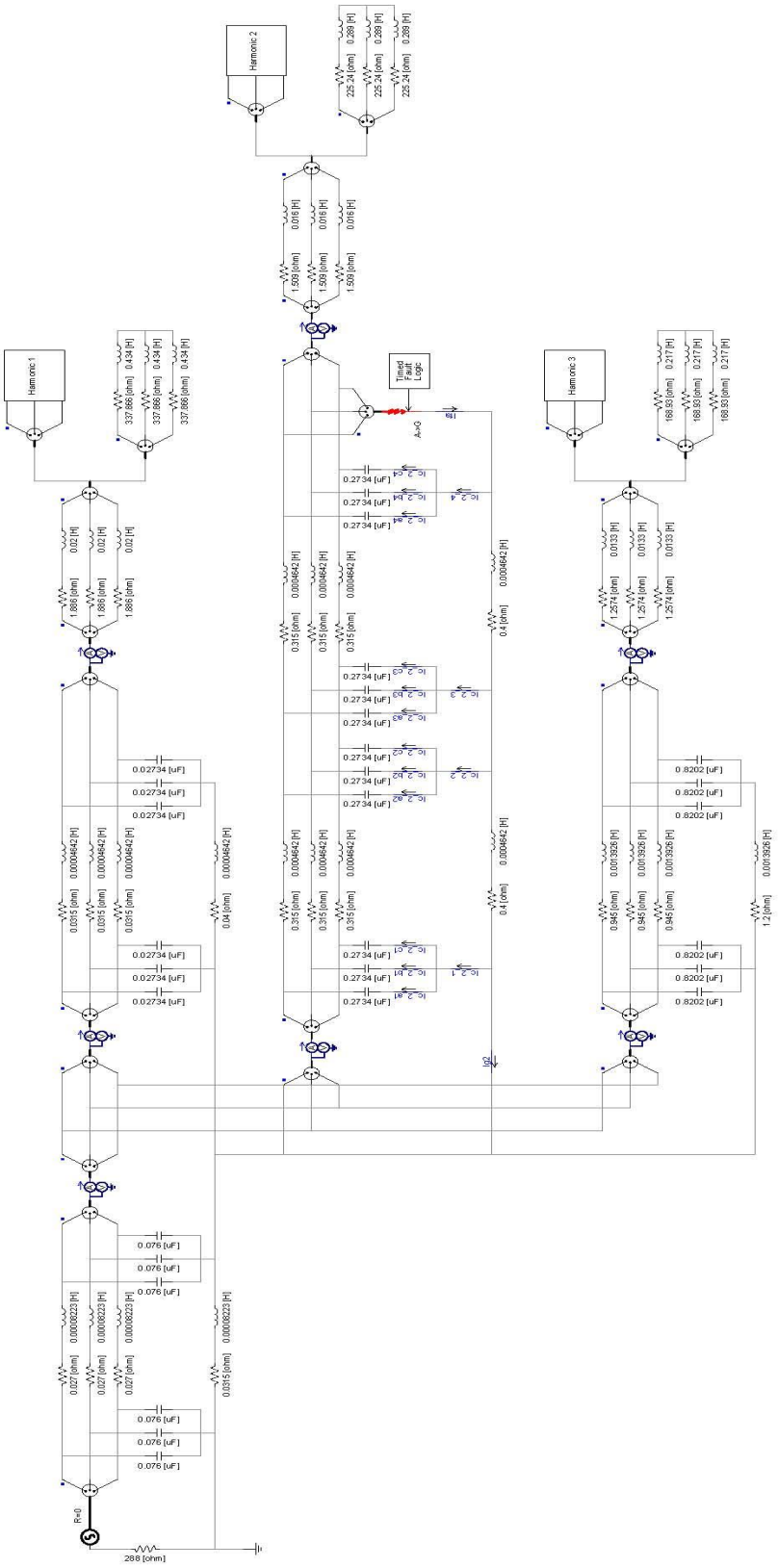

Figure 4.8. Three-phase simulation model with fault occurs at the end of branch 2.

Table 4.6. Simulation results and fault current prediction comparison with fault occurring at the end of branch 2.

	I_{21}	I_{22}	I_x	I_{fa}	$\lvert I_{fa} - I_x \rvert$
1st	51.31∠12.2 º	28.21∠-27.1 º	34.47∠43.4 º	34.46∠43.4 º	0.01
5th	8.34∠178.0 º	8.06∠179.1 º	0.33∠149.6 º	0.34∠149.9 º	0.01
7th	8.62∠177.4 º	8.03∠179.2 º	0.65∠154.4 º	0.68∠154.9 º	0.03
11th	8.13∠175.5 º	6.66∠179.2 º	1.54∠159.3 º	1.63∠159.6 º	0.09
13th	9.04∠173.6 º	6.64∠179.0 º	2.51∠159.2 º	2.65∠159.5 º	0.14
17th	6.76∠163.9 º	3.30∠178.3 º	3.65∠150.9 º	3.88∠151.0 º	0.22
19th	10.17∠145.6 º	3.29∠177.7 º	7.58∠132.7 º	8.05∠132.8 º	0.48
23rd	2.16∠39.2 º	1.31∠175.2 º	3.23∠22.9 º	3.45∠22.9 º	0.22
25th	0.89∠29.6 º	1.27∠173.2 º	2.06∠8.1 º	2.20∠8.1 º	0.14
29th	0.07∠88.2 º	0.59∠171.8 º	0.58∠-1.3 º	0.63∠-1.3 º	0.05
31st	0.11∠129.5 º	0.56∠171.0 º	0.48∠-0.6 º	0.52∠-0.6 º	0.04

Results obtained from this simulation model indicate that when the single line-to-ground fault occurs at the load end of the faulted branch, the subtractions of the two measured faulted phase currents are still very close to the ground fault currents at the fundamental and each harmonic frequencies, and the errors are small enough to be negligible.

According to the results obtained from these three simulation studies shown above, the predicted ground fault currents are equal or very close to the actual value, at both the fundamental and each harmonic frequency. Errors occur with the change of fault locations, and largest values appears when the fault occurs at the load end of the faulted branch. Harmonic components of the ground fault current also have the largest magnitude when the fault locates at the load side. It is because the distributed capacitance between the fault location and the bus (switchhouse) create return paths and part of the ground fault currents flow through this capacitance and back into the system. Therefore, the prediction errors can be considered being caused by part of the faulted branch distributed capacitance which is a small portion of the entire system capacitance so that the errors can be very small (less than 0.5 A) and neglected.

4.3. Chapter Summary

In this chapter, a novel method to predict the fundamental and harmonic components of ground fault currents was introduced. The principle of the novel prediction method can be identified as the ground fault current is equal or very close to the subtraction of two currents, which are measured on the faulted phase at each side of the faulted branch.

A simplified three-branch distribution system with a single line-to-ground fault occurring on phase A at the middle of branch 2 is used to simulate the fault situation of a coal mine distribution system. The corresponding three-phase and sequence networks of the three-branch distribution system are developed to analyze the current path and relationships during a single line-to-ground fault occurrence. The novel prediction method is derived at the fundamental frequency first without harmonic signals. Then three harmonic sources are added at the load end of each branch and parallel with the load. Simulation results indicate that the novel prediction method can be generalized to the fault current of each harmonic frequency. To analyze the correctness of the novel method under different fault location conditions, two similar simulation models are developed: one has the ground fault located at the source side of the distribution cable, and another one has the fault placed close to the load. Results obtained from these two simulation models have verified the feasibility of the novel method when the fault occurs at different locations. It is noticed that small errors appear in all these simulations which is mainly caused by the distributed capacitance of the faulted branch.

CHAPTER 5

THE IMPLEMENTATION OF GROUND FAULT CURRENT NUTRALIZATION AND FAULT LOCATION DETECTION

5.1. Introduction

In the previous chapter, a novel method for predicting ground fault current was developed and verified by a three-branch distribution system simulation model. According to the simulation results, the prediction method has the ability to predict not only the fundamental component of fault current, but also the harmonic components. The predicted value of the ground fault current at each frequency is determined as the difference between current at the source end and the load end of the each branch. Errors between the predicted values and the "actual" value as calculated by the simulation model exist at several frequencies, but they are small enough to be negligible.

After making predictions for the ground fault current, the magnitude and phase angle of the fault current at each frequency is known and can be neutralized. In this chapter, an injection method is used to actively neutralize the ground fault current, including the fundamental and harmonic components, by injecting current signals into the distribution system neutral point, i.e., the substation transformer neutral. Also, a fault location method is described based on the prediction method to determine the faulted branch in order to isolate the fault and avoid nuisance tripping.

5.2. Ground Fault Current Neutralization

5.2.1. Introduction

During a single-line-to-ground fault, the ground fault current consists of the fundamental and also harmonic components. According to the different types of injected current, two types of compensation systems are presented and analyzed. The first one is a combination of passive and active compensation. It has been shown that Petersen coil applications have the ability to control the fault current fundamental component; therefore, the injected current only needs to compensate the harmonic components in this case. Another compensation system is an optimization of a high-resistance grounded system, which injects both fundamental and harmonic signals to fully compensate the ground fault currents. The three-branch system with a single line-to-ground fault located at the load end of branch 2 is modeled and the simulation results are compared and the advantages and disadvantages are discussed.

5.2.2. Compensation with Petersen Coil Involved

In a traditional application, the Petersen coil is connected between the system neutral point and the ground. It is tuned such that its 60-Hz reactance is equal to the absolute value of the reactance of the distributed 60-Hz capacitive reactance of the system to drive the ground fault current fundamental to nearly zero. In the simulation model, the neutral grounding resistor is replaced by an inductor with an inductive reactance equal to the absolute value of the system distributed capacitive reactance. A current source is connected in parallel with the Petersen coil to inject compensating harmonic signals. Figure 5.1 illustrates the structure of this compensation system, where L_{pc} and R_{pc} represent the inductance and resistance of the Peterson coil. Subsequently, simulation is performed to determine the effectiveness of this compensation system.

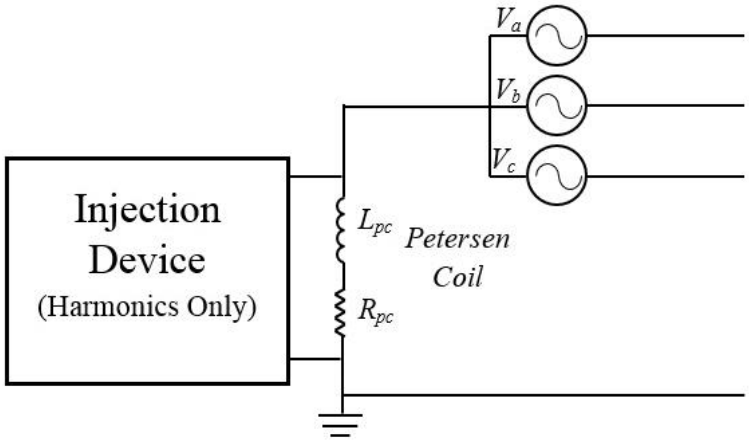

Figure 5.1. Structure of the compensation system of a Petersen coil in parallel with an active current injection device.

5.2.2.1. Petersen Coil Inductance Calculation

The Petersen coil inductance is calculated on the basis of the system total distributed capacitance. According to the simulation model parameters, the system lumped per-phase capacitance is calculated as:

$$C_{1-\emptyset} = 0.1520 + 0.0547 + 1.0936 + 1.6404 = 2.9407\ \mu F \tag{5.1}$$

The per-phase system lumped capacitive reactance is:

$$X_{c1-\emptyset} = -\frac{1}{2 \times \pi \times f \times C_{1-\emptyset}} = -902.024\ \Omega \tag{5.2}$$

where f is the system fundamental frequency of 60Hz.

Thus, the required value of the Petersen coil can be calculated as:

$$L_{pc} = -\frac{\frac{-X_{c1-\emptyset}}{3}}{2 \times \pi \times f} = 0.798\ H \tag{5.3}$$

with the Petersen coil 60-Hz inductive reactance of :

$$X_{L-pc} = 2 \times \pi \times f \times L_{pc} = 300.839\ \Omega \tag{5.4}$$

Thus, the maximum rms value of the current flow through the Petersen coil can be calculated as:

$$I_{pc} = \frac{V_{\emptyset}}{X_{L-pc}} = \frac{7200}{300.839} = 23.933\ A \tag{5.5}$$

In the simulation model, the Petersen coil is modeled as a 0.798 H inductor connected in series with a 0.10 Ω resistor. The 0.10 Ω resistor represents the resistance of the Petersen coil.

5.2.2.2. Harmonic Signal Injection

In the simulation model, a customized block is connected in parallel with the Petersen coil to represent the current injection device. It injects the 5^{th}, 7^{th}, 11^{th}, 13^{th}, 17^{th}, 19^{th}, 23^{rd}, 25^{th}, 29^{th}, and 31^{st} harmonic signals. It is important to note that the magnitude and angle of each injected signal is not simply equal to the predicted value of the fault current. At the fundamental frequency, the system inductance and reactance characteristics have little effect because of the relatively low supply frequency. However, for the harmonic frequencies, the system capacitance and inductance play a relatively significant role, especially at the higher frequencies, because the system harmonic reactance values are a function of frequency. When a current at a certain harmonic frequency is injected into the system neutral point, it will flow through the distribution system and be affected by the system characteristics. When this current signal arrives at the fault location, its magnitude and angle will be different from the initial injected value. Therefore, in order to obtain the desired compensation signal at the fault location, it is necessary to find the magnitude and phase angle relationships between the initial injecting current and its corresponding signal at the fault location. This relationship is determined by a coefficient termed the *injection factor* and its value at each frequency can be obtained by several measurements. After the distribution system is established, a single line-to-ground fault can be artificially created at each branch, and the ground fault current can be

determined under this circumstance. Current signals of magnitude 1.0 A and phase angle 0 º are injected into the system from the neutral point at each harmonic frequency, thus, their corresponding signals for each branch can be measured at the fault location. Then the injection factor at each harmonic frequency of all branches can be recorded in a data acquisition system. Once a single line-to-ground fault occurs, these injection factors will be called and the required injecting current can be calculated as:

$$I_{injected} = \frac{I_{predicted}}{X} = \frac{I_1 - I_2}{X} \tag{5.6}$$

where I_1 and I_2 are the measured phase currents at the source and load ends of the faulted branch and X is the injection factor. Values are recorded from the simulation model current signal at each harmonic frequency with 1.0 A magnitude and 0.0 ºphase angle injected into the system neutral point. The results are shown in Table 5.1. After applying EQ 5.6, the injection factor X is calculated at each harmonic frequency and the results are presented in Table 5.2.

Table 5.1. Ground fault current measurements from injection of 1.0∠0º A into the system neutral point.

Harmonic	$I_{injected}$ (A)	I_{fault} (A)	Harmonic	$I_{injected}$ (A)	I_{fault} (A)
5th	1.0∠0 º	1.053∠-1.7 º	19th	1.0∠0 º	4.853∠-29.0 º
7th	1.0∠0 º	1.108∠-2.1 º	23rd	1.0∠0 º	3.291∠-159.3 º
11th	1.0∠0 º	1.341∠-3.7 º	25th	1.0∠0 º	1.643∠-171.0 º
13th	1.0∠0 º	1.560∠-5.6 º	29th	1.0∠0 º	0.626∠-178.8 º
17th	1.0∠0 º	2.710∠-14.0 º	31st	1.0∠0 º	0.409∠179.2 º

Table 5.2. The injection factor, X, at each harmonic frequency with a Petersen coil in parallel with the injection device.

Harmonic	X	Harmonic	X
5th	1.053∠-1.7 º	19th	4.853∠-29.0 º
7th	1.108∠-2.1 º	23rd	3.291∠-159.3 º
11th	1.341∠-3.7 º	25th	1.643∠-171.0 º
13th	1.560∠-5.6 º	29th	0.626∠-178.8 º
17th	2.710∠-14.0 º	31st	0.409∠179.2 º

In a practical distribution system, the injection factor can be measured and saved by simulating a fault. Subsequently, when a ground fault occurs in the system, the processing module receives the measurements of I_1 and I_2 and calls the saved injection factor for each harmonic frequency, and the required injection currents can be calculated by using EQ 5.6.

5.2.2.3. Simulation Results and Analysis

Simulations were performed to check the prediction of the fault current. Two conditions, with and without harmonic injection, are simulated to demonstrate the effect of the harmonic signal compensation. Both simulations are run for five seconds; the single-line-to-ground fault occurs at one second and remains for the remainder of the simulation time. Figure 5.2 shows the ground fault current waveform without the active compensation and the magnitude of ground fault current at each harmonic frequency is shown in Table 5.3. It is observed that the fault current is still significant with only the fundamental neutralized by the Petersen coil. Figure 5.3 shows the ground fault current waveform before and after the fault occurrence with the harmonic injection system included. After the fault occurs, the injection device takes 0.20 sec to receive the calculated values and perform the active injection. The simulation result is presented in Table 5.4.

Table 5.3. Magnitude of ground fault current without harmonic injection system.

	Total (A)	1st (A)	5th (A)	7th (A)	11th (A)	13th (A)	17th (A)	19th (A)	23rd (A)	25th (A)	29th (A)	31st (A)
I_{fa}	11.11	0.03	0.3	0.66	1.63	2.65	4	9.06	3.73	2.26	0.63	0.50

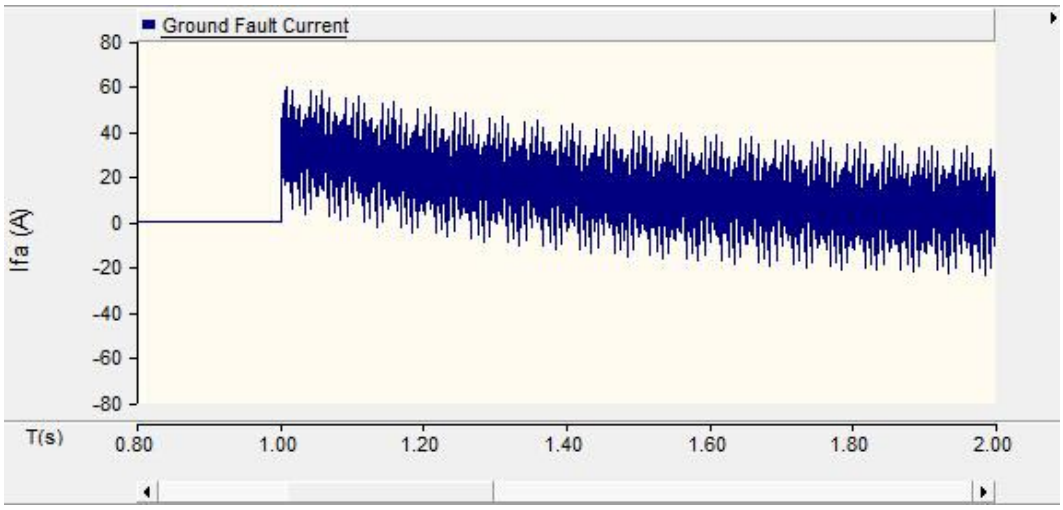

Figure 5.2. Plot of ground fault current waveform without harmonic injection.

Table 5.4. Magnitude of ground fault current, I_{fa}, and the current through Petersen coil, I_{pc}, at each frequency with harmonic injection system.

	Total (A)	1st (A)	5th (A)	7th (A)	11th (A)	13th (A)	17th (A)	19th (A)	23rd (A)	25th (A)	29th (A)	31st (A)
I_{fa}	0.53	0.03	0.02	0.02	0.04	0.14	0.21	0.38	0.26	0.07	0.02	0.04
I_{pc}	24.78	23.84	0.34	0.62	1.19	1.61	1.77	1.77	1.03	1.27	0.87	1.05

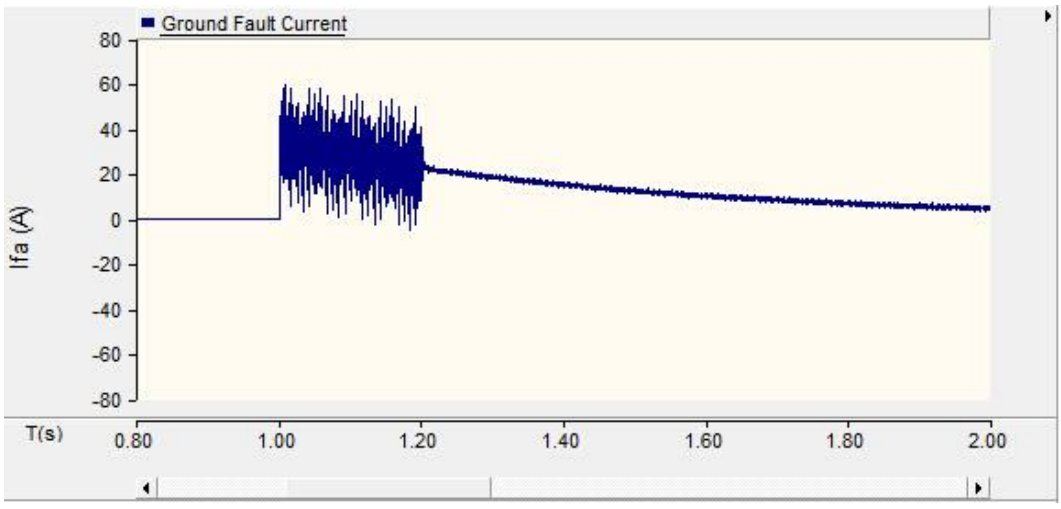

Figure 5.3. Plot of ground fault current with Petersen coil and the harmonic injection system connected in parallel.

From these simulation results, it is clear that the Petersen coil is able to drive ground fault fundamental to nearly zero. Meanwhile, the harmonic components of the ground fault current are also driven close to zero after the harmonic compensation signals are injected.

These results show that the proposed compensation system could limit the fundamental and harmonic components of ground fault current to very low values. However, the proposed system drives the fault current to a very low value, traditional zero-sequence relaying cannot be used for ground fault detection. Consequently, a different ground fault location technique must be developed. It is to some extent limiting the implementation of this compensation system.

5.2.3. Full-Current Compensation

Another type of compensation system is to use the neutral grounding resistor and directly connect an injection device in parallel with it. This can be considered as an improvement over the presently used high-resistance grounded system. Different from the one discussed previously, the injection device is required to compensate both the fundamental and the harmonic components of the ground fault current due to the absence of the Petersen coil; therefore, it is defined as full compensation. Figure 5.4 demonstrates the structure of this compensation system, where the neutral grounding resistor resistance is 288 Ω.

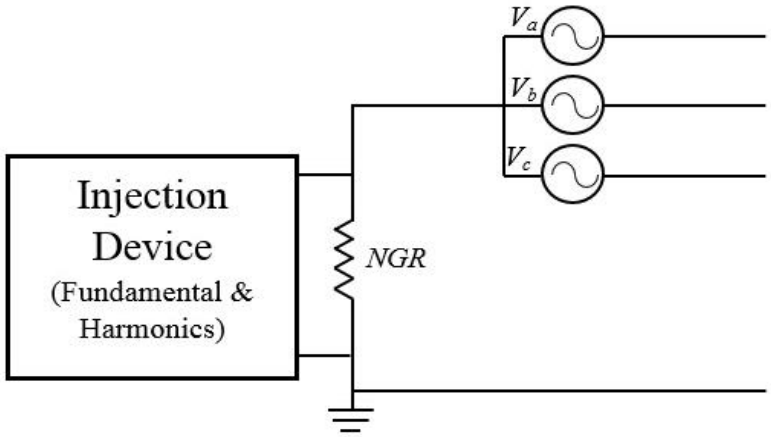

Figure 5.4. Structure of the compensation system of a neutral grounding resistor in parallel with the injection device.

5.2.3.1. Harmonic Injection Factor Measurements

Similar to the first compensation system, the harmonic injection factor, *X*, needs to be determined at each harmonic frequency. Signals with magnitude of 1.0 A and phase angle of 0.0˚ for each harmonic frequency are injected into the system neutral point and the results are presented in Table 5.5. It can be observed that by replacing the Petersen coil with the NGR, the injection factor at each harmonic frequency is different from the values determined for the previous compensation system. Because the fundamental frequency is 60 Hz, which is relatively low, the injected fundamental signal would have the same magnitude and phase angle as the prediction.

Table 5.5. Injection factor, X, at each harmonic frequency for a grounding system with the NGR in parallel with the injection device.

Harmonic	X	Harmonic	X
5th	1.047∠-2.4 º	19th	4.292∠-39.3 º
7th	1.107∠-3.2 º	23rd	3.027∠-150.4 º
11th	1.328∠-6.0 º	25th	1.599∠-165.8 º
13th	1.543∠-8.6 º	29th	0.620∠-175.8 º
17th	2.612∠-20.1 º	31st	0.388∠178.4 º

5.2.3.2. Simulation Results and Analysis

Simulation is conducted to determine the performance of the protection system for a single-line-to-ground fault. As with the previous model, the simulation period is 5.0 seconds and the single-line-to-ground fault occurs at 1.0 sec and remains for the remainder of the simulation time. After the fault occurs, the injection device takes 0.20 sec to receive calculated values and perform active compensation.

5.2.3.2.1. Level of Ground Fault Current

The simulation results are presented in Table 5.6 and the ground fault current waveforms are shown in Figure 5.5.

Table 5.6. Magnitude of ground fault current and the current through the neutral grounding resistor at each frequency.

	Total (A)	1st (A)	5th (A)	7th (A)	11th (A)	13th (A)	17th (A)	19th (A)	23rd (A)	25th (A)	29th (A)	31st (A)
I_{fa}	0.66	0.23	0.01	0.02	0.09	0.14	0.23	0.48	0.22	0.15	0.05	0.08
I_{NGR}	24.57	23.67	0.31	0.58	1.15	1.61	1.39	1.75	1.04	1.22	0.81	1.03

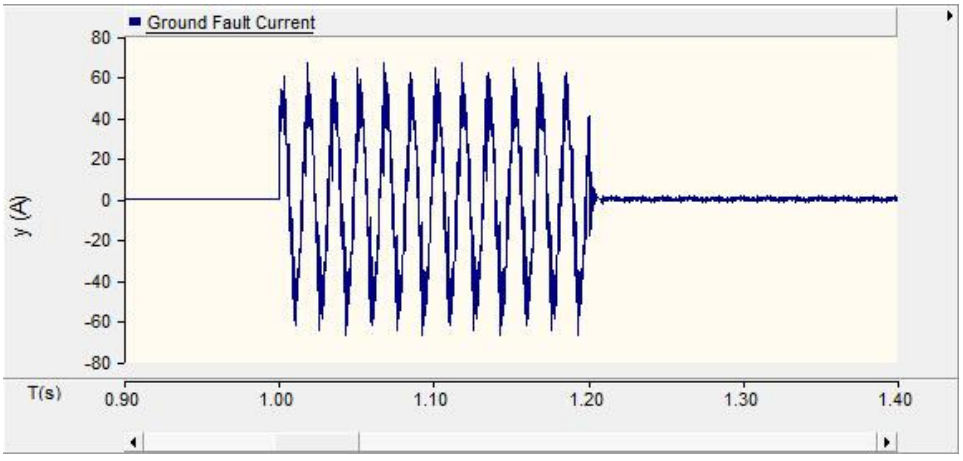

Figure 5.5. Plot of ground fault current with 288Ω NGR and injection system connected in parallel.

From the simulation results shown, the ground fault current can be driven to nearly zero after injecting both fundamental and harmonic compensation signals. The error at fundamental frequency is a little larger than with the Petersen coil because the fundamental injection factor is neglected, but it is still under 0.5 A.

5.2.3.2.2. Fault Branch Identification

The compensation system using an injection device connected in parallel with the neutral grounding resistor also effectively limits the level of ground fault current to nearly zero. Due to the absence of the Petersen coil, the fundamental component of the ground fault current cannot be canceled immediately after the fault occurs; instead, a short period of 0.20 s is required for the active compensation system. During this period, the system identifies the faulted branch by comparing the phase angle measured by the zero-sequence current transformer at the source end of each branch. Figure 5.6 demonstrates the zero-sequence current in the three-branch distribution system with a fault occurring at branch 2. Because of the system capacitance, zero-sequence current through unfaulted branch are capacitive with the phase angle of nearly -90 º(the reference is at 0 º) and the direction is from the bus to loads, but the zero-sequence current through the faulted branch will flow from loads to the bus and the phase angle is not close to -90 º. By comparing the zero-sequence current phase angle measurements from each branch, it is straightforward to identify the faulted branch.

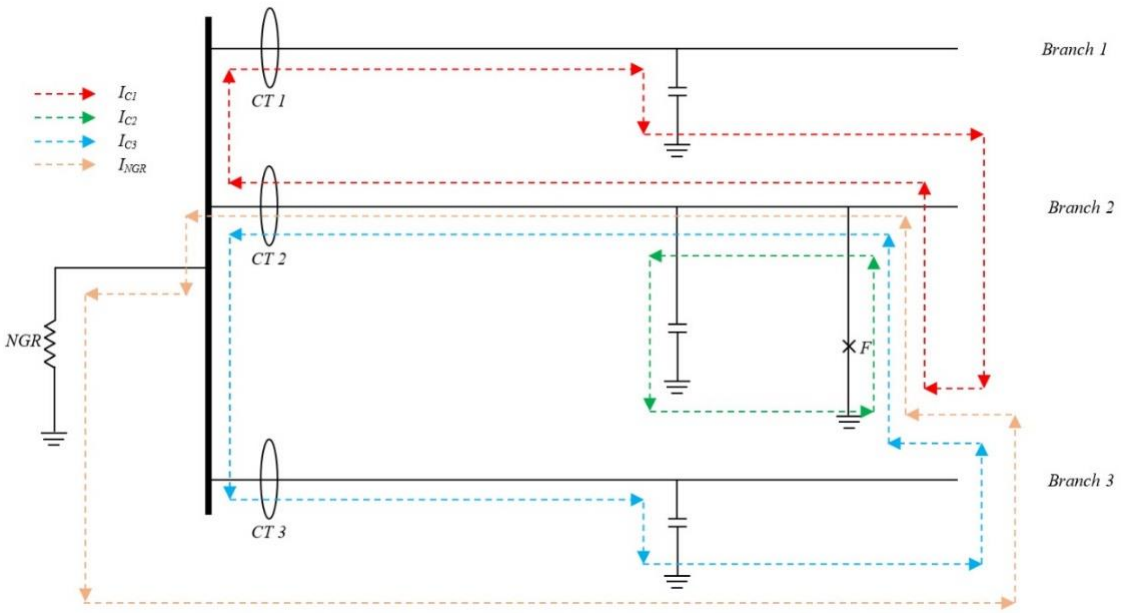

Figure 5.6. Zero-sequence currents flows in a three-branch distribution system with a fault occurring at branch 2.

Simulation results are shown in Table 5.7 to verify the feasibility of this ground fault location detection method. The results are obtained before the compensation system begins operation and it is obvious that the zero-sequence current on unfaulted branches (i.e., 1 and 3) have a phase angle of approximately -90 ºwhile the faulted branch (2) has a phase angle of approximately 30 °.

Table 5.7. Phase angle of the zero-sequence current measured at each branch.

	Branch 1	Branch 2	Branch 3
Phase Angle	-90.41º	30.62º	-90.45º

5.2.4. Flowchart of the Active Current Injecting Compensation System

Figure 5.7 shows a flowchart of the active current injecting compensation system for a practical situation. The system is initially operating under balanced conditions. At a specified time, a

single-line-to-ground fault occurs on an unknown branch, and the ground fault current is partially limited by the neutral grounding resistor. The processor reads phase angles at the source end of each branch and performs a comparison to identify the faulted branch. Then the phase currents at both sides of the faulted branch are measured and sent to the processor. Meanwhile, the processor calls the injection factor at each harmonic frequency (saved in the system database). After the processor calculates the required compensation current magnitude and phase angle at each frequency, the signals are injected into the neutral point of the system. Once the injection system starts, the distribution system can remain in operation for a short period to permit an orderly shutdown. After the faulted branch is isolated and disconnected from the distribution system for repair, the injection system ceases operation. The system returns to normal operation once the fault is cleared.

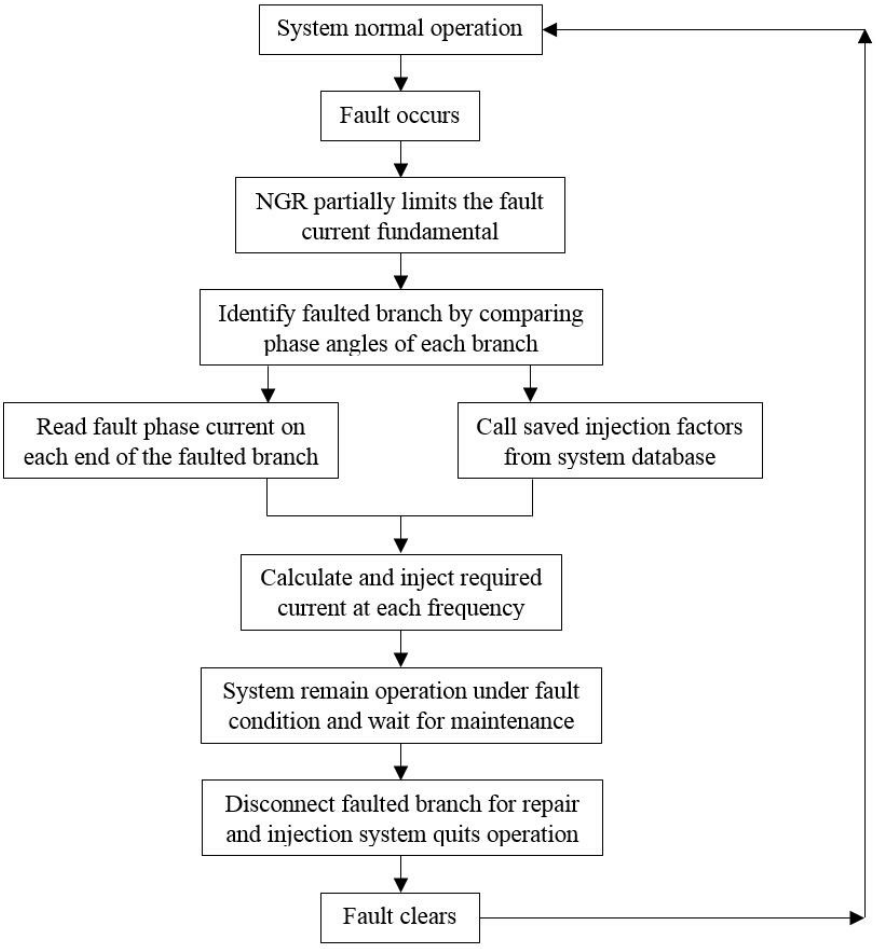

Figure 5.7. Flowchart of the active current injection compensation system.

5.3. Chapter Summary

This chapter has presented a theory using an active current injection method to fully compensate the ground fault current based on the prediction method described in Chapter 4. Two types of compensation systems are proposed and representative simulations are performed.

The first compensation system is to connect a Petersen coil in parallel with the injection system so that the fault current fundamental can be neutralized by the Petersen coil and the harmonics can be compensated by the injected currents. The simulation results show that the level of ground fault current is effectively reduced, but a separate system must be used for detecting the fault.

In the second compensation system, the Petersen coil is replaced by a neutral grounding resistor which allows the NGR to partially limit the fault current fundamental, while the residual fundamental current and harmonic currents are all neutralized by the injection system. The simulation results indicate that this compensation system can, not only drive the fault current close to zero, but also easily detect the fault location.

After comparing both results, it is recommended to choose the second compensation system for a coal mine distribution system. Finally, the flowchart of the chosen compensation system is presented for a practical situation to demonstrate how the compensation system works.

CHAPTER 6

CONCLUSIONS AND RECOMMENDED FUTURE WORK

6.1. Conclusions

The current practice in U.S underground coal mine high-voltage distribution systems is to limit ground fault current to 25 A with a pickup (i.e., trip) setting of 10 A. However, the combination of shielded cables and extensive distribution systems can cause system charging current to be several times higher than 25 A. Consequently, the 25 A limit is not truly the ground fault limit. Moreover, with the development of modern mining technologies, a variety of control devices and non-linear loads are increasing the level of harmonic currents in the distribution system. These harmonic currents flow through the entire distribution system and once a single-line-to-ground fault occurs, they can be a significant part of the ground fault current. To help improve underground safety, all components of the ground fault current should be driven close to zero, in order to eliminate arcing and the potential of fire or injury.

A Power System CAD (PSCAD/EMTDC) simulation model of a simplified three-branch distribution system was developed to represent a typical mine power distribution system. A wye connected three-phase voltage source is used as the secondary side of the substation transformer and the neutral point is grounded. Mine power cables, including borehole and mine power feeders, are represented by π-equivalent circuits. Loads and transformers are converted to distribution voltage level and represented by resistance and inductance. Harmonic sources are simulated in parallel with the load on each branch. After the simulation model is established, hand calculations of voltages and currents are performed to verify the model's correctness.

Subsequently, simulations are performed on the three-branch distribution system simulation model to investigate problems associated with distributed capacitance. In a ground fault simulation conducted for high-resistance grounding as currently practiced by U.S. coal mines, it is observed that the ground fault current exceeds the NGR current limit. (Although the simulation results of the three-branch distribution system show the predicted fault current is 1.5 times the NGR current, more extensive systems found in mining will have significantly higher capacitance charging current.) Loss of relay selectivity is also observed, which causes difficulty in isolating the faulted branch. Moreover, simulations are performed to investigate the issues associated with harmonics. After connecting harmonic sources at the end of each branch, simulation results indicate that the harmonic components of the ground fault current can be significant. Even with the fundamental component reduced by use of a Petersen coil, the harmonics fault current could cause arc and flash hazards.

The difficulty associated with harmonics is that the Petersen coil is a passive device and is tuned to eliminate the 60-Hz ground fault current. Therefore, a prediction method is developed to predict the fundamental and harmonic ground fault currents in real-time. A corresponding sequence network simulation model of the simulated three-branch distribution system is established to help analyze the faulted condition. By analyzing the sequence network, it is recognized that the ground fault current can be predicted by a novel application of differential relaying, i.e., comparing the source side current with the load side current. Subsequently, simulations are performed to verify the proposed prediction method. Results indicate that the magnitudes and angles of the predicted ground fault currents are very close to the results of the simulation model. Additional simulations are also performed to verify the correctness of the prediction method when a fault occurs at different locations.

After successfully predicting the fault current's harmonic components, it is possible to use active current injection to compensate for the ground fault current. Two different types of compensation systems are developed and simulated in PSCAD/EMTDC. The first compensation system is to connect a Petersen coil in parallel with the injection system so that the fault current fundamental is neutralized by the Petersen Coil and the harmonics are neutralized by the injected currents. The simulation results show that the level of ground fault current is reduced significantly, but it is difficult to detect the fault location and impossible to

control overvoltages. In the second compensation system, the Petersen coil is replaced by a neutral grounding resistor to partially limit the fault current fundamental, while the residual fundamental current and harmonic currents are all neutralized by the injection system. A fault branch detection method based on this compensation system is also developed and discussed. The simulation results and analysis indicate that this compensation system can, not only drive the fault current close to zero, but it is also possible to detect the fault location and limit overvoltages. Therefore, it is believed that the second compensation system would be more appropriate for a coal mine distribution system. Finally, a flowchart of the chosen compensation system is developed.

6.2. Recommended Future Work

This research has shown that the proposed compensation system with an active current injection device connected in parallel with the neutral grounding resistor has the potential to fully eliminate the ground fault current, especially the harmonic components. However, there are still several development needs to be considered before such as system can be implemented. Therefore, several recommendations are made for future research.

First, a lab-scale experimental system should be constructed to demonstrate the effect of the proposed compensation system. Due to the lack of financial support, the construction of such a system was not possible.

Second, a suitable data acquisition and communication system needs to be developed and tested. This is necessary to collect current data from each branch of the distribution system, save the injection factor data of each branch, and perform phase angle comparisons for each branch. This system must also contain a calculation module to calculate the predicted magnitude and phase angle of ground fault currents. This system would also need to operate very quickly to neutralize ground fault current as soon as possible to minimize safety hazards.

Finally, additional studies should be conducted to evaluate the proposed system under different fault conditions. For example, the present simulation system assumes the ground fault

resistance is zero; however, in some cases, there could be a significant fault resistance; therefore, the effect of a variable fault resistance on the system performance should be evaluated.

REFERENCES

1. Ai, B., 2011, Application of Fault Line Selection Apparatus Based on Transient Current Principle in Small Current Grounding System of WISCO Grid, Metallurgical Power, Vol. 6, No. 3, pp. 8-11.

2. Amoh, M. A., 2006, Analysis of Electrical Grounding Practices in the Aggregate Industry, M. S. Thesis, Department of Mining Engineering, University of Kentucky, August, 150 pp.

3. Anon., 1976, Mining Cable Engineering Handbook, Anaconda Wire and Cable Company, Greenwich, Connecticut, pp. 40-69.

4. Anon., 1993, IEEE Recommended Practice for Electric Power Distribution for Industrial Plants (IEEE Red Book), IEEE Std. 141-1993 (R1999), The Institute of Electrical and Electronics Engineers, New York.

5. Anon., 2001, IEEE Recommended Practice for Protection and Coordination of Industrial and Commercial Power Systems, IEEE Std. 242-2001, The Institute of Electrical and Electronics Engineers, New York, pp. 231-284.

6. Anon., 2003, Title 30 of the Code of Federal Regulations: Mineral Resources, Office of the Federal Register, National Archives and Records Administration, Washington, DC, 90-128, pp. 510-541.

7. Anon., 2010, PSCAD/EMTDC Experimental Guidance and Manual, Smart Power System Lab, Xi'an University of Technology, pp. 2-3.

8. Anon., 2013, Tiger Brand Mining Cables, AmerCable Inc., [Online] Available from: http://www.amercable.com, [Accessed December 2013]

9. Blackburn, J. L., 1993, Symmetrical Components for Power Systems Engineering, Marcel Dekker, Inc., New York, 427 pp.

10. Blackburn, J. L., 1997, Protective Relaying: Principles and Applications, 2nd Edition, CRC Press, pp. 70-128, 190-230.

11. Chen, D., 2011, Harmonics Analysis and Control in Coal Mine Power System, Energy Technology and Management, Vol. 3, pp. 147-148.

12. Chen, Z., Wu, W., Chen, J. and Zhang, Q., 2005, Study on Damping Rate and Out-of-resonance Degree of Power Compensation Network, *Relay,* Vol. 33, No. 4, Feburay, pp. 36-44.

13. Coyle, T., 2002, Performance Testing Low-Voltage Ground-Fault Protection, IEEE Transactions on Industry Applications, Vol. 38, No.4, July/August, pp. 981-989.

14. Du, Y., 2003, A Summary of Automatic Tuning Principles of Arc-suppression Coil, Colliery Mechanical & Electrical Technology, Vol. 2, No. 4, pp. 37-40.

15. Faulkenberry, L. M. and Coffer W., 1996, Electric Power Distribution and Transmission, Prentice Hall, Inc., New Jersey, pp. 71-296.

16. Fortescue, C. L., 1918, Method of Symmetrical Co-Ordinates Applied to the Solution of Polyphase Networks, *AIEE Transactions*, Vol. 37, part II, pp. 1027-1140.

17. Fu, Z. and Wan, G., 2002, Methods of Fault Line Selection for Single Phase to Earth Fault in Networks with Ungrounded Neutral, Low Voltage Apparatus, Vol. 3, No. 1, pp. 43-47.

18. Granger, J. J. and Stevenson, W. D., Jr., 1994, Power System Analysis, McGraw-Hill Book Co., Singapore, pp. 416-430.

19. Hao, S. and Zhan, X., 2010, Simulation of Fault Branch Selection using Fifth-order Harmonic Method, Mechanical and Electrical Information, Vol. 1, No. 30, pp. 74-75.

20. Li, F., 1993, Neutral Point Non-effictively Grounded System Operation, China Waterpower Press, Beijing, pp. 57-59.

21. Li, X., 2010, Research on Flexible Zero-Residual-Current Arc Suppression Coil, Ph.D Dissertation, Department of Information and Electrical Engineering, Chinese University of Mining and Technology, pp. 26-38.

22. Miller, R. H. and Malinowski, J. H., 1994, Power System Operation, 3rd Edition, McGraw-Hill Book Company, New York, pp. 185-212.

23. Morley, L. A., 1990, Mine Power Systems, Information circular: 9258, United States Department of the Interior, Bureau of Mines, Supt. of Docs. no.: I 28.27:9258, pp.159-345.

24. Mu, L. and Meng, Q., 2003, Power Distribution Safety Technology, China Machine Press, Beijing, pp. 67-99.

25. Mu, L., 1999, Principle of Selective Grounding Fault Protection Based on Active Component Direction of Zero-sequence Current, Power System Technology, Vol. 23, No. 9, September, pp. 60-62.

26. Nasar, S. A. and Trutt, F.C., 1999, Electric Power Systems, CRC Press, pp. 105-167.

27. Nelson, J. P., 2002, System Grounding and Ground-Fault Protection in the Petrochemical Industry: A Need of Better Understanding, IEEE Transactions on Industry Applications, Vol. 38, No. 6, November/December, pp.1633-1640.

28. Novak, T., 1998, Analysis of Very-High Resistance Grounding in High-Voltage Longwall Power System, Proceedings of the 1998 IEEE Industry Applications Conference, Thirty-Third IAS Annual Meeting, Volume 3, October 12-15, pp. 2175-2183.

29. Novak, T., 2001, The Effects of Very-High-Resistance Grounding on the Selectivity of Ground-Fault Relaying in High-Voltage Longwall Power Systems, IEEE Transactions on Industry Applications, Vol. 37, No. 2, March/April, pp. 398-406.

30. Roberts, J., Hou, D., Calero, F., and Altuve, H. J., 2001, New Directional Ground-Fault Elements Improve Sensitivity in Ungrounded and Compensated Networks, Schweitzer Engineering Laboratories, Technical Paper, pp. 1-27.

31. Sottile, J. AND Novak, T., 2001, Electrical Safety, Mine Health and Safety Management, Society for Mining, Metallurgy, and Exploration, Inc. (SME), pp. 409-436.

32. Stevenson, W. D., Jr., 1982, Elements of Power System Analysis, 4th Edition, McGraw Hill, Inc., New York, pp. 380-530.

33. Tripathi, A. K., 2007, Techniques for Improving the Performance of High-Resistance Grounded Underground Coal Mine Distribution Systems, Ph.D Dissertation, Department of Mining Engineering, University of Kentucky, pp. 2-82.

34. Trutt, F. C. and Morley, L. A., 1998, Mine Power System Analysis, IEEE Transactions on Industry Applications, Vol. 24, No. 5, September/October, pp. 839-845.

35. Wang, C., 1999, Power System Neutral Grounding and Petersen Coil, Chinese University of Mining and Technology Press, pp. 39-48.

36. Xue, Y., Xu, B. and Du, J., 2007, Analysis of Fault Branch Selection in Resonance Grounding Systems, *Eelctrical Equipment,* Vol. 8, No. 11, pp. 5-9.

37. Yang, W., Cao, J. and Pei, M., 2010, Research on Harmonic Detection of Power System in Coal Mine, Sci-Tech Information Development & Economy. Vol. 20, No. 24, pp. 166-168.

38. Yao, H., 2001, The Resonance Grounding of the Electrical Power System, China Electic Power Press, Beijing, pp. 34-36.

39. Yu, L., Chow, M., and Bowen, J., 1998, Safety and Ground Fault Protection in Electrical Systems, IEEE Industry Applications Magazine, March – April, pp. 32-36.

40. Zipse, D. W., 2001, Earthing – Grounding Methods: A Primer, IEEE Industry Application Society 48th Annual Petroleum and Chemical Industry Conference, pp. 11-30.

41. Bridger, B. Jr., 1983, High-Resistance Grounding, IEEE Transaction on Industry Application, Vol. 1A-19, No. 1, January/February, pp. 15-21.

42. Cai, X. and Liu, Y., 2004, Magnetic Bias Based Arc-Suppression Transformer with Three Phases and Five Columns and Its Tuning, Automation of Electric Power System, Vol. 28, No. 2, pp. 83-88.

43. Cai, X., Li, S., Du, Y. and Chen, G., 2004, An Integrated Controller of Multi-Tap Arc-Suppression with Variational Damp and Detection of Earth Fault Feeder, Automation of Electric Power Systems, Vol. 28, No. 5, March, pp. 85-89.

44. Cai, X., Liu, Y., Hu, C. and Zuo, H., 2004, New Resonance Earth System with Magnetic Bias and Its Protection, Proceedings of CSEE, Vol. 24, No. 6, June, pp. 44-49.

45. Champe, W. C. and Voigtlander, F. V., 1938, System Analysis for Petersen Coil Application, Electrical Engineering Transaction, Vol. 57, December, pp. 663-676.

46. Chen, G., Cai, X. and Jiang, D., 2003, A New Tuning Method for Petersen-Coil with Magnetic Bias, Proceedings of the EPSA, Vol. 15, No. 1, February, pp. 15-21.

47. Chen, H. and Chen W., 2003, The Measurement of Capacitive Current in Distribution Networks Using Controllable Arc-Extinguishing Coil with High Speed Response, High Voltage Engineering, Vol. 29, No. 4, pp. 9-10.

48. Chen, H., Zheng, J. and Yu, Z., 2003, Proof of Mounting of Harmonics Removing

Damping Device for Arc Removing Coil of 66 kV System, Metallurgical Power, No. 4, pp. 1-4.

49. Chen, K., Tang, Y. and Meng, Q., 2006, Detecting Single-Phase-to-Ground Faulted Feeder in Resonant Grounded Power Distribution System, Journal of China University of Mining and Technology, Vol. 35, No. 1, January, pp. 104-108.

50. Chen, X., 1996, A Three-Phase Multi-Legged Transformer Model in ATP Using the Directly-Formed Inverse Inductance Matrix, IEEE Transactions on Power Delivery, Vol. 11, No. 3, July, pp. 1554-1562.

51. Cheng, J., Chen, B. and Huangpu, C., 2006, Automatic Tuning TSC Arc Suppression Coil Grounding Device Based on Signal Injection, High Voltage Apparatus, Vol. 42, No. 1, February, pp. 63-65.

52. Doln´ık, B. and Kurimsk´y, J., 2011, Contribution to earth fault current compensation in middle voltage distribution networks, Przeglad Elektrotechniczny, No. 2, pp. 220-224.

53. Hu, T., Wang, C. and Mu, L., 2000, Method of Measuring Insulation Parameters to Ground for Mining Power System, Journal of China University of Mining and Technology, Vol. 29, No. 4, July, pp. 385-387.

54. Hu, Z., Li, X. and Shi, J., 2006, Analysis of Earth Fault Selection Based Residual Current and Current Angle Integration, Relay, Vol. 34, No. 7, April, pp. 6-9.

55. Huang, J., Liu, H. and Lv, Y., 2006, Distribution Grid Earth Gault Line Detection Study by the Traveling Wave Wavelets Coefficient Maximum Polarities Redundancy Voting, Relay, Vol. 34, No. 7, April, pp. 13-17.

56. Huo, L. and Chen, L., 2014, Study on Coal Mine Power System Harmonic Cancelation, [Online] Available from http://www.paper.edu.cn/, [Accessed March 2014], pp. 1-5.

57. Ji, F., Wang, C., Mu, L., Liu, J. and Chen, C., 2004, New Type of Arc Suppression Coil Based on Symmetry and Phase Tuning Principle, Automation of Electric Power Systems, Vol. 28, No. 22, November, pp. 73-77.

58. Ji, J. and Pu, W., 2003, Principle of Selecting Earthing Wire for Single-Phase Ground of Arc-Suppression Coil Grounding System, Zhejiang Electric Power, No. 3, pp. 51-54.

59. Jia, C., 2014, Research of Key Technologies on Full Current Compensation Arc Suppression Coil, Ph.D Dissertation, Department of Information and Electrical Engineering, Chinese University of Mining and Technology, pp. 26-72.

60. Kong, R., Dong, X. and Bi, G., 2006, Test of Gault Line Selector Based on Current Traveling Wave, Automation of Electric Power Systems, Vol. 30, No. 5, March, pp. 63-67.

61. Li, D., Chen, Q. and Jia, Z., 2003, A Novel Principle of Adjustable Reactor Based on Magnetic Flux Controllable, Proceedings of CSEE, Vol. 23, No. 2, February, pp. 116-120.

62. Li, J., Chen, Q., Zhang, Y. and Yao, J., 2007, Grounding Fault Line Detection Based on Magnetic-Flux Controllable Arc Suppression Coil Using Current Injection Technology, Electric Power Automation Equipment, Vol. 27, No. 1, January, pp. 61-64.

63. Li, L., Hu, X. and Liu, C., 2011, Analysis and Research on Harmonic Wave Control

of Electric Power Supply System in Mine Enterprise, Coal Mine Machinery, Vol. 32, No. 6, January, pp. 235-237.

64. Li, L., Sun, H. and Wang, X., 2003, A New Automatic Tuning Method for Resonance Grounding Power Network, Proceedings of CSEE, Vol. 23, No. 6, June, pp. 77-80.

65. Lin, X., Weng, H., Wu, K., Liu, H. and Liu, P., 2006, A Novel Adaptive Protection Principle of the Single-Phase Earth Fault of the Non-Effectively Grounded Power System, Proceedings of CSEE, Vol. 26, No. 2, January, pp. 52-57.

66. Ma, H., Chen, X., Zeng, X., Li, Z. and Wang, Y., 2005, Petersen Coil Automatic Tuning and Earth Fault Identification in a Compensated Distribution Network, Journal of Changsha University of Science and Technology (National Science), Vol. 2, No. 2, June, pp. 48-51.

67. North, J. R. and Eaton, J. R., 1934, Petersen Coil Tests on 140-kV System, Electrical Engineering, January, pp. 63-74.

68. Oliver, J. M. and Eberhardt, W. W., 1926, Operating Performance of a Petersen Earth Coil-II, A.I.E.E. Transaction, February, pp. 165-168.

69. Pan, Z., Zhang, H., Zhang, F. and Sang, Z., 2007, Analysis and Modification of Signal Injection Based Fault Line Selection Protection, Automation of Electric Power Systems, Vol. 31, No. 4, February, pp.71-75.

70. Papadopoulos, T. A., Tsiamitros, D. A. and Papagiannis, G. K., 2010, Impedances and Admittances of Underground Cables for the Homogeneous Earth Case, IEEE Transactions on Power Delivery, Vol. 25, No. 2, April, pp. 961-969.

71. Qu, Y., Dong, Y., Tan, W. and Yang, Y., 2007, Research on New Type Arc-Suppression Coil Base on Single-Phase Active Power Filter Technology, Relay, Vol. 35, No. 3, February, pp. 29-33.

72. Shan, X., 2006, Discussion on Instantaneous Reactive Power P-Q Theory, High Voltage Engineering, Vol. 32, No. 5, May, pp. 100-110.

73. Shu, H. and Si, D., 2006, New Approach for Fault Line Selection in Distribution System with Arc Suppression Coil Grounding Using Decaying DC Component, Electric Power, Vol. 39, No. 2, February, pp. 1-4.

74. Su, J. and Chen, C., 2003, Steady State Operation Performance Study of TCR with New Type of Petersen-Coil, Electric Power Automation Equipment, Vol. 23, No. 1, pp. 11-17.

75. Tang, Y., Chen, K., Chen, Q. and Fang, Y., 2003, Research on the Full Current Compensation of One-Phase-to-Ground-Fault, Journal of China University of Mining and Technology, Vol. 32, No. 5, September, pp. 558-562.

76. Wang, C., Liu, J. and Dong, X., 1999, Analysis on Principle of Operation and Wave Shape of the Arc-Suppression Coil with Three Phase and Five Columns Controlled by Silicon Controller, Journal of China Coal Society, Vol. 24, No. 6, December, pp. 638-642.

77. Wang, X., Li, Q. and Chen, X., 2004, Study on Fault Feeder Detection for Single-Phase-to-Earth Fault in Compensated Distribution Network, Electric Power Automation Equipment, Vol. 24, No. 4, April, pp. 39-41.

78. Wang, Z., Sun, H., Xin, Y. and Li, G., 2008, Design of New Capacitor Automatic Tuning Arc-Suppression Coil Based on PSCAD, Power Electronics, Vol. 42, No. 3,

March, pp. 46-48.

79. Xie, Y., 2008, Study on Power System Harmonics and its Suppression Technology, M. S. Thesis, Department of Electrical Engineering, Dalian University of Technology, December, pp. 1-33.

80. Xiong, R., Zhang, H., Zhang, C. and Lv, Y., 2006, Study on Intelligent Selection Device in Indirect-Grounded Fault System, Relay, Vol. 34, No. 6, March, pp. 6-10.

81. Xu, Y. and Wang, M., 2006, Fault Line Detection for Distribution Networks Based on Transient Current of Non-Fault-Phase, Journal of North China Electric Power University, Vol. 33, No. 2, March, pp. 45-49.

82. Xu, Y., Zeng, X., Liu, Z. and Yi, W., 2008, Novel Control Techniques of Petersen-Coil, Proceedings of the IEEE International Conference on Industrial Technology, Chengdu, April 21-24, pp. 1-4.

83. Ye, G., 2006, Petersen Coil Auto Tuning Technology Based on Signal Injection Method, Hunan Electric Power, Vol. 26, No. 2, pp. 32-36.

84. Zeng, X., Xu, Y. and Wang, Y., 2010, Some Novel Techniques for Insulation Parameters Measurement and Petersen-Coil Control in Distribution Systems, IEEE Transaction on Industrial Electronics, Vol. 57, No. 4, April, pp. 1445-1451.

85. Zeng, X., Yi, X., Yu, Y. and Chen, D., 2000, New Method for Control and Protection Relay in a Compensated Medium Voltage Distribution Network Based on Injecting Various Frequency Current, Proceedings of the CSEE, Vol. 20, No. 1, January, pp. 29-36.

86. Zeng, X., Yu, Y., Zhou, Y. and Yang, Q., 1998, Online Distinguishing Between

Resonance and One-Phase Grounding in Distribution Network, Automation of Electric Power Systems, Vol. 22, No. 8, August, pp. 41-43.

87. Zhang Z., Zhou, Y. and Wang, N., 2006, Single-Phase Earthing Line Selection Based on Fundamental Current Injection, Relay, Vol. 34, No. 9, May, pp. 70-72.

88. Zhang, F., Pan, Z., Zhang, H., Xu, A. and Song, L., 2006, New Criterion of Fault Line Selection in Non-Solidly Earthed Network Based on the Maximum of Zero-Sequence Transient Current, Automation of Electric Power Systems, Vol. 30, No. 4, February, pp. 45-48.

89. Zhang, H., Wang, H., Wang, S. and Tian, Z., 2001, Syntonic Earthing and Faulty Line Identifying and Faulty Point Location Technique with S's Signal Injection Method, Electrical Equipment, Vol. 2, No. 3, September, pp. 26-44.

90. Zhang, L. and Liu, R., 1999, The Neutral Spot Displacement Analysis of Erasing Electric Arc Coil in All Kind of Compensative Conditions, Journal of Electric Power, Vol. 14, No. 3, pp. 157-160.

91. Zhang, X., 2012, Analysis and Control Measures of Coal Mine Power Network Harmonics, Electric Switchgear, No. 3, pp. 98-99.

92. Zhao, H., 2002, System Analysis of Arc Suppression Coil with Tapping Switch, Modern Electric Power, Vol. 19, No. 6, December, pp. 65-70.

93. Zheng, P., 2003, Engineering Practice and Discussion of Weak Current Grounding Wire Selection, Electric Power Automation Equipment, Vol. 23, No. 6, June, pp. 82-85.

VITA

Yigong Zhang was born in Jiaozuo City, Henan Province, China. He started undergraduate studies in the Henan Polytechnic University in China for 3 years, and then joined the exchange program and transferred to the University of Kentucky. He obtained his Bachelor of Science degree in Electrical Engineering from University of Kentucky in May 2010. Since August 2010, he has been pursuing Doctoral degree in Mining Engineering with specialization of Mine Power System at the University of Kentucky, Lexington, KY, USA. He is a member of SME and IEEE.